

EGG-TMI-6630
June 1984
DRAFT

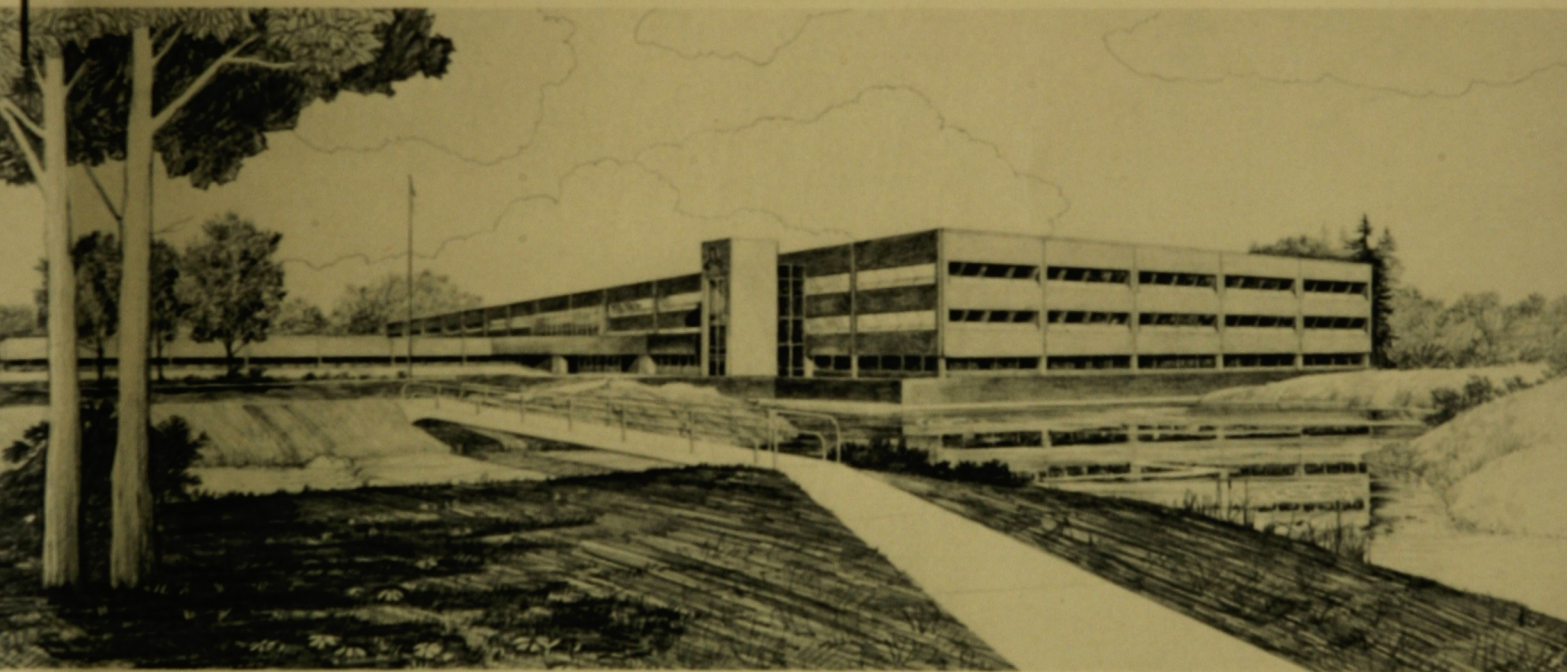
DRAFT PRELIMINARY REPORT:
TMI-2 CORE DEBRIS GRAB SAMPLES - ANALYSIS OF FIRST
GROUP OF SAMPLES

D. W. Akers

B. A. Cook

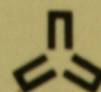
Idaho National Engineering Laboratory

Operated by the U.S. Department of Energy



This is an informal report intended for use as a preliminary or working document

Prepared for the
U.S. DEPARTMENT OF ENERGY
Under DOE Contract No. DE-AC07-76ID01570

 **EG&G** Idaho

DISCLAIMER

This book was prepared as an account of work sponsored by an agency of the United States Government. Neither the United States Government nor any agency thereof, nor any of their employees, makes any warranty, express or implied, or assumes any legal liability or responsibility for the accuracy, completeness, or usefulness of any information, apparatus, product or process disclosed, or represents that its use would not infringe privately owned rights. References herein to any specific commercial product, process, or service by trade name, trademark, manufacturer, or otherwise, does not necessarily constitute or imply its endorsement, recommendation, or favoring by the United States Government or any agency thereof. The views and opinions of authors expressed herein do not necessarily state or reflect those of the United States Government or any agency thereof.

EGG-TMI-6630
Draft

DRAFT PRELIMINARY REPORT
TMI-2 CORE DEBRIS GRAB SAMPLES
ANALYSIS OF FIRST GROUP OF SAMPLES

D. W. Akers
B. A. Cook

EG&G Idaho, Inc.
Idaho Falls, Idaho 83415

Prepared for the
U.S. Department of Energy
Idaho Operations Office
Under DOE Contract No. DE-AC07-76ID01570

ACKNOWLEDGMENT

Many people contributed to the analysis of the core debris samples. Special thanks go to the following individuals: C. Rowsell and the staff at the Radiation Measurement Laboratory for their timely gamma spectrometry analysis of the samples. Y. D. Harker and P. R. Napper for their development of the fast neutron flux measurement facility and performance of the fissile/fertile material analysis. O. D. Simpson for his critical review of the data, and to J. O. Carlson, T. E. Cox, M. R. Martin, J. K. Jacoby, R. R. Hobbins, and H. W. Reno for their assistance in analysis of data and review of the manuscript.

SUMMARY

Six samples of particulate debris were removed from the TMI-2 core rubble-bed. These samples were acquired in order to obtain data on the extent and nature of the debris and the post-accident condition of the TMI-2 core. Five samples are being examined at EG&G Idaho. The remaining sample (No. 2) is being examined at the Babcock & Wilcox Lynchburg Research Center.

The first phase of the examination is presented in this report. It centers on GPU Nuclear's data needs to support reactor recovery. The first phase consisted of the following activities: unpackaging, bulk weighing, photo-visual survey, sieving (to determine particle size distribution), sieve fraction weighing, ferromagnetic material content test, pyrophoricity tests, gamma spectrometry and fissile/fertile material analysis. Discrete particles were selected from the larger diameter sieve fraction sizes ($\geq 1000 \mu\text{m}$) and aliquots from the smaller ($< 1000 \mu\text{m}$) sieve fraction sizes for use during the gamma spectrometry and fissile/fertile examinations.

A brief summary of the findings from this phase of the examination is outlined below:

- o Most material (~90%) is larger than $1000 \mu\text{m}$ (1 mm); less than 1% is smaller than $300 \mu\text{m}$.
- o The samples contain fuel pellet fragments and shards of cladding or guide tubes. Most particles are a conglomerate mixture of nonuniform combinations of fuel (UO_2) and non-fuel materials. Further analyses of those materials are planned.
- o The following gamma emitting radionuclides were present: ^{60}Co , ^{106}Ru , $^{110\text{m}}\text{Ag}$, ^{125}Sb , ^{134}Cs , ^{137}Cs , ^{144}Ce , ^{154}Eu , ^{155}Eu , and ^{241}Am .

- o No pyrophoric (combustible) materials were observed during the pyrophoricity test.
- o The ferromagnetic content of the examined sample was <1% of the total sample weight and was principally within the size range between 300 μm and 4000 μm .
- o The measured average enrichments at the H8 and E9 locations were 2.4 and 2.8% respectively, indicating that peripheral core materials generally were not present at the center of the core (i.e., H8).
- o A comparison of the measured data with the ORIGEN-2 code was performed. Preliminary evaluations indicated that some fission products (i.e., ^{144}Ce , ^{154}Eu , and ^{155}Eu) remained primarily with the fuel whereas large percentages (>50%) of other fission products (principally ^{134}Cs , ^{137}Cs) were no longer associated with the fuel material.

CONTENTS

ACKNOWLEDGMENTS	11
SUMMARY	111
1. INTRODUCTION	1
2. UNPACKAGING, PHOTO-VISUAL AND PARTICLE SIZING	6
3. FERROMAGNETIC ANALYSIS	20
4. PYROPHORICITY TESTS	22
5. GAMMA SPECTRAL MEASUREMENTS	24
6. FISSILE/FERTILE MEASUREMENTS	25
7. DISCUSSION OF RESULTS	26
8. CONCLUSIONS/OBSERVATIONS	45
9. REFERENCES	47
APPENDIX A--PHOTOGRAPHS OF DISCRETE PARTICLES	A-1
APPENDIX B--CORE DEBRIS GAMMA SPECTROMETRY DATA	B-1
APPENDIX C--FISSILE/FERTILE MATERIAL ANALYSIS	C-1

FIGURES

1. TMI-2 core debris sampling schematic	4
2. Summary schematic showing the TMI-2 core debris sample acquisition	8
3. TMI core debris sampling tools	10
4. Sample 1 - location H8 at the surface of the debris bed	11
5. Sample 1A, fuel rod segment from surface of debris bed at H8 location	13
6. Sample 3 - location H8 at 22-inches with debris in the sampler	14
7. Sample 3 - location H8 at 22-inches	15
8. Sample 4 - location E9 at surface	16

9. Sample 5 - location E9 at 2-inches	17
10. Sample 6 - location E9 at 22-inches	18
11. Ferromagnetic particle removed from the 1000 μ m size fraction of Sample 6	21
12. Tesla coil pilot ignition test	23
13. Propane torch pilot ignition test	23
14. Core debris sample frequency distribution histogram	27
15. Core debris sample particle size distribution	28
A-1 through A-27 photographs of individual particles	

TABLES

1. Summary of photo-visual and gross radioactivity levels	7
2. Particle size analysis results	9
3. Radionuclide distribution for Sample 1-Location H8 at surface	30
4. Radionuclide distribution for Sample 3-Location H8 at 22-inches	31
5. Radionuclide distribution for Sample 4-Location E9 at surface	32
6. Radionuclide distribution for Sample 5-Location E9 at 3-inches	33
7. Radionuclide distribution for Sample 6-location E9 at 22-inches	34
8. Non-fuel core material radionuclide content	35
9. Percent of fission products retained in the fuel	36
10. Weight fraction of fissile/fertile material	38
11. Average uranium enrichment	39
12. TMI-2 core fission product inventory	40
13. Measured to predicted fission product/uranium core inventory ratios	41
B1-B5 Core debris sample radionuclide concentrations	B-1
C1-C5 Core debris sample fissile/fertile material content	C-1

DRAFT PRELIMINARY REPORT

TMI-2 CORE DEBRIS GRAB SAMPLES ANALYSIS OF FIRST GROUP OF SAMPLES

1. INTRODUCTION

On 28 March 1979, the Unit 2 pressurized water reactor at Three Mile Island underwent an accident that resulted in severe damage to the reactor's core. As a consequence of the TMI-2 accident, numerous aspects of light water reactor safety have been questioned and the Nuclear Regulatory Commission (NRC) has embarked on a thorough review of reactor safety issues, particularly the causes and effects of severe core damage accidents. The nuclear community acknowledges the importance of examining TMI-2 in order to understand the nature of the core damage. Immediately after the TMI-2 accident, four organizations with interests in both plant recovery and accident data acquisition formally agreed to cooperate in these areas. These organizations, commonly referred to as the GEND Group--General Public Utilities, Electric Power Research Institute, Nuclear Regulatory Commission, and Department of Energy--are presently involved in post accident evaluations. The Department of Energy (DOE) is providing a portion of the funds for reactor recovery (in those areas where accident recovery knowledge will be of generic benefit to the light water reactor industry of the United States). In addition, DOE is funding acquisition and analysis of severe accident data (such as the examination of the damaged core).

Acquisition and examination of the core debris grab samples are part of the core internals examination program recommended by the TMI Reactor Assessment/Fission Product Behavior Technical Evaluation Group (TEG). The objectives and interests of the examinations and data presented in this report support data requirements of GPU Nuclear for reactor recovery. The examinations are being performed to acquire data on the extent and nature of damage and post-accident condition of the core that will assist GPU Nuclear in assessing the tooling and procedures required to defuel the TMI-2 reactor. The principal reactor recovery issues being addressed in the core debris examinations include:

- o What is the physical form of the particulate core debris (particle size, shape, morphology, origin, etc.)?
- o What are the chemical forms of the debris (fuel, cladding, control material, structural material, reaction product, etc.)?
- o What are the identity and quantity of fission products retained in the debris?
- o What are the release rates of radioisotopes from existing and freshly created surfaces?
- o Are pyrophoric materials present in the debris, and if so to what extent?
- o Does the core debris present any unanticipated defueling equipment concerns (filtration properties, settling rate, etc.)?
- o What is the airborne potential for radioactive particles (fines). This issue will be addressed in subsequent examinations. It is not part of this report.
- o Can the water that is physically or chemically entrained in the debris be removed readily to facilitate shipping and storage of the core? What drying conditions are required? This issue will be addressed in subsequent examinations. It is not part of this report.

Data designed to address these issues will aid TMI-2 defueling planning in numerous ways. The physical form of the debris (particle size and structure) is significant since small sized particles may be suspended during defueling and cause cloudiness in the water. Particle size distribution and filterability will also determine the type and effectiveness of filters, cyclones, and so forth, used for cleaning the water. Evidence of the physical state of debris particles (e.g., presence of previously molten materials) may provide a clue to the nature of the core material underneath the loose debris layer. The physical and mechanical properties of the core materials will influence the design of tools and methods for defueling. The retained fission product content of the debris is also important since it represents a potential radiological source that must be controlled. The rate at which

radioisotopes can be leached from the debris will affect the level of radioactivity dissolved in the water during defueling. The presence of pyrophoric materials may suggest that larger concentrations of pyrophoric materials could exist below the loose debris, which could be hazardous during preparation for shipping. Water entrained in debris materials represents a potential for the radiolytic buildup of hydrogen and oxygen gas in closed storage containers.

This report provides preliminary data on the physical characteristics and radionuclide concentrations of the five debris samples being examined at the INEL. The follow-on examinations will supplement these data and assist in resolving the principal issues discussed above. In addition, these data will be used along with the data from other tasks described in the Core Examination Plan to aid in defining the behavior of a commercial reactor core under the accident conditions that occurred at TMI-2. Specifically, this report presents the bulk sample and individual particle geometry, including particle size analysis, the ferromagnetic content, results of pyrophoricity tests, gamma spectral measurements of the sieve fractions and some individual particles, and fissile/fertile measurement data. The data are discussed and a summary of observations is presented.

Six samples of particulate debris from within the TMI-2 rubble bed were obtained in September-October 1983 by lowering sampling devices through leadscrew openings at two locations in the TMI-2 core, H8 (mid-core) and E9 (mid-radius). The samples are from three depths: surface of the rubble bed, 3-inches and 22-inches deep in the bed. After their removal, the six samples were shipped to EG&G Idaho. Sample (No. 2) was then shipped to Babcock and Wilcox (B&W) for examination and analysis. The grab samples are the first material to be extracted from the rubble bed.

Two different sampling devices were used to extract the samples from the rubble bed. One was a clamshell type tool used to take the surface samples. The other was a rotating tube device with doors on each side of two tubes. Figure 1 shows the TMI-2 core debris sampling schematic.

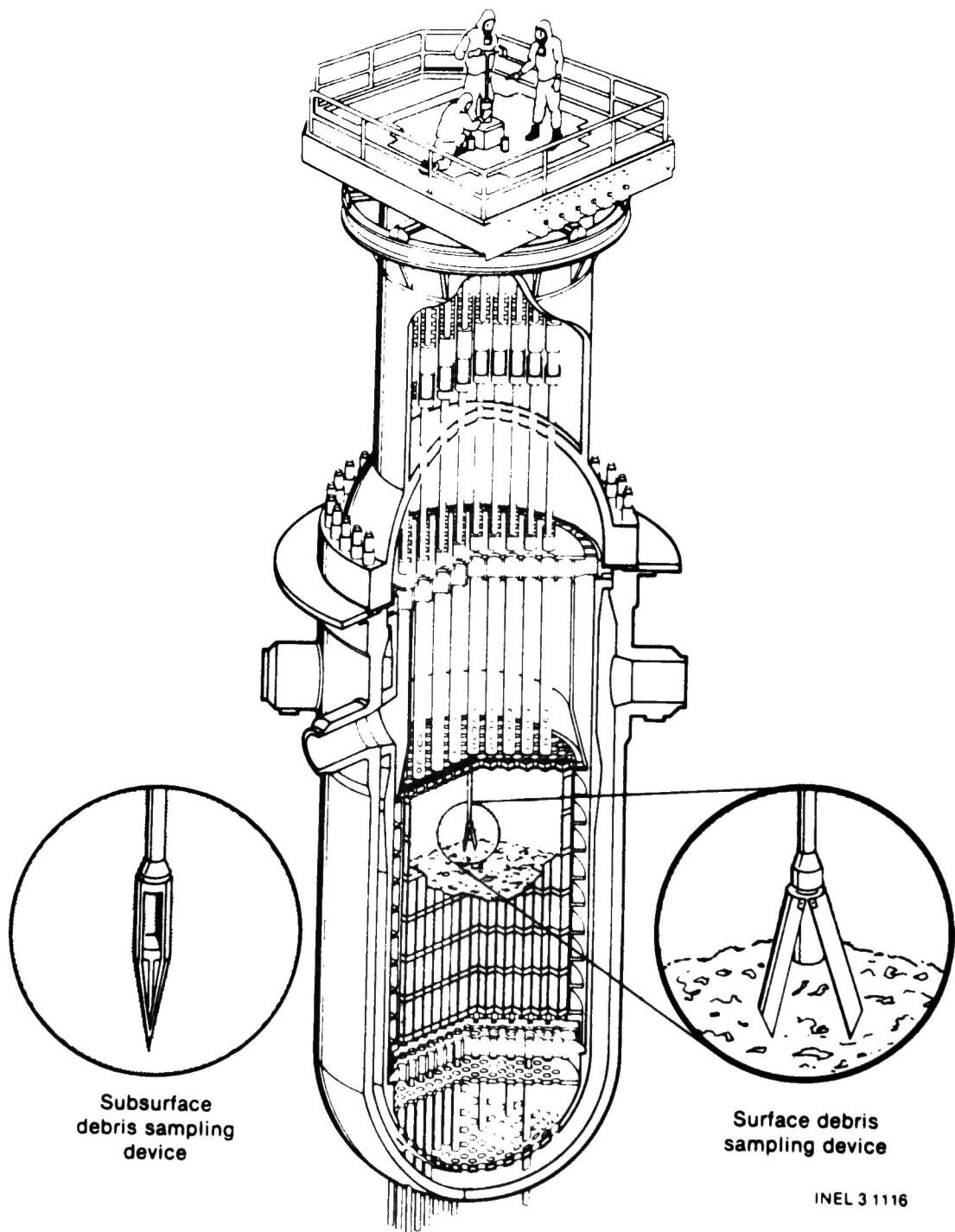


Figure 1. TMI-2 core debris sampling schematic.

Eventually, examination results from B&W of sample Number 2 (3-inch into the debris bed at core location H8) will be combined and analyzed with these data. A report will be prepared which contains both the EG&G Idaho and B&W results.

2. UNPACKAGING, PHOTO-VISUAL, AND PARTICLE SIZING

After their receipt from TMI, the five bulk samples (1, 3, 4, 5, and 6) retained at EG&G Idaho were unpackaged and photo-visually inspected. A summary of the bulk examination is presented in Table 1. Figure 2 is a summary schematic showing the core debris grab sample acquisition (core location and photos of each bulk sample) at TMI-2. Figure 3 shows the sampling tools used to acquire the samples.

The bulk samples were subjected to a particle size distribution analysis. This analysis was done by sieving the bulk samples into a number of progressively smaller particle sized groups (8 for most samples). The number and size division were determined during the visual examination of the bulk samples and, in general, match those used by B&W. The results of these analyses are shown in Table 2. Both wet (freon wash) and dry sieving techniques were employed. For the larger particle size fraction (i.e., $\geq 1000 \mu\text{m}$) dry sieving was used. For the size groups $< 1000 \mu\text{m}$, wet sieving (i.e. freon wash) was used to reduce suspension of the smaller size particles. The freon wash was used because it does not react chemically with the core debris materials. These data are discussed further in Section 7.

Discrete particles from the larger ($\geq 1000 \mu\text{m}$) sieve fraction sizes were selected and photographed in preparation for follow-on examination. Photographs of these particles are shown in Appendix A. A detailed description of each of the five samples follows:

Sample 1, the surface sample from the H8 location, was obtained using a clamshell sampler (see Figure 3). The sampler contained approximately 71 grams of very black debris with a wide range of particle sizes. The particle sizes in this sample ranged from $30 \mu\text{m}$ to greater than $4000 \mu\text{m}$, with the majority of the material being greater than $1000 \mu\text{m}$ in size. The overall photograph of Sample 1 is shown in Figure 4. The most unique particle in Sample 1 is a large fuel rod remnant, approximately $19000 \mu\text{m}$ long,

TABLE 1. SUMMARY OF PHOTO-VISUAL, ANA GROSS RADIATION LEVELS

Sample Number	Sampler Type	TMI-2 Core Location	Location of Sample in Rubble Bed	Gamma Radiation Level at 1-in. (Rads)	Visual Characteristics
1	Clamshell	H8	307 ft 0 in. (surface)	16	A pile of very black, damp debris with a fairly wide range of particle sizes (dimensions ranging from 1/16 to 1/2 in.); several rounded surfaces; sporadic rust color throughout.
3	Rotating Tube	H8	22-in. into debris bed	36	Very black debris, slightly damp, wide range of particle sizes (dimensions 1/16 to 1/4-in.), small chunks to fine debris; similar to Sample 1.
4	Clamshell	E9	306 ft 9 in. (surface)	3	Thirteen major chunks, dry, black with rust colored sides, basically sharp edges with one or two chunks having rounded edges; dimensions ranging from 1/4 to 3/8 in.
5	Rotating Tube	E9	3 in. into debris bed	18	Similar to Sample 4 with the following distinctions: many more pieces; greater size range (1/16 to 3/8 in.); some surfaces more reflective. Again, very dry.
6	Rotating Tube	E9	22-in. into debris bed	36	Very black debris, small chunks to fine debris, slightly damp, some pieces blackish gray. A couple of pieces resembled metal shards similar to Sample 3.

TMI-2 Core Debris Grab Samples

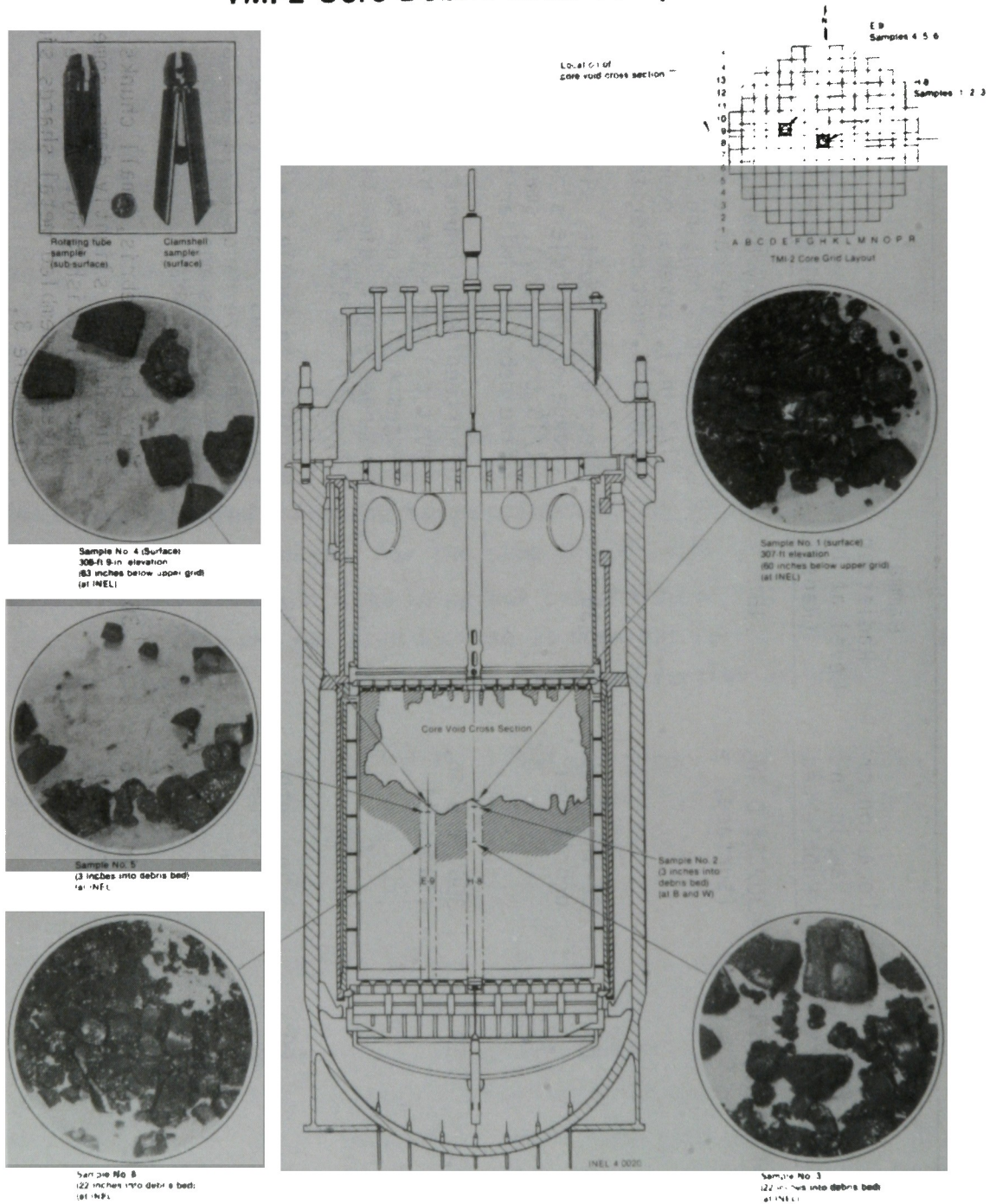


Figure. 2 Summary schematic showing TMI-2 core debris grab sample acquisition.

TABLE 2. PARTICLE SIZE ANALYSIS RESULTS

Particle Size Range (μm)	Sample No. 1 ^a		Sample No. 3		Sample No. 4 ^b	Sample No. 5 ^c		Sample No. 6		Sample No. 6
	(gms)	(%)	(gms)	(%)	(gms)	(gms)	(%)	(gms)	(%)	(gms)
>4000	12.62	18.4	63.75	42.9		69.57	77.1	57.99	42.0	0
1680 to 4000	27.82	40.6	51.45	34.7		13.96	15.5	49.39	35.8	0.39
1000 to 1680	15.64	22.8	19.19	12.9		6.25	6.9	13.88	10.1	0.30
% >1000		81.8		90.5			99.5		87.9	
<1000						0.44	0.49			
707 to 1000	7.80	11.4	5.49	3.7				8.93	6.5	0.25
297 to 707	3.20	4.7	6.34	4.3				5.99	4.3	0.19
149 to 297	0.87	1.3	1.27	0.86				0.97	0.70	0.025
74 to 149	0.44	0.64	0.77	0.52				0.67	0.48	0.024
30 to 74	0.17	0.25	0.18	0.12				0.22	0.16	NA
<30	NA ^e	--	0.013	0.01				NA	-0-	NA
Summed wt	68.56		148.45			90.22		138.04		1.178
Initial wt	70.88		152.71		16.59	90.96		140.73		
Loss	2.32	3.3	4.26	2.8		0.74	0.8	2.69	1.9	

a. Sample numbers shown correspond to sample numbers listed in Table 1.

b. Sieving was not done. Sample consisted only of large pieces.

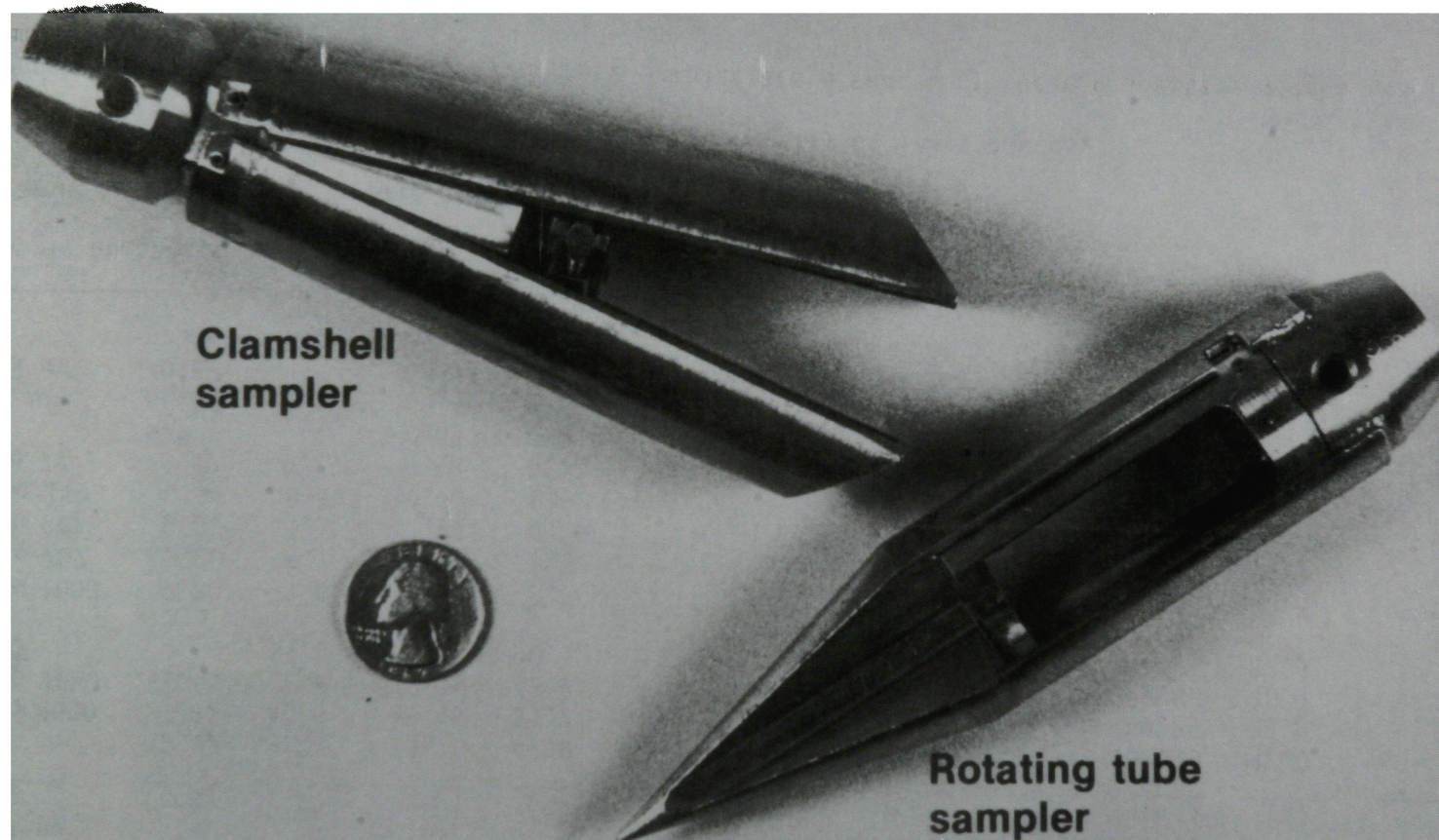
c. Sieving was limited to 4 sizes. Sample consisted mostly of large pieces.

d. Ferromagnetic sample weights (gms). These samples are a subset of their respective weight fractions for Sample No. 6.

e. None detected (not measurable).

f. The loss fraction defines an uncertainty in the quantity of material present, however, the loss fraction particle size distribution is not known.

TMI-2 Core Debris Sampling Tools



Clamshell
sampler

Rotating tube
sampler

S3 3538

Figure 3 TMI-2 core debris sampling tools.



Figure 4. TMI-2 core debris sample #1 (surface-H8).

consisting of zirconium cladding with pieces of fuel attached (Figure 5). The outer surface of the cladding and all fracture surfaces appear smooth. Several other particles within the debris also have smooth surfaces and rounded corners. There are no sharp fracture surfaces apparent on the particles. Several particles were selected from Sample 1 for detailed analysis. Photographs of these particles are presented in Appendix A.

(SAMPLE 2 DATA FROM B&W TO BE ADDED)

Sample 3, the 22-inch deep sample from the H8 position was obtained using a rotating tube sampler (see Figure 3). Figure 6 shows the debris contained in this sample. The material was stratified within the sampler, with the larger particles toward the top and the finer particles nearer the bottom. This may have occurred during shipment. The particle sizes in this sample ranged from 30 μm to greater than 4000 μm as shown in Table 2, with a majority of the particles (90%) greater than 1000 μm in size. This sample contained several particles that appeared to be fractured fuel pellets. The sample is shown in Figure 7.

Sample 4, the E9 surface sample consisted of thirteen larger sized particles ($>1000 \mu\text{m}$) requiring particle size analysis of this sample unnecessary. All pieces have the appearance of fractured fuel pellets (see Figure 8). Sample 5, the E9 three inch deep sample, contained almost all larger ($>1000 \mu\text{m}$) particles (see Figure 9). It appeared similar in nature to Sample 4. The lack of smaller particles ($<1000 \mu\text{m}$) in these two samples coincides with the in-core closed circuit television (CCTV) video inspections which show the E9 and adjacent area to contain larger sized particles on the surface of debris bed. Also, the E9 location coincides with a steep slope in the debris bed, as determined from the core topography.¹ It may be that the E9 location is at an area in the debris bed of preferential coolant flow so that the fine material in the upper layers would have been swept away.



Figure 5. Sample 1A, fuel rod segment from surface of debris bed at H8 location.

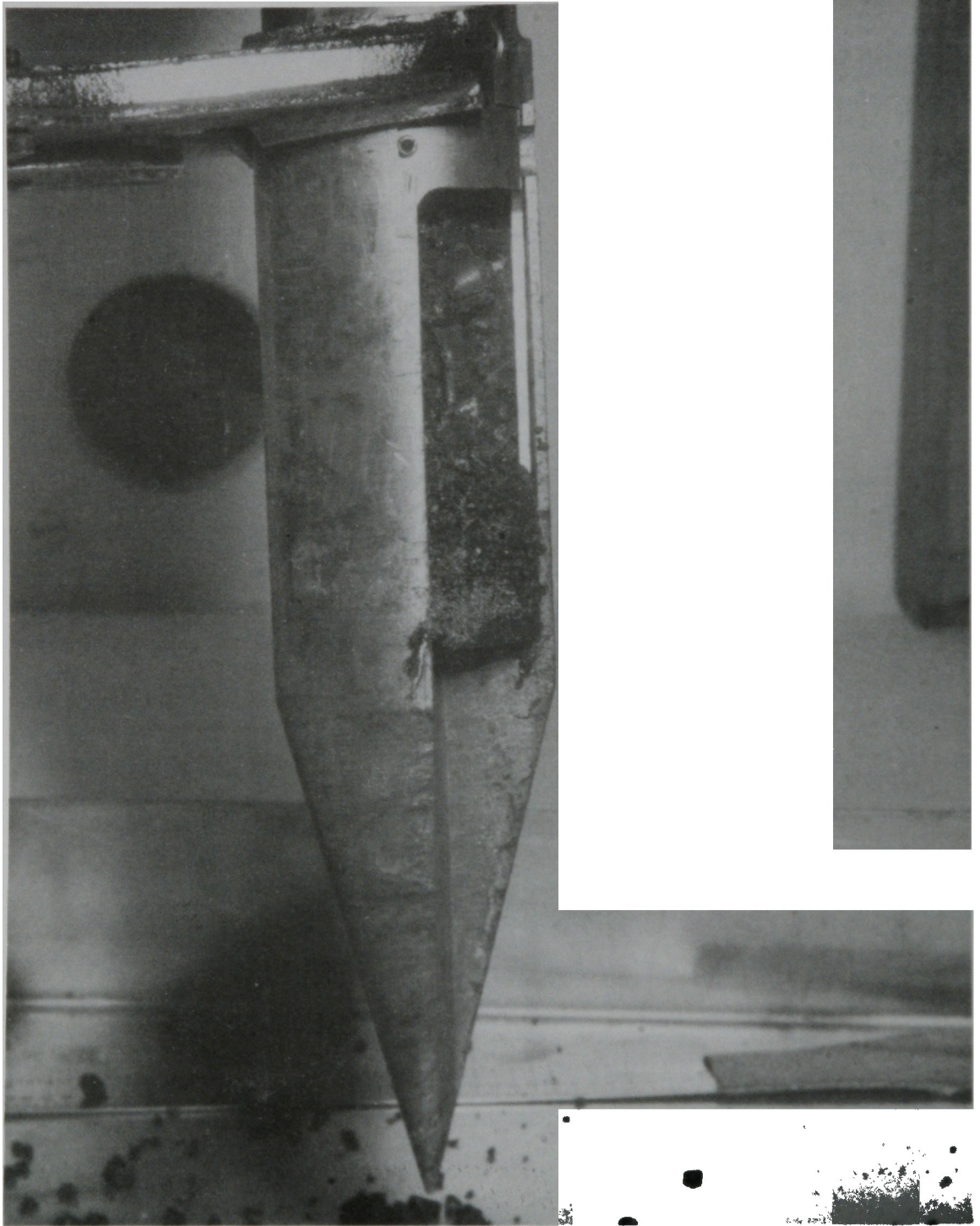


Figure 6 TMI-2 core debris sample #3 being removed from the rotating tube (22" deep-H8).

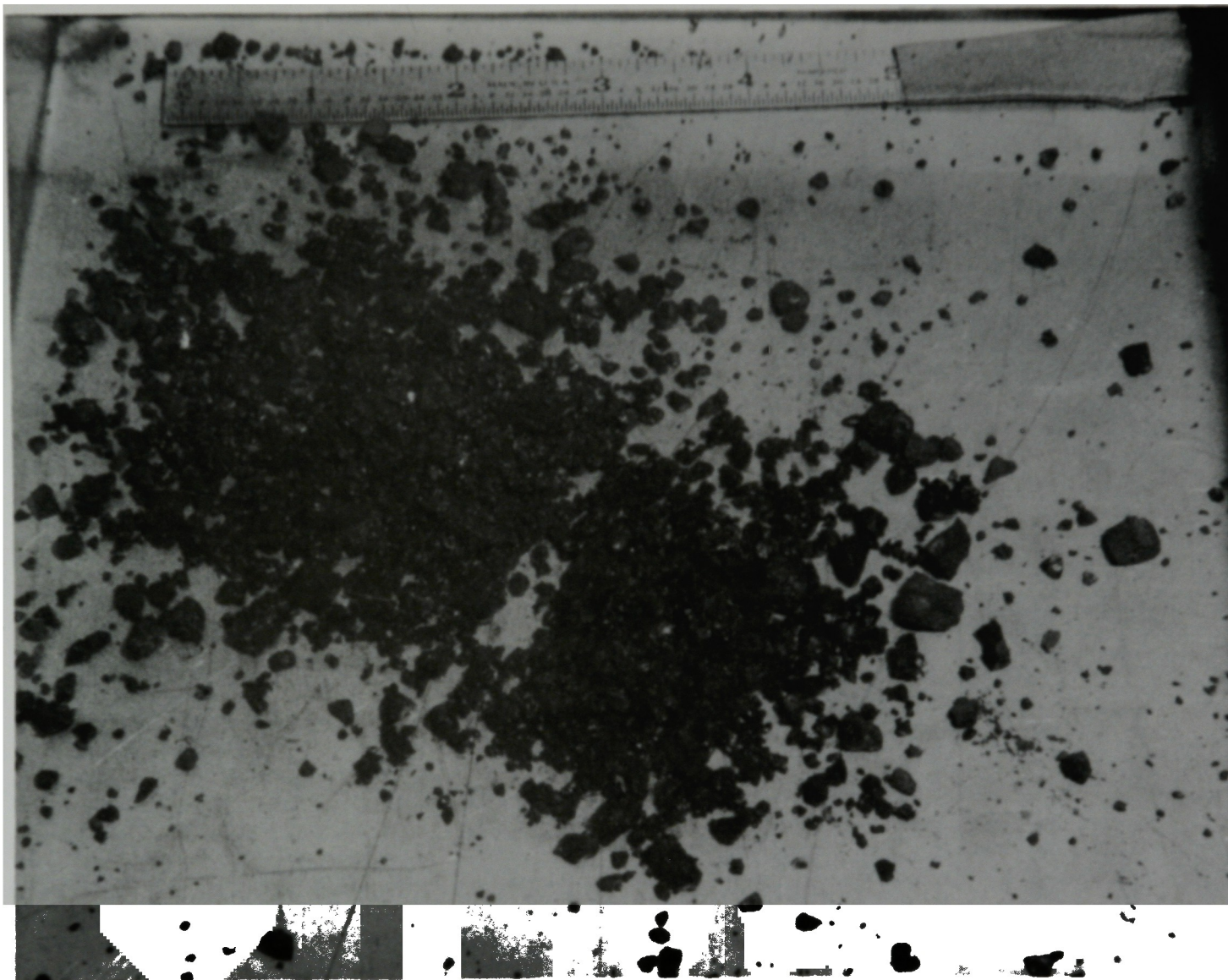


Figure 7 TMI-2 core debris sample #3 (22" deep-H8).

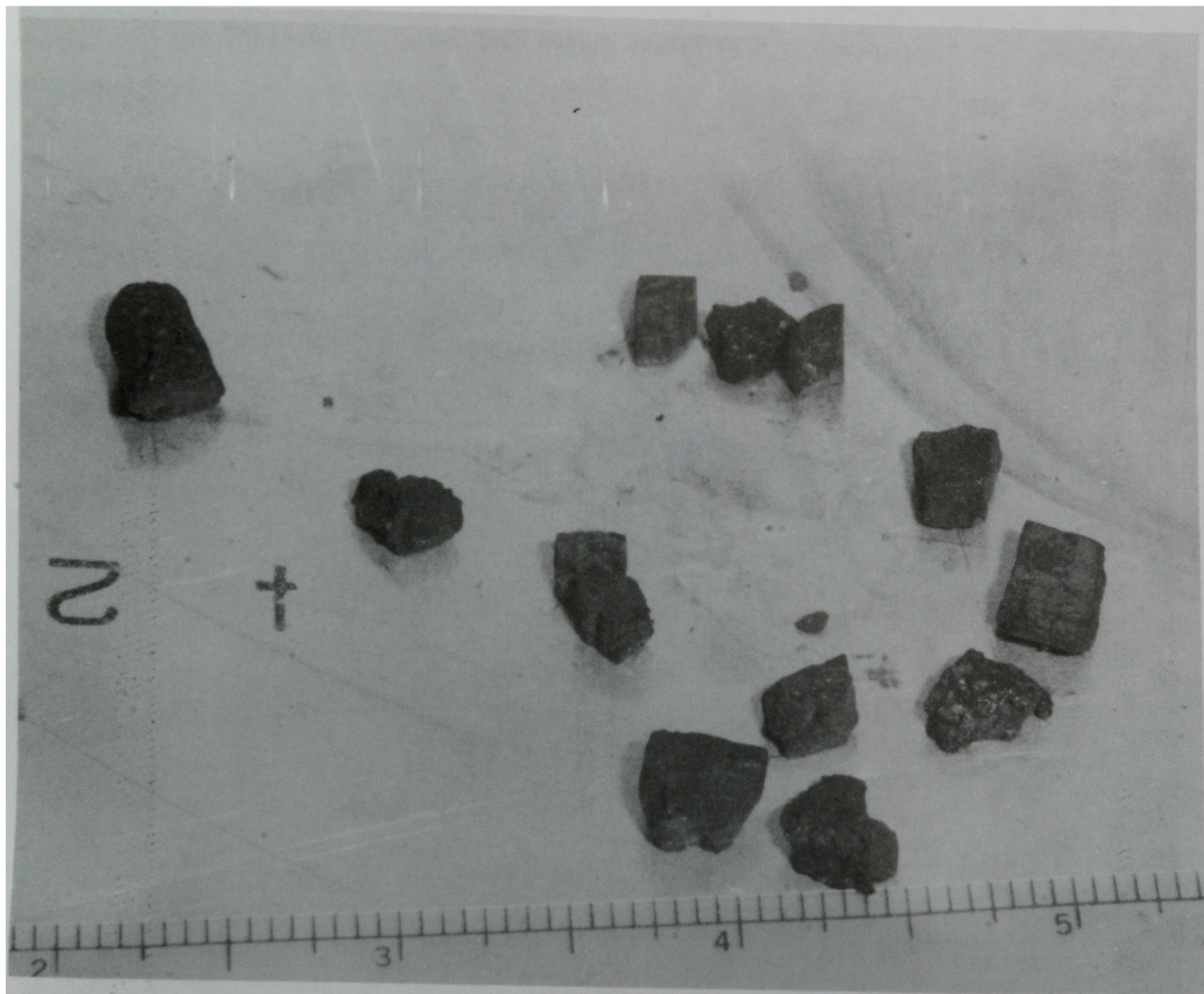


Figure 8. TMI-2 core debris sample #4 (surface-E9).



Figure 9 TMI-2 core debris sample #5 (3" deep-E9).

Sample 6, the E9 deep (22-in.) sample shown in Figure 10 is very similar in quantity and appearance to Sample 3, the H8 deep (22-in.) sample. In general, 80% or more of the debris examined (by weight) was greater than 1000 μm in size. This may indicate that the TMI-2 core materials were fractured into relatively large chunks when quenched during reflood. Smaller particles may be absent from the debris bed due to washout or settling. Evidence of washout is demonstrated through examination of the TMI-2 makeup system filters and the B8 and H8 leadscrews which revealed particles in the 0.5 to 6 μm range.

A number of particles in all of the samples appear to be partially covered with rust. There exists extensive coverage on some surfaces and a lack of coverage on others of the same particle. The origin of the rust is unknown.

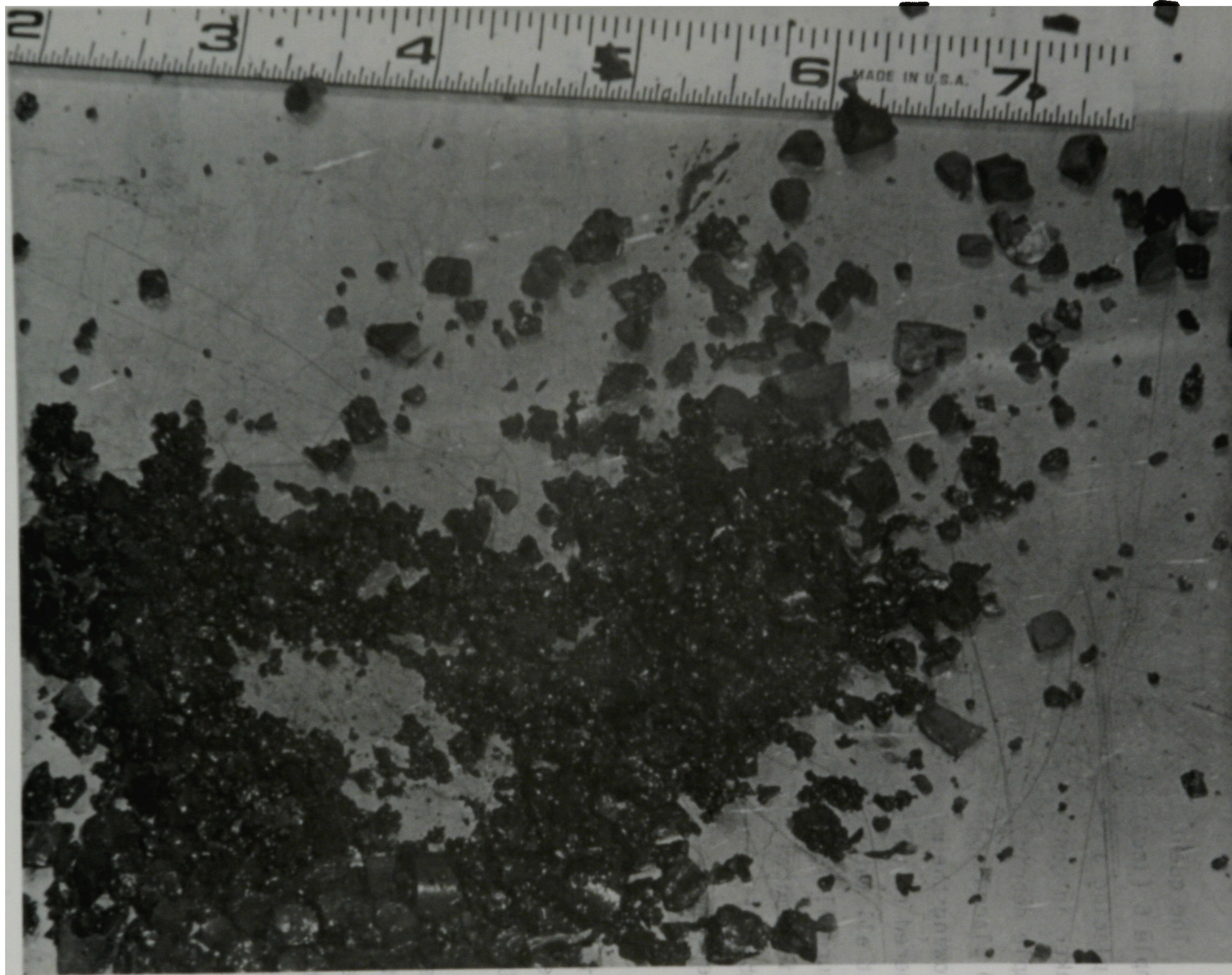


Figure 10. TMI-2 core debris sample #6 (22" deep-E9).

SECTION 3

FERROMAGNETIC ANALYSIS

The quantity of ferromagnetic material present in the sieve fractions for Sample 6 (location E9 at 22-inches) was measured. This analysis was performed by placing a small (2 lb. pull) magnet in a small beaker and then placing the beaker in contact with each sieve fraction. After stirring the beaker in the sample debris, the magnet, beaker and attached magnetic material were removed and placed in a sample container. The magnet was then removed from the beaker allowing the magnetic material to drop into the sample container. No material adhered to the glass after removal of the magnet; therefore, it was assumed that all material in the sample container had a ferromagnetic component. Figure 11 is a photograph of a magnetic particle which was removed for radiochemical analysis (Particle Number 6F). The rough exterior of particle Number 6F is characteristic of most particles observed in the ferromagnetic material.

Table 2 lists the quantity of ferromagnetic material in each of the individual size fractions. From these data the quantity of ferromagnetic material present is divided into two groups. The first group (297 to 1680 μm) contains 95% of the total weight and the second group (30 to 297 μm) contains 5%. Therefore, the fracturing forces which effected these materials produced no large chunks of material (i.e., >1680 μm) and very little material <297 μm indicating little powdering of the ferromagnetic core components occurred. Stainless steel was the principal core material containing iron. There was approximately 4.5×10^3 kg of stainless steel ($\sim 68\%$ Fe) present in the core area.² This compares with the total core material mass of 1.25×10^5 kg. The fraction of ferromagnetic material found in the sample ($\sim 0.9\%$) was magnetite, however the quantity of hematite (Fe_2O_3) formed from the stainless steel is not known as this compound is not magnetic.

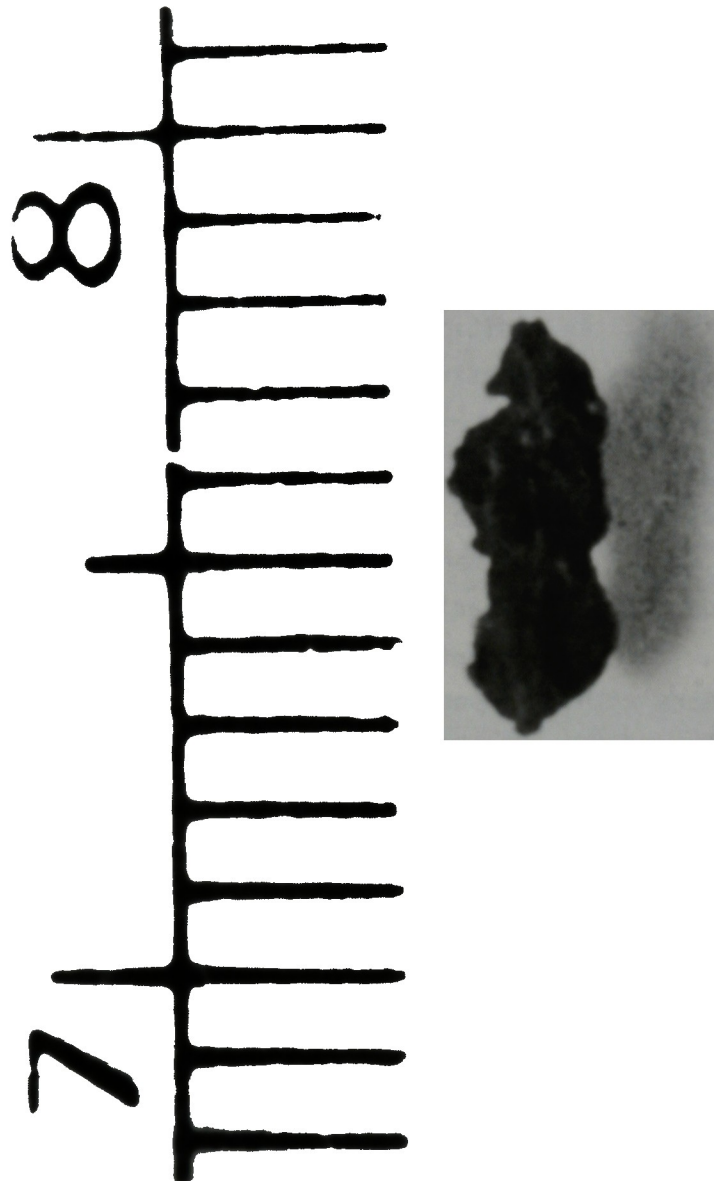


Figure 11. Ferromagnetic particle removed from the 100 μm size fraction of Sample 6 (particle number 6F).

SECTION 4

PYROPHORICITY TESTS

Pyrophoricity (i.e., pilot ignition) tests were performed on the core debris samples to evaluate potential safety hazards to core recovery operations. To demonstrate the test procedure, tests were performed on zirconium hydride powder using a small tesla coil (Fisher Scientific Model BD 10) rated at 50,000 volts. The ignition of this powder was recorded both by video tape and still photography before beginning the actual core debris pyrophoricity tests. An additional method used to produce higher temperatures (a propane torch) was also tested on the same type powder prior to beginning the actual measurements.

The samples chosen for the pyrophoricity testing were the sieve fractions from Samples 3 and 6. Tests were performed on all size fractions from 30 to 4000 μm . The quantity of material used for each test was in the range of 0.25-0.5 grams. The small quantity of material was selected to maintain personnel exposure within reasonable limits. Tests were performed under both "dry" and "wet" conditions. The dry condition was attained by warming the sample for approximately 30 minutes at 100°C before the sieving procedure. The wet condition was attained by adding two drops of water to the material.

Analyses were performed on individual wet and dry samples portions. No sample was used for both analyses. Figure 12 shows a portion of Sample 3 being exposed to the tesla coil to determine if pilot ignition occurred. No visible pilot ignition was observed for any sample.

Figure 13 shows a small piece of suspected zircaloy material being heated with a propane torch. Two pieces of core material were exposed to the propane torch and no pilot ignition was observed.

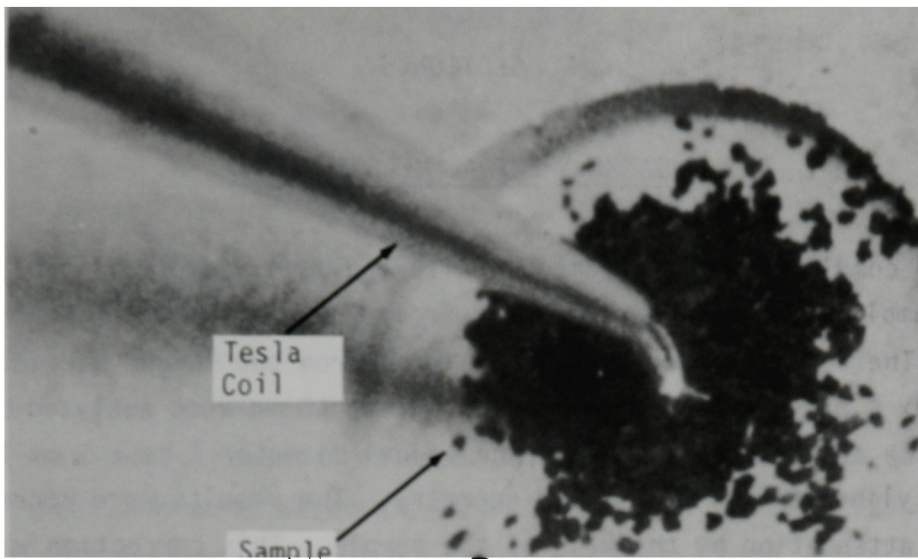


Figure 12. Tesla coil pilot ignition test on material removed from the 149-297 μm size fraction from sample no. 3 using a Fisher Scientific Co. Model BD10 tesla coil which is rated at 50,000 volts maximum.

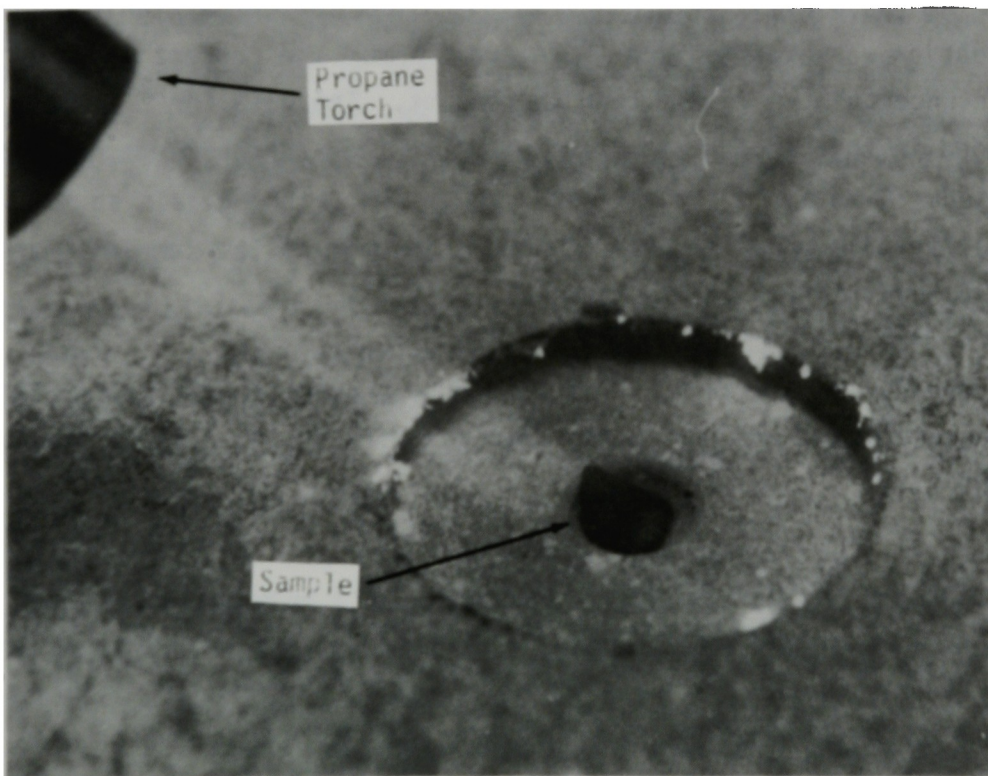


Figure 13. Propane torch pilot ignition test on core structure material.

SECTION 5

GAMMA SPECTRAL MEASUREMENTS

After completion of the particle size analysis, sample aliquots (i.e., typical sample fractions) were removed from each size group of the five bulk samples. The aliquots and fragmented pieces from the larger particles shown in Appendix A ranging in size between 5 mg and 50 mg were analyzed by gamma spectrometry after being placed in individual diameter 1 cm x 5 cm long sealed aluminum cylinders in a calibrated geometry. The results were corrected for gamma ray attenuation by the mass of the sample. This correction was performed by comparing high and low energy gamma rays from specific radionuclides. From the data, primarily ^{144}Ce , a correction factor was calculated which allowed the effects of the sample mass attenuation to be subtracted from the gross analysis results. The gamma ray energies used to calculate the radionuclide content of each sample were: ^{60}Co (1332 KeV), ^{106}Ru (622 KeV), $^{110\text{m}}\text{Ag}$ (885 KeV), ^{125}Sb (601 KeV), ^{134}Cs (605 KeV), ^{137}Cs (662 KeV), ^{144}Ce (2185 KeV), ^{154}Eu (1274 KeV), ^{155}Eu (80 KeV), and ^{241}Am (59.5 KeV). The only radionuclides for which significant mass attenuation was expected are ^{155}Eu and ^{241}Am . The correction for ^{155}Eu has an uncertainty of less than 20 percent. The data for ^{241}Am are not included in this report as effective correction factors have not yet been verified. Aluminum cylinders were chosen for this analysis so that the fissile/fertile material analysis could be made on the samples fractions without transferring sample material.

Appendix B tabulates and segregates the gamma spectrometry analytical data according to particle size. The analysis of the data is discussed in Section 7.

SECTION 6

FISSILE/FERTILE MATERIAL ANALYSIS

The fissile/fertile material analyses were performed at the Coupled Fast Reactivity Measurement Facility (CFRMF) by delayed neutron analysis.³ The total fissile/fertile content of the samples was measured by remotely exposing the individual 1 cm x 5 cm sample containers to a fast spectrum neutron flux which is located in the central region of the core in the facility. The canister was then removed after a one minute exposure and the delayed neutrons being emitted, measured after a specific time (~40 seconds) using a He₃ detector in a hydrogen moderator.

To obtain the distribution between fissile and fertile material content, the sample canister was then exposed to a thermal neutron flux spectrum which causes only the ²³⁵U plus ²³⁹Pu elements within the sample to fission and emit delayed neutrons. It was assumed that the quantity of ²³⁹Pu is insignificant. Based on theoretical predictions discussed in Section 7, the ²³⁹Pu content is less than 0.2 weight percent. However, a five to eight percent bias may result. The sample was then analyzed using the He₃ detection system. The fissile and fertile material contents of the sample were determined by subtracting the measured fissile material content from the total fissile/fertile material content using appropriate calibrations.

In preparation for the core debris fissile/fertile material analysis, calibration standards were prepared from highly enriched uranium, depleted uranium, and light water reactor grade enriched uranium (~4.3 wt%). In addition, calibration standards were prepared at different weights (between 5 mg and 1 gram) to permit correction of the data for neutron attenuation caused by the mass of the sample.

The available measured fissile/fertile material data at the time of the preparation of this report are listed in Appendix C. These data are discussed in Section 7.

SECTION 7

DISCUSSION OF RESULTS

The data of principal interest presented in this report are the particle size analysis of the core debris samples, the radionuclide content of the individual size fractions, the fissile/fertile content of specific samples and the comparison of these data with the core inventory as calculated by ORIGEN-2.⁴

From the particle size data, some preliminary observations concerning the characteristics of the material may be made. They are:

1. At the H8 core location, the surface sample (No. 1) is finer than the deep subsurface sample (No. 3), as would be expected if the granular core debris had been suspended by pump flow and then gravity settled.
2. There is no significant particle size difference among the H8 and E9 deep samples (No. 3 and 6), thus they may be used with some confidence as typical of the subsurface bulk debris bed.
3. Only about 0.3 weight percent of the debris bed is smaller than 100 μm in size.
4. The E9 surface sample (No. 4) and the E9 near surface sample (No. 5) are similar in that they contain only large particles greater than 1000 μm .

The tabular particle size data are presented in Table 2. These data have been plotted two ways to aid interpretation. Figure 14 is a frequency distribution histogram showing the fraction of particles within a size range relative to the average particle size of the range. Figure 15 is a log-log plot (Rosin-Rammler plot) showing cumulative percent under a certain particle size. The latter plot may be used for interpolation and extrapolation.⁵

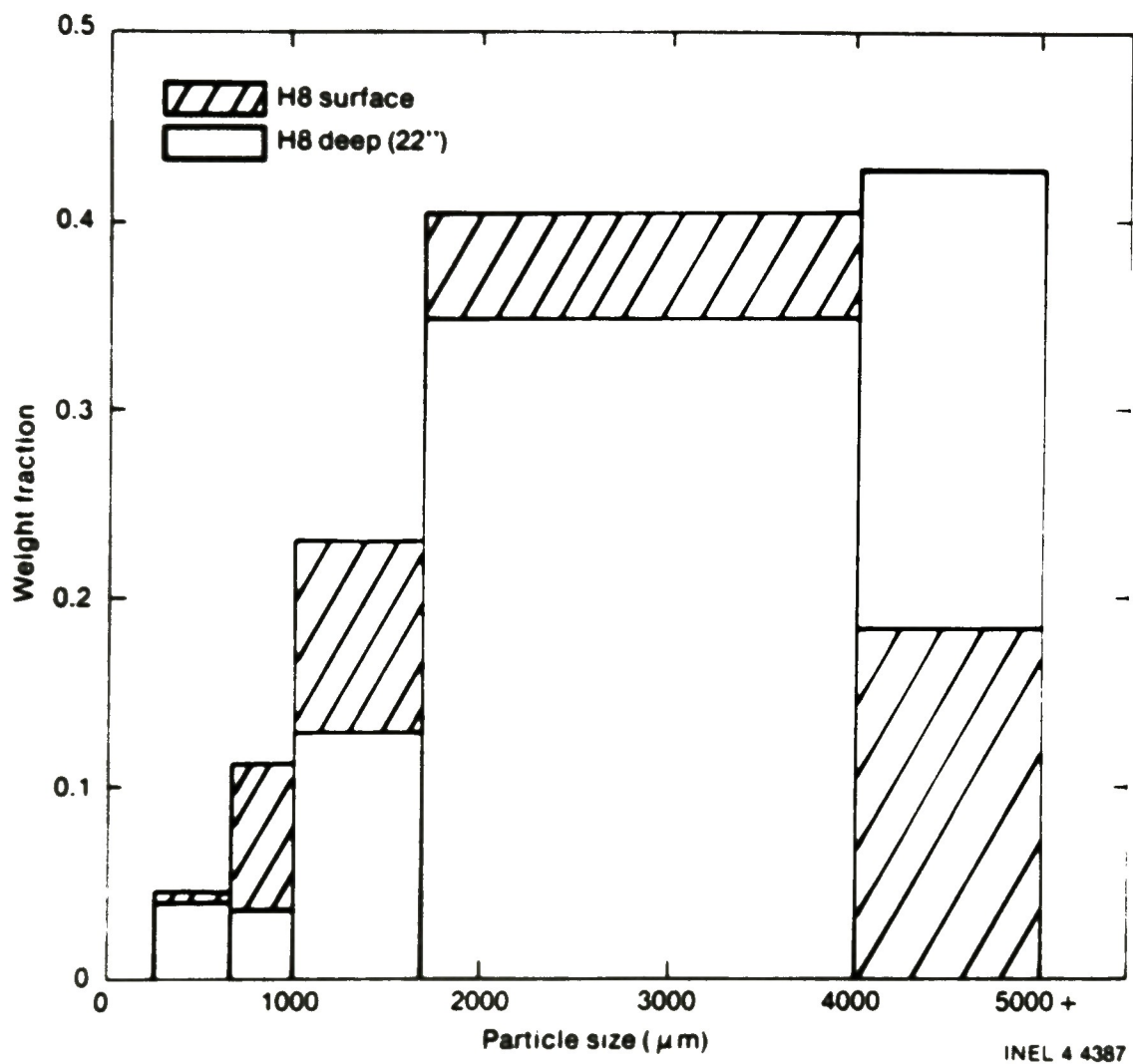


Figure 14. TH1-2 Core Debris Samples Frequency Distribution Histogram

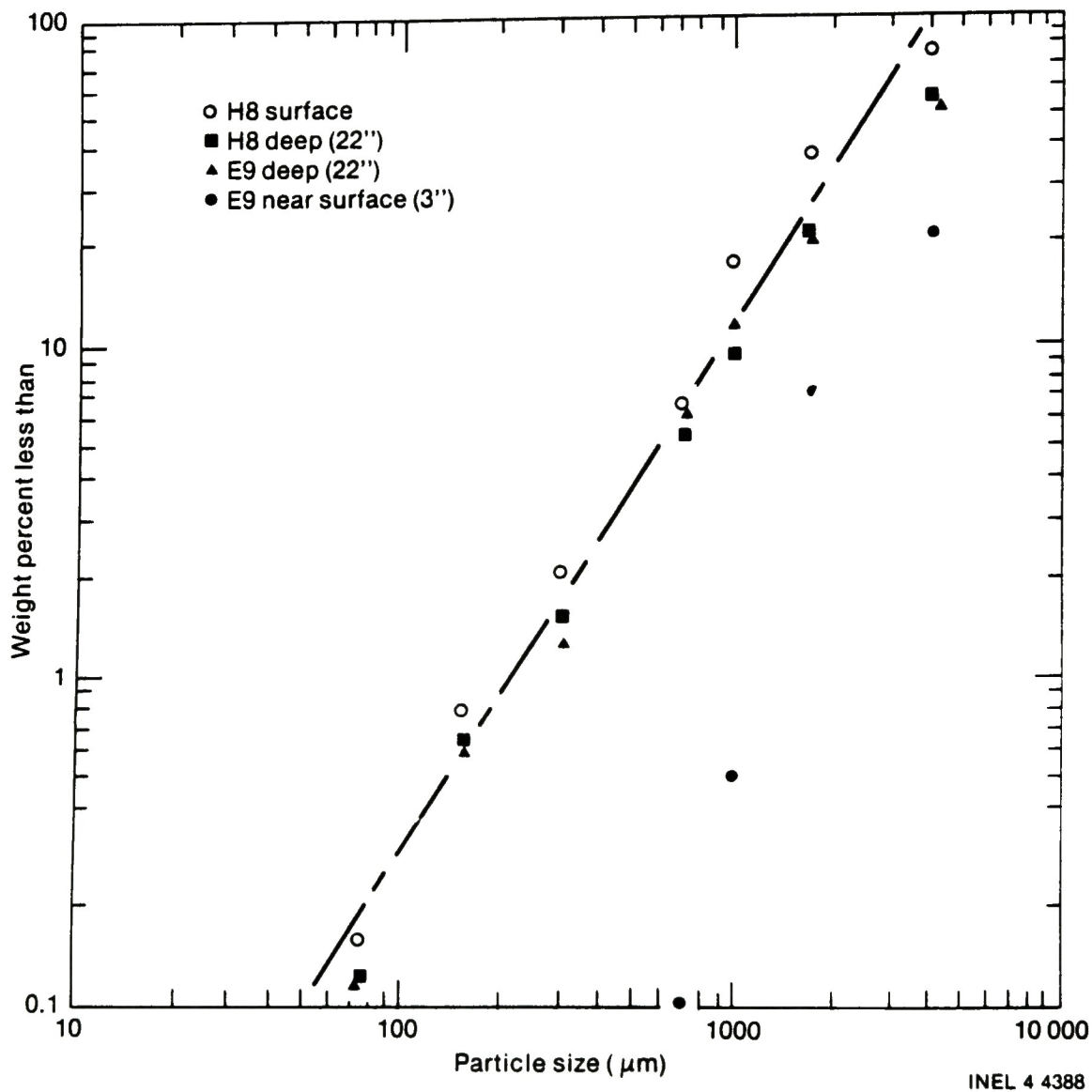


Figure 15. TMI-2 Core Debris Samples Particle Size Distribution

The gamma spectrometry analysis of individual particles and sample aliquots may be used to provide estimates of the fission product inventory remaining in the debris bed. In Tables 3 through 7 the gamma spectrometry results for all sample fractions are summarized according to particle size. For particle size fractions where more than one sample was removed (i.e., 1000 -4000 μm) the data are presented as an average radionuclide concentration ($\mu\text{Ci/gram}$) with the range of the concentrations. Fission product concentrations for sample aliquots <1000 μm are relatively consistent for all samples indicating that the material in these size fractions is relatively homogeneous. For the large size fractions (i.e., ≥ 1000 μm) there appears to be a much wider range of radionuclide contents among individual particles. In some instances, these results are due to the obvious presence of structural materials (see Appendix A). These materials have been included in the measurement data to provide information on the radionuclide content of materials other than fuel present in the core. Table 8 lists the identification and the data from pieces of material which were determined by fissile content to be nonfuel components. These data indicate significantly lower levels of fission product content than other particles which are composed at least partially of fuel material.

The core debris sample fission product data were normalized using the total sieve fraction weights and total sample weights for each of the five bulk samples analyzed. A weighted average value for each gamma emitting radio nuclide detected in the core debris was calculated and divided by the ORIGEN-2 fission product inventory per gram of UO_2 to determine the percent of each of the radio nuclides remaining in the fuel. The results of this comparison are given in Table 9. It should be noted that the sample aliquots removed were not completely representative of the bulk sample. Therefore, these data may not be representative of the average core fission product contents. However, these data indicate that the majority of the Ruthenium, Cerium, and Europium remained with the fuel, while the majority of the Cobalt, Antimony and Cesium were released.

TABLE 3. RADIONUCLIDE DISTRIBUTION FOR SAMPLE 1 LOCATION H8 AT SURFACE
($\mu\text{Ci/g}$)

Radionuclide	4000 μm ^a		1680 μm		1000 μm	
	Average	Range	Average	Range	Average	Range
⁶⁰ Co	1.8(+1)	8.7(0) - 2.6(+1)	3.2(+1)	8.1(0) - 7.8(+1)	8.9(0)	1.9(0) - 1.7(+1)
¹⁰⁶ Ru	5.7(+2)	6.7(+1) - 1.6(+3)	7.5(+1)	4.4(+1) - 1.1(+2)	4.2(+1)	8.9(0) - 7.0(+1)
^{110m} Ag	ND	--	ND	--	7.4(0) ^b	--
¹²⁵ Sb	6.3(+1)	1.4(+1) - 1.2(+2)	1.8(+1)	1.5(+1) - 1.8(+1)	7.2(+2)	1.1(0) - 2.2(+3)
¹³⁴ Cs	2.6(+1)	3.7(0) - 7.6(+1)	7.3(+1)	6.3(0) - 1.1(2)	2.4(+1)	3.1(0) - 6.3(+1)
¹³⁷ Cs	5.4(2)	6.7(+1) - 1.3(+3)	1.3(+3)	1.1(+2) - 2.0(+3)	4.3(+2)	5.5(+1) - 1.1(+3)
¹⁴⁴ Ce	2.1(+3)	1.7(+2) - 3.8(+3)	2.5(+3)	2.2(+3) - 3.1(+3)	9.4(+2)	0 - 2.5(+3)
¹⁵⁴ Eu	3.3(+1)	8.0(-1) - 5.9(+1)	4.1(+1)	3.0(+1) - 5.7(+1)	1.8(+1)	9.8(-1) - 4.8(+1)
¹⁵⁵ Eu	6.8(+1)	1.2(+1) - 1.6(+2)	1.0(+2)	9.5(+1) - 1.2(+2)	3.7(+1)	0 - 1.0(+2)

Radionuclide	707 μm	297 μm	149 μm	74 μm	30 μm
⁶⁰ Co	2.3(+2)	4.9(+1)	8.1(+1)	1.1(+2)	6.6(+1)
¹⁰⁶ Ru	5.6(+3)	1.5(+2)	1.5(+2)	2.7(+2)	1.1(+2)
^{110m} Ag	3.7(0)	1.1(0)	1.3(0)	1.8(0)	1.0(0)
¹²⁵ Sb	1.9(+3)	2.2(+2)	3.4(+2)	4.8(+2)	2.0(+2)
¹³⁴ Cs	5.6(+1)	2.7(+1)	4.4(+1)	5.1(+1)	3.2(+1)
¹³⁷ Cs	1.1(+3)	6.5(+2)	9.1(+2)	1.0(+3)	6.1(+2)
¹⁴⁴ Ce	2.3(+3)	2.4(+3)	1.6(+3)	1.7(+3)	7.1(+2)
¹⁵⁴ Eu	4.5(+1)	4.3(+1)	2.4(+1)	3.4(+1)	1.1(+1)
¹⁵⁵ Eu	1.1(+2)	9.7(+1)	6.7(+1)	6.9(+1)	2.6(+1)

a. Two pieces of zircaloy included in the average.

b. Only one particle showed ^{110m}Ag.

TABLE 4. RADIONUCLIDE DISTRIBUTIONS FOR SAMPLE 3 - LOCATION H8 AT 22-INCHES
($\mu\text{Ci/g}$)

Radionuclide	4000 μm		1680 μm		1000 μm	
	Average	Range	Average	Range	Average	Range
^{60}Co	4.8(+1)	2.0(0) - 1.3(+1)	6.1(0)	3.3(0) - 8.6(0)	3.1(+1)	6.4(0) - 7.1(+1)
^{106}Ru	7.8(+2)	3.8(0) - 1.46(+3)	9.4(+2)	5.1(+1) - 2.6(+3)	1.4(+2)	4.2(+1) - 2.4(+2)
^{125}Sb	6.6(+1)	6.9(0) - 1.3(+2)	4.0(+1)	6.1(0) - 9.6(+1)	2.3(+1)	9.0(0) - 4.4(+1)
^{134}Cs	2.3(+1)	5.0(-1) - 5.7(+1)	4.9(+1)	1.1(+1) - 9.2(+1)	2.1(+1)	4.6(0) - 4.8(+1)
^{137}Cs	3.8(+2)	4.6(+1) - 9.5(+2)	9.1(+2)	3.9(+2) - 1.6(+3)	4.0(+2)	7.3(+1) - 9.3(+2)
^{144}Ce	2.2(+3)	5.8(+1) - 3.9(+3)	3.2(+3)	5.7(+2) - 7.0(+3)	2.0(+3)	9.3(+2) - 2.6(+3)
^{154}Eu	3.7(+1)	7.1(-1) - 6.8(+1)	5.3(+1)	4.3(0) - 1.2(+2)	3.5(+1)	1.6(+1) - 4.7(+1)
^{155}Eu	8.8(+1)	2.9(0) - 1.6(+2)	1.4(+2)	2.8(+1) - 3.1(+2)	8.7(+1)	4.0(+1) - 1.1(+2)

Radionuclide	707 μm	297 μm	149 μm	74 μm	30 μm	20 μm
^{60}Co	9.2(+1)	2.2(+1)	6.6(+1)	8.6(+1)	1.4(+2)	1.0(+2)
^{106}Ru	2.1(+2)	1.2(+2)	3.1(+2)	2.3(+2)	6.5(+2)	2.5(+2)
^{125}Sb	3.4(+1)	1.9(+1)	1.1(+2)	1.9(+2)	2.2(+2)	1.8(+2)
^{134}Cs	3.1(+1)	3.5(+1)	4.3(+1)	5.2(+1)	5.2(+1)	2.9(+1)
^{137}Cs	5.4(+2)	8.4(+2)	9.0(+2)	9.0(+2)	8.9(+2)	6.6(+2)
^{144}Ce	2.4(+3)	1.8(+3)	1.6(+3)	1.5(+3)	1.2(+3)	7.5(+2)
^{154}Eu	4.5(+1)	3.2(+1)	2.6(+1)	2.3(+1)	1.7(+1)	1.0(+1)
^{155}Eu	1.0(+2)	3.8(+1)	8.2(+3)	6.3(+1)	4.9(+1)	3.1(+1)

TABLE 5. RADIONUCLIDE DISTRIBUTION FOR SAMPLE 4 - LOCATION E9 AT SURFACE
($\mu\text{Ci/g}$)

	Large Particles ($>1000\mu\text{m}$)	Range
^{60}Co	8.6(+1)	2.75 - 2.5(+2)
^{106}Ru	1.5(+3)	2.4(+2) - 3.3(+3)
$^{110\text{m}}\text{Ag}$	ND	
^{125}Sb	9.9(+1)	6.8(0) - 2.0(+2)
^{134}Cs	6.5(+1)	1.7(0) - 1.8(+2)
^{137}Cs	1.3(+3)	3.6(0) - 3.9(+3)
^{144}Ce	4.3(+3)	7.8(+2) - 8.6(+3)
^{154}Eu	6.5(+1)	9.3 - 150
^{155}Eu	1.4(+2)	30 - 315
^{241}Am		

TABLE 6. RADIONUCLIDE DISTRIBUTION FOR SAMPLES 5 - E9 AT 3-INCHES
($\mu\text{Ci/g}$)

Radionuclide	4000 μm		1680 μm		1000 μm		< 1000 μm
	Average	Range	Average	Range	Average	Range	
^{60}Co	4.9(+1)	2.8(0) - 1.2(+2)	1.6(+1)	2.1(0) - 3.1(+1)	3.4(+1)	6.6(-1) - 1.0(+2)	5.5(+1)
^{106}Ru	1.2(+3)	6.4(+2) - 2.2(+3)	6.2(+2)	5.6(+2) - 6.9(+2)	1.8(+3)	1.3(+3) - 2.8(+3)	6.5(+2)
^{125}Sb	1.4(+2)	2.5(+1) - 3.0(+2)	3.8(+1)	1.3(+1) - 6.3(+1)	2.8(+2)	1.0(+2) - 6.1(+2)	8.0(+1)
^{134}Cs	1.5(+1)	6.8(0) - 2.3(+1)	1.6(+1)	2.9(0) - 2.9(+1)	1.4(+2)	3.2(+1) - 3.6(+2)	9.9(+1)
^{137}Cs	3.4(+2)	1.5(+2) - 3.9(+2)	4.1(+2)	3.8(+1) - 7.9(+2)	2.5(+3)	5.1(+2) - 6.5(+3)	1.7(+3)
^{144}Ce	3.5(+3)	1.8(+3) - 6.6(+3)	2.1(+3)	1.9(+3) - 2.4(+3)	6.0(+3)	3.6(+3) - 1.1(+4)	2.2(+3)
^{154}Eu	5.5(+1)	1.6(+1) - 1.2(+2)	2.3(+1)	1.7(+1) - 2.9(+1)	1.1(+2)	6.2(+1) - 2.2(+2)	3.5(+1)
^{155}Eu	1.4(+2)	8.1(+1) - 2.7(+2)	8.8(+1)	7.4(+1) - 1.0(+2)	2.7(+2)	1.4(+2) - 5.1(+2)	1.1(+2)

TABLE 7. RADIONUCLIDE DISTRIBUTION FOR SAMPLE 6 - LOCATION E9 AT 22-INCHES
($\mu\text{Ci/g}$)

Radionuclide	4000 μm ^a		1680 μm		1000 μm	
	Average	Range	Average	Range	Average	Range
⁶⁰ Co	2.5(0)	0 - 6.1(0)	1.9(0) ^b	0 - 4.9(0)	7.1(0)	6.9(0) - 7.3(0)
¹⁰⁶ Ru	4.2(+2)	1.3(0) - 1.1(+3)	6.1(+2)	7.0(0) - 1.0(+3)	4.4(+2)	2.9(+2) - 5.8(+2)
¹²⁵ Sb	1.1(+2)	2.4(+1) - 3.0(+2)	6.5(+1)	1.5(+1) - 1.0(+2)	5.0(+1)	1.8(+1) - 8.2(+1)
¹³⁴ Cs	2.2(+1)	2.2(0) - 5.5(+1)	8.3(+1)	3.2(+1) - 1.7(+2)	8.8(+1)	5.0(-1) - 1.7(+2)
¹³⁷ Cs	5.7(2)	4.4(+1) - 1.3(+3)	1.8(+3)	6.2(+2) - 3.8(+3)	2.0(+3)	1.1(+1) - 4.1(+3)
¹⁴⁴ Ce	1.3(+3)	1.9(0) - 3.6(+3)	1.8(+3)	1.8(+1) - 3.1(+3)	2.0(+3)	6.9(+2) - 3.5(+3)
¹⁵⁴ Eu	1.3(+1) ^b	0 - 3.2(+1)	2.3(+1) ^b	0 - 4.3(+1)	3.2(+1)	1.3(+1) - 5.1(+1)
¹⁵⁵ Eu	5.5(+1) ^b	0 - 1.5(+2)	8.7(+1) ^b	1.24(+2) - 1.37(+2)	3.3(+1)	3.2(+1) - 3.5(+1)

Radionuclide	707 μm	297 μm	149 μm	74 μm	30 μm
⁶⁰ Co	1.4(+2)	5.2(+1)	9.2(+1)	1.1(+2)	1.2(+2)
¹⁰⁶ Ru	4.2(+2)	2.2(+2)	2.9(+2)	3.7(+2)	5.2(+2)
¹²⁵ Sb	8.8(+1)	9.8(+1)	1.5(+2)	1.9(+2)	1.7(+2)
¹³⁴ Cs	5.7(+1)	5.8(+1)	5.4(+1)	4.8(+1)	5.0(+1)
¹³⁷ Cs	1.2(+3)	1.1(+3)	1.1(+3)	9.6(+2)	9.5(+2)
¹⁴⁴ Ce	2.3(+3)	2.1(+3)	1.4(+3)	1.3(+3)	1.1(+3)
¹⁵⁴ Eu	3.6(+1)	3.6(+1)	2.2(+1)	2.1(+1)	1.8(+1)
¹⁵⁵ Eu	1.1(+2)	9.2(+1)	6.7(+1)	7.8(+1)	4.5(+1)

a. Average includes two zircaloy pieces (known).

b. No measurable data included in average.

c. Excludes ferromagnetic particles - high ⁶⁰Co.

TABLE 8. NON-FUEL CORE MATERIAL RADIONUCLIDE CONTENT
($\mu\text{Ci/g}$)

Radionuclide	Sample 1	Sample 3	Sample 6	Sample 6
	Particle 1J	Particle 3B	Particle 6E	Particle 6F
^{60}Co	1.9(0)	5.9(+1)	1.2(0)	4.9(0)
^{106}Ru	8.9(0)	3.8(0)	1.3(0)	7.0(0)
^{125}Sb	1.1(0)	6.9(0)	2.4(+1)	1.5(+1)
^{134}Cs	3.1(0)	5.0(-1)	2.2(0)	3.2(+1)
^{137}Cs	5.5(+1)	1.2(+1)	4.4(+1)	6.2(+2) ^a
^{144}Ce	3.2(+2)	5.8(+1)	1.9(0)	1.8(+1)
^{154}Eu	5.4(0)	7.2(-1)	ND	ND
^{155}Eu	1.2(+1)	2.9(0)	ND	ND
^{241}Am	ND	3.6(-1)	ND	ND
Fissile Material (mg)	<0.02	<1.6(-2)	<0.02	<0.02

a. This data point is higher than other ^{137}Cs concentrations. The reason is not known.

TABLE 9. PERCENT OF FISSION PRODUCTS RETAINED IN FUEL PER GRAM UO_2

Nuclide	Debris Concentration ^a ($\mu Ci/gm$)	Concentration 5/1/84 ^b ($\mu Ci/gm$ UO_2)	Percent Retained ^c In Fuel per Gram of UO_2
Co-60	31	740	4.0 ^d
Ru-106	760	1060	72
Sb-125	130	470	28
Cs-134	40	330	12
Cs-137	810	8130	10
Ce-144	2410	2650	91
Eu-154	38	60	63
Eu-155	98	175	56

a. These radionuclide concentrations are the weighed average of all five samples using individual sample fraction weights and total sample weights.

b. Concentrations calculated by ORIGEN-2.

c. These values represent data compared to an ORIGEN-2 calculation is a core wide average of fission products. Local core averages may vary.

d. Values rounded to nearest whole percent.

Table 10 lists the percentage of each sample containing fissile/fertile material. These data are calculated by dividing the weight of UO_2 in each sample as listed in Appendix B by the weight of the sample fraction analyzed. The fissile material measurements include ^{239}Pu which is the equivalent of 5 to 8 percent of the actual ^{235}U content according to ORIGEN-2 calculations.⁴

Observations that can be made concerning these data are as follows: (a) less than 15 percent of the particles analyzed contain >90% uranium dioxide, indicating that most particles analyzed are agglomerates of fuel and nonfuel materials, (b) there is a tendency among particles <707 μm towards decreasing percent of fuel content with decreasing particle size, and (c) the smaller particle size ranges (<707 μm) display a relatively consistent fuel content when compared to the larger particles indicating that they may have all been formed by a similar mechanism.

Table 11 lists the average fissile/fertile enrichments for the samples analyzed at the date of the report. For comparison purposes, the actual fuel enrichments at each location are listed in the footnote. These average data, which represent preliminary results, have a range of approximately 20%. There is a general trend in the data which indicates a higher enrichment (2.8%) at the E9 location. These data indicate fuel mixing at E9 between the 2.96% enriched fuel from the core periphery and 1.98% from the E9 fuel assembly. The data at the H8 location suggests a mixing of the 1.98 and 2.64% enriched fuels to provide the measured average enrichment of 2.4%.

Table 12 lists the fission product inventory per gram of UO_2 calculated by the ORIGEN-2 code.

Table 13 lists the ratios of the measured fission product content to the ORIGEN-2 predicted fission product content/gram ^{235}U for Sample 1. These data were calculated using the following equation:

TABLE 10. WEIGHT FRACTION OF FISSILE/FERTILE MATERIAL ^a

Size Fraction	Sample 1 H8-Surface	Sample 3 H8-22-inch	Sample 4 E9-Surface	Sample 5 E9-2-inch	Sample 6 E9-22-inch
>4000 μm Particle 1	0.11	0.44	NA	NA	NA
>4000 μm Particle 2	0.11	0	0.22	100	NA
>4000 μm Particle 3	0.66	NA	NA	NA	0.04
>4000 μm Particle 4	0.98	0.94	NA	NA	0.88
>4000 μm Particle 5	0.22	0.94	NA	0.43	0
1680-4000 μm Particle 1	0.79	NA		0.66	0
1680-4000 μm Particle 2	0.56	NA		NA	0.90
1680-4000 μm Particle 3	0.53	0.62		NA	0.10
1000-1680 μm Particle 1	0	NA		NA	0.11
1000-1680 μm Particle 2	0.8	0.20		0.85	0.15
1000-1680 μm Particle 3	0.45	0.47		0.82	0.09
<16 mesh	--	--		0.06	0.06
707-1000 μm aliquot	0.73	NA			0.54
297-707 μm aliquot	0.57	NA			0.42
149-297 μm aliquot	0.45	NA			0.43
74-149 μm aliquot	0.52	0.32			0.29
30-74 μm aliquot	0.24	0.43			
20-30 μm aliquot					

a. Calculated assuming all fissile/fertile material was in the form of UO_2 . Also, these data assume that the ^{239}Pu component of the fuel is a negligible component of the total fissile material control (i.e., <0.2 wt% from ORIGEN-2 calculations).

TABLE 11. AVERAGE MEASURED URANIUM ENRICHMENT^a

<u>Sample Number</u>	<u>Average Enrichment</u>	<u>Number of Analyses</u>
1 - H8 surface	2.4	15
3 - H8 22-inches	2.3	8
4 - E9 surface	3.0	2
5 - E9 3-inches	2.8	7
6 - E9 22-inches	2.8	12

a. There are three fuel assembly enrichments in the TMI-2 core. The peripheral fuel assemblies are 2.96% enriched. The inner fuel assemblies alternate between 1.98 and 2.64% enriched. The H8 and E9 fuel assemblies were originally enriched to 2.64 and 1.98%, respectively.

TABLE 12. TMI-2 CORE FISSION PRODUCT INVENTORY^a

<u>Radionuclide</u>	<u>Total Inventory (curies)</u>	<u>Fission Product Content Per Gram UO₂^b (curies)</u>
⁶⁰ Co ^c	6.97(+4)	7.49(-4)
¹⁰⁶ Ru	1.02(+5)	1.10(-3)
^{110m} Ag ^c	1.25(+5)	1.77(-4)
¹²⁵ Sb	3.48(+4)	3.75(-4)
¹³⁴ Cs	3.18(+4)	3.42(-4)
¹³⁷ Cs	7.26(+5)	8.16(-3)
¹⁴⁴ Ce	2.57(+5)	2.76(-3)
¹⁵⁴ Eu ^c	5.47(+3)	5.88(-5)
¹⁵⁵ Eu ^c	1.57(+4)	1.69(-4)

a. Data obtained from ORIGEN 2 code analysis of core inventory assuming 2.57% enrichment and 3250 MWd/MTu.

b. ²³⁵U content is 2.27(-2) grams/gram UO₂.

c. Activation and/or fission product.

TABLE 13. MEASURED TO PREDICTED FISSION PRODUCT/URANIUM CORE INVENTORY RATIOS
(Sample 1 - H8 surface)

Radionuclide	>4000 μm	>4000 μm	>4000 μm	>4000 μm	>4000 μm	1680-4000 μm
	Particle 1A	Particle 1B	Particle 1C	Particle 1D	Particle 1E	Particle 1F
^{60}Co	2.8(-1)	2.9(-2)	1.9(-2)	3.0(-2)	8.6(-2)	1.5(-2)
^{106}Ru	5.2(-1)	1.7(0)	9.9(-2)	9.3(-1)	1.2(0)	5.2(-2)
$^{110\text{m}}\text{Ag}$	--	--	--	--	--	--
^{125}Sb	5.5(0)	5.3(-1)	1.1(-1)	8.7(-2)	2.5(0)	1.6(-1)
^{134}Cs	1.3(-1)	1.3(-2)	3.6(-1)	3.6(-2)	4.9(-1)	4.6(-1)
^{137}Cs	2.8(-2)	9.8(-3)	2.6(-1)	2.8(-2)	4.9(-1)	3.5(-1)
^{144}Ce	5.1(-1)	1.7(0)	1.7(0)	1.3(0)	1.3(0)	1.6(0)
^{154}Eu	1.1(-1)	1.2(0)	1.3(0)	8.9(-1)	8.5(-1)	1.4(0)
^{155}Eu	4.6(-1)	1.1(0)	1.1(-1)	8.4(-1)	9.8(-1)	1.0(0)
Fissile Material Grams fissile/ Gram Sample	2.8(-3)	1.9(-2)	1.4(-2)	2.0(-2)	4.8(-3)	1.6(-2)

TABLE 13. (continued)

Radionuclide	1680-4000 μm Particle 1G	1680-4000 μm Particle 1H	1000-1680 μm Particle 1I	1000-1680 μm Particle 1J	1000-1680 μm Particle 1K
^{60}Co	2.6(-2)	1.8(-1)	ND	3.7(-2)	1.9(-2)
^{106}Ru	1.4(-1)	1.7(-1)	ND	1.1(-1)	7.3(-2)
$^{110\text{m}}\text{Ag}$	--	--	--	--	--
^{125}Sb	2.1(-1)	1.5(-1)	ND	8.8(-2)	4.8(-2)
^{134}Cs	6.0(-1)	3.2(-2)	ND	1.3(-1)	2.6(-2)
^{137}Cs	4.3(-1)	2.5(-2)	ND	9.6(-2)	1.9(-2)
^{144}Ce	1.7(0)	1.4(0)	ND	1.6(0)	1.6(0)
^{154}Eu	1.2(0)	9.0(-1)	ND	1.3(0)	1.4(0)
^{155}Eu	1.2(0)	9.8(-1)	ND	1.0(0)	1.0(0)
Fissile Material Grams UO_2 / Gram Sample	1.1(-2)	1.3(-2)	0	1.6(-3)	1.3(-2)

TABLE 13. (continued)

Radionuclide	707-1000 μm Aliquot	297-707 μm Aliquot	149-297 μm Aliquot	74-149 μm Aliquot	30-74 μm Aliquot
^{60}Co	4.6(-1)	1.1(-1)	2.7(-1)	3.3(-1)	5.4(-2)
^{106}Ru	7.7(0)	2.2(-1)	3.4(-1)	1.1(0)	6.1(-2)
$^{110\text{m}}\text{Ag}$	3.2(+2)	1.0(-2)	1.8(-2)	2.3(-2)	3.5(-3)
^{125}Sb	1.6(+1)	2.0(0)	4.8(0)	6.1(0)	1.7(0)
^{134}Cs	2.5(-1)	1.3(-1)	3.2(-1)	3.4(-1)	5.8(-2)
^{137}Cs	2.0(-1)	1.3(-1)	2.8(-1)	2.8(-1)	4.6(-2)
^{144}Ce	1.3(0)	1.4(0)	1.4(0)	1.4(0)	1.6(-1)
^{154}Eu	1.2(0)	1.2(0)	1.0(0)	1.3(0)	1.2(-1)
^{155}Eu	9.9(-1)	9.3(-1)	9.9(-1)	9.3(-1)	9.3(-2)
Fissile Material Grams Fissile/ Gram Sample	1.5(-2)	1.4(-2)	9.1(-3)	1.0(-2)	3.7(-2)

$$R = \frac{C_F}{C_u \times C_p}$$

R = Ratio of measured to ORIGEN predicted fission product concentrations per gram UO_2 .

C_F = Measured fission product content - uCi/gram (Appendix B).

C_u = Measured fissile/material content - ^{235}U content in grams (Appendix C).

C_p = Predicted ORIGEN-2 fission product concentration (uCi/gram ^{235}U).

These data indicate that there are radionuclides that remain generally associated with the fuel. These radionuclides are ^{144}Ce , ^{154}Eu and ^{155}Eu . The ORIGEN-2 code analysis was done for the core average enrichment, which may account for some ratios being >1. Actual measured enrichment for the listed samples may vary by 20 percent from the average. A discussion with individuals familiar with the ORIGEN-2 code indicated that the listed values are well within the expected range of values.⁶ The fission products ^{134}Cs , ^{137}Cs , ^{110m}Ag , ^{106}Ru , and ^{125}Sb were generally found in quantities less than 50% of the core inventory.

SECTION 8

CONCLUSIONS/OBSERVATIONS

The following is a summary of conclusions and observations based on the preliminary analysis of the available data:

1. At the H8 core location, the surface sample (No. 1) is composed of finer particles than the deep subsurface sample (No. 3). This might be expected if the finer, granular core debris had been suspended by pump flow and then allowed to settle to the top of the debris bed.
2. There is no significant particle size difference between the H8 and E9 deep samples (No. 3 and 6). They may be typical of the subsurface debris bed.
3. Only about 0.3 weight percent of the core debris samples is smaller than 100 μm in particle size.
4. The E9 surface sample (No. 4) and the E9 near surface sample (No. 5) are similar. They are comprised of mostly larger sized particles ($> 1000 \mu\text{m}$).
5. The fission product concentrations ($\mu\text{Ci/g}$) are relatively consistent for all samples $< 707 \mu\text{m}$.
6. The fission product content for nonfuel material as indicated by the fissile material analysis is significantly less than for fuel associated material.

7. Based upon fissile/fertile material analyses, there are <15% of the particles measured contain >90% fuel indicating that both fuel and nonfuel material are generally contained in the particles.
8. The average fissile/fertile enrichment data indicate that the core samples at E9 had some contamination from the peripheral 2.96% enrichment fuel whereas this was not observed at the H8 location.
9. A comparison with the ORIGEN-2 data indicate that the ^{144}Ce and $^{154,155}\text{Eu}$ are principally associated with fuel particles; whereas, ^{134}Cs , ^{137}Cs , $^{110\text{m}}\text{Ag}$, ^{106}Ru , and ^{125}Sb were generally found in quantities less than 50% of the predicted fuel core ratio and therefore these radionuclides have been partially removed (e.g., by leaching or some other process) from the particles.

SECTION 9.

REFERENCES

1. L. S. Beller and H. L. Brown, Design and Operation of the Core Topography Data Acquisition System for TMI-2, GEND-INF-012, May 1984.
2. D. L. Evans, TMI-2 Fuel Recovery Plant Feasibility Study, EGG-TMI-6130, December 1982.
3. Y. D. Harker, "Feasibility of Measuring the Fissile Content of Irradiated Fuel Samples," REA-83-022, February 16, 1983.
4. A. G. Groff, ORIGEN-2--A Revised and Updated Version of the Oak Ridge Isotope Generation and Depletion Code, ORNL-5621, July 1980.
5. H. M. Burton letter to G. R. Eidam, "Core Debris Samples Particle Size Data," HMB-98-84, April 23, 1984.
6. Personal communication between D. W. Akers and B. G. Schnitzler, May 29, 1984.

APPENDIX A

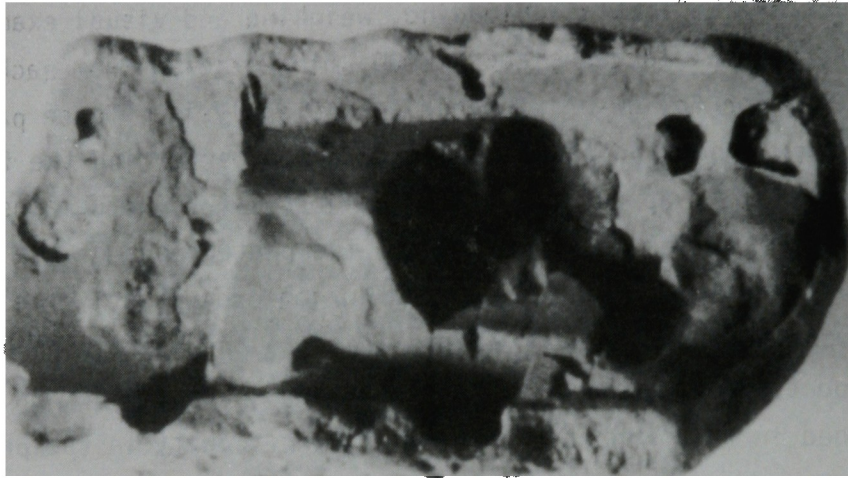
PHOTOGRAPHS OF DISCRETE PARTICLES

APPENDIX A

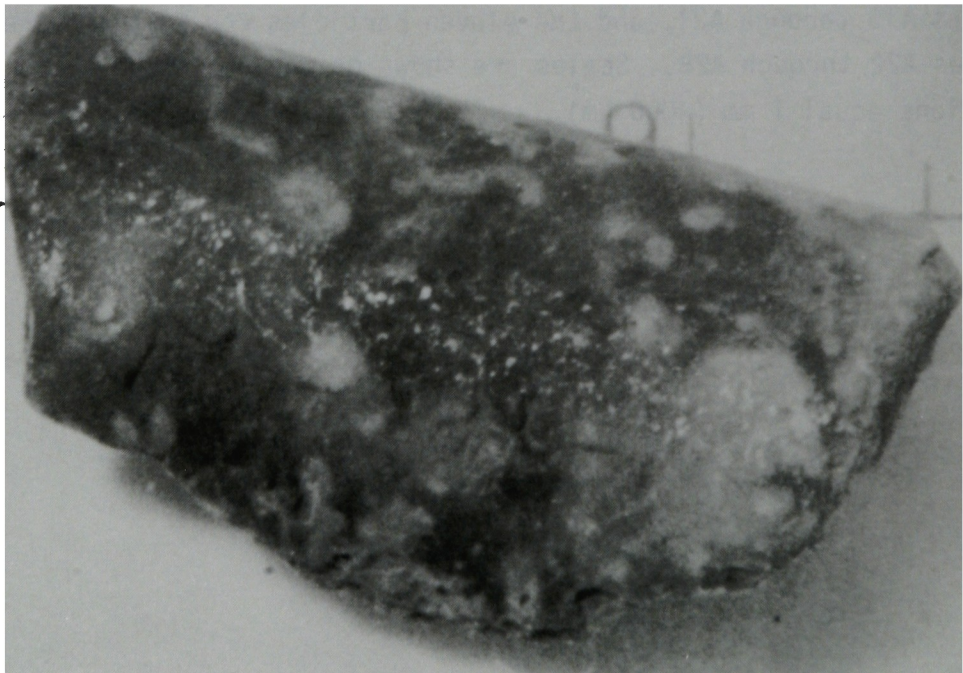
PHOTOGRAPHS OF DISCRETE PARTICLES

As part of the initial unloading, weighing and visual examination activities, several larger sized ($\geq 1000 \mu\text{m}$) particles from each sample were selected for follow-on examination and analysis. These particles were individually weighed and photographed prior to performing the follow-on examinations. This appendix contains copies of the photographs for all particles from Samples 1, 4, 5, and 6. The photographs of the individual particles from Sample 3 were misplaced during processing. These particles will be rephotographed and the photos added to the final core debris grab sample report. Photographs of individual particles smaller than $1000 \mu\text{m}$ are not included in this report due to the lack of acuity in the photos.

Photographs for the eleven particles from Sample 1 are shown in Figures A1 through A10. The five particles from Sample 4 are shown in Figures A11 through A15. The eleven particles from Sample 5 are shown in Figures A16 through A21, and the eleven particles for Sample 6 are shown in Figures A22 through A28. Scales are shown on the photographs and the divisions equal 1 mm ($1000 \mu\text{m}$).



Front



Back

Figure A-1. Particle 1A from Sample 1 (surface of debris bed at H8 location), size range: $>4000 \mu\text{m}$.

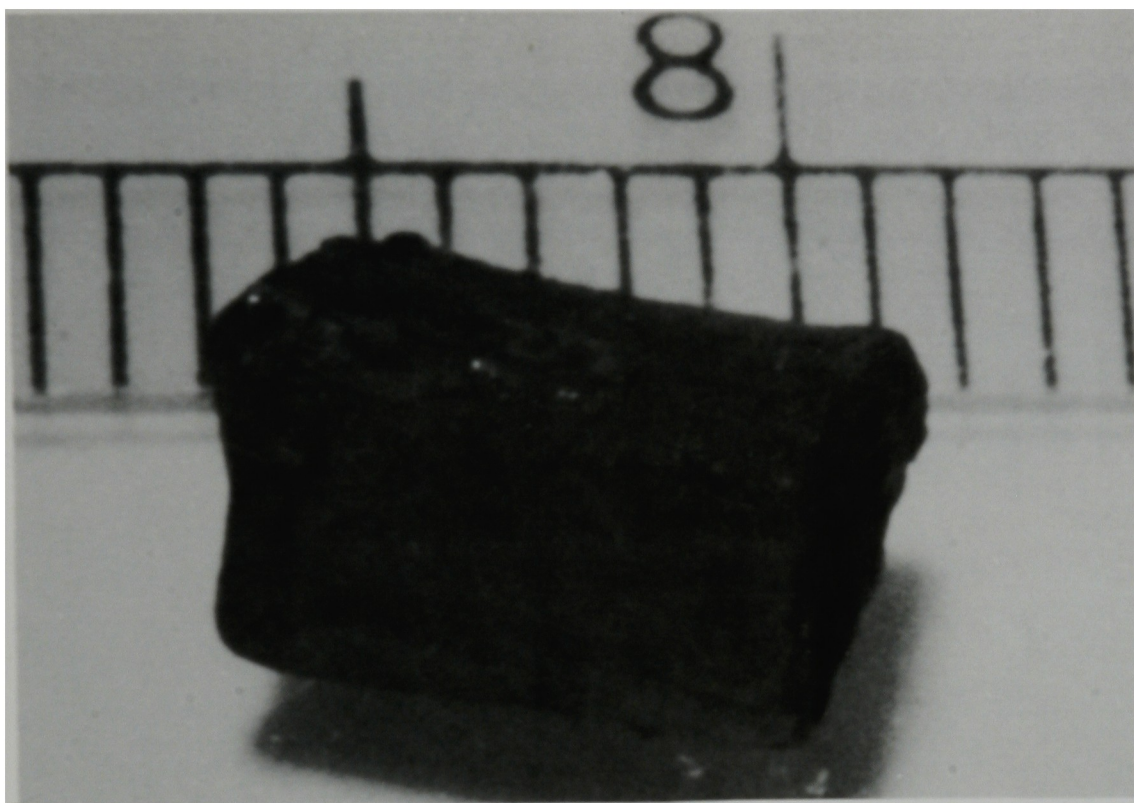


Figure A-2. Particle 1b from Sample 1 (surface of debris bed at H8 location), size range: $>4000 \mu\text{m}$.

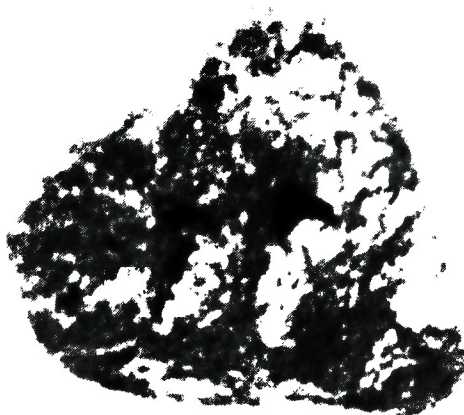


Figure A-3. Particle 1C from Sample 1 (surface of debris bed at H8 location), size range: $>4000\ \mu\text{m}$.

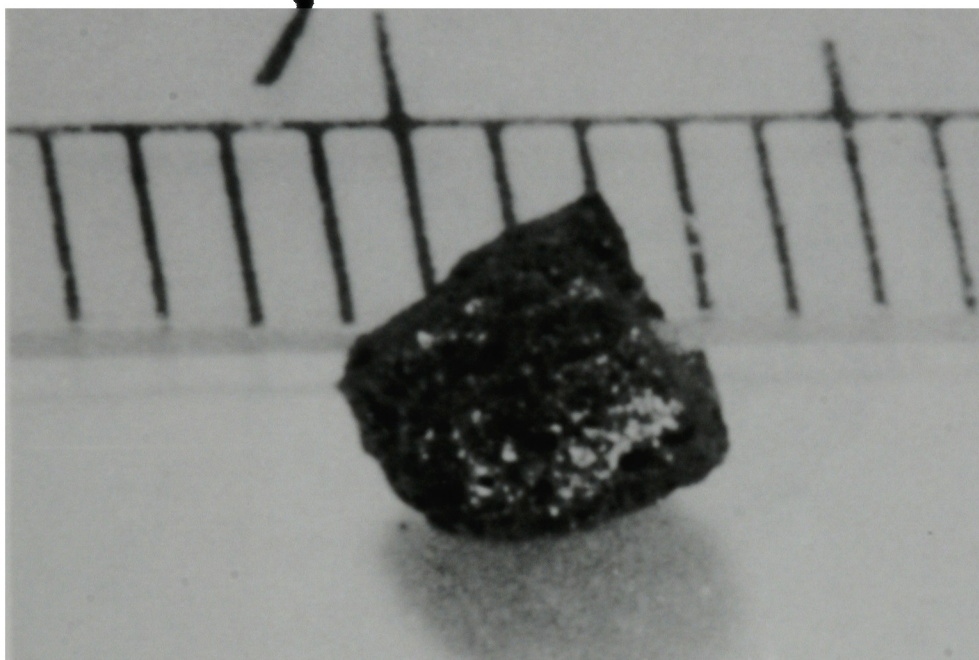


Figure A-4. Particle 1D from Sample 1 (surface of debris bed at H8 location), size range: $>4000\ \mu\text{m}$.

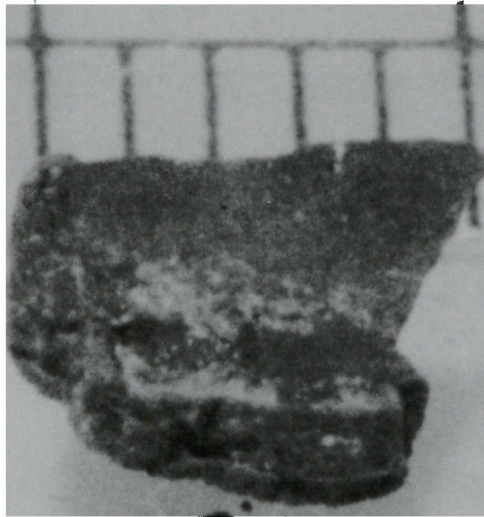


Figure A-5. Particle 1E from Sample 1 (surface of debris bed at H8 location), size range: $>4000\ \mu\text{m}$.

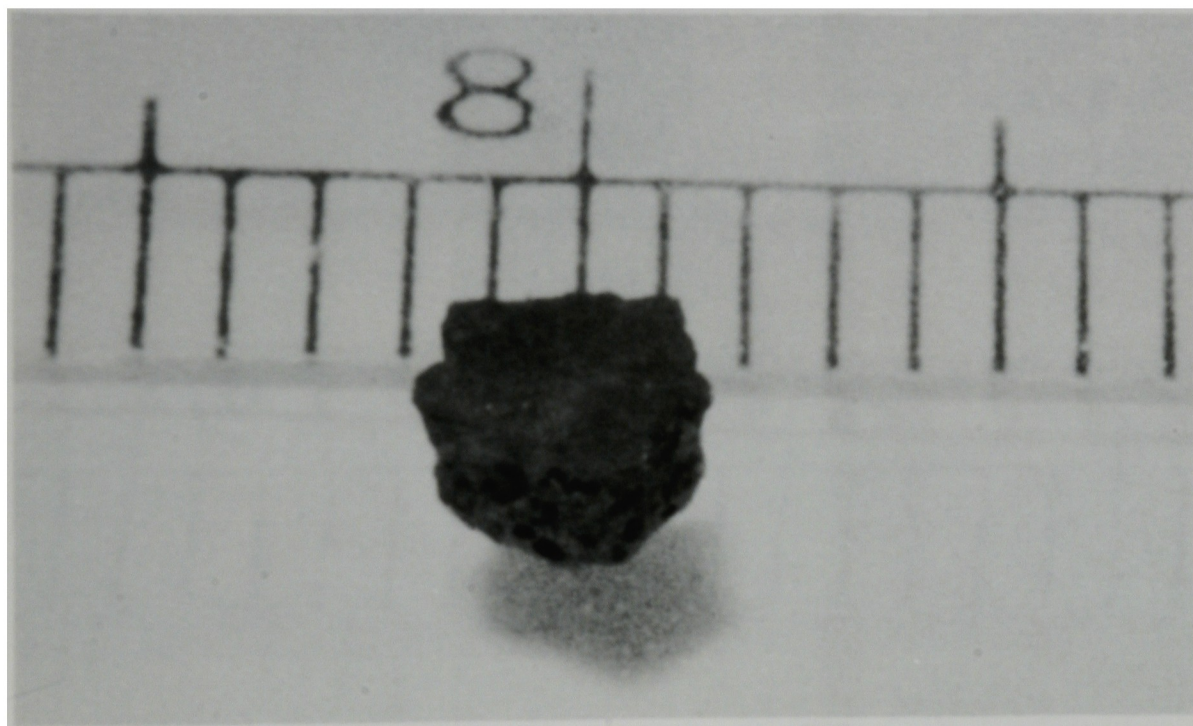
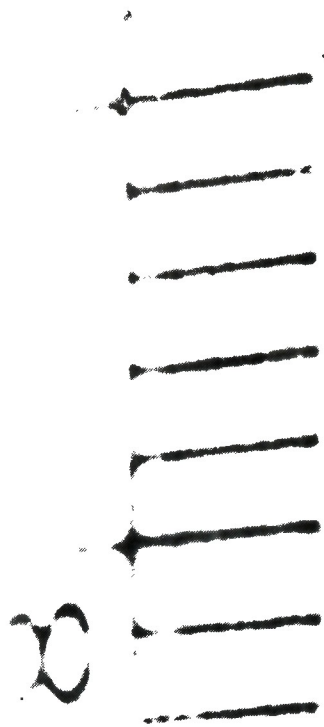


Figure A-6. Particle 1F from Sample 1 (surface of debris bed at H8 location), size range: 1680-4000 μm .



Front



Back

Figure A-7. Particle 1G from Sample 1 (surface of debris bed at H8 location), size range: 1680-4000 μm .

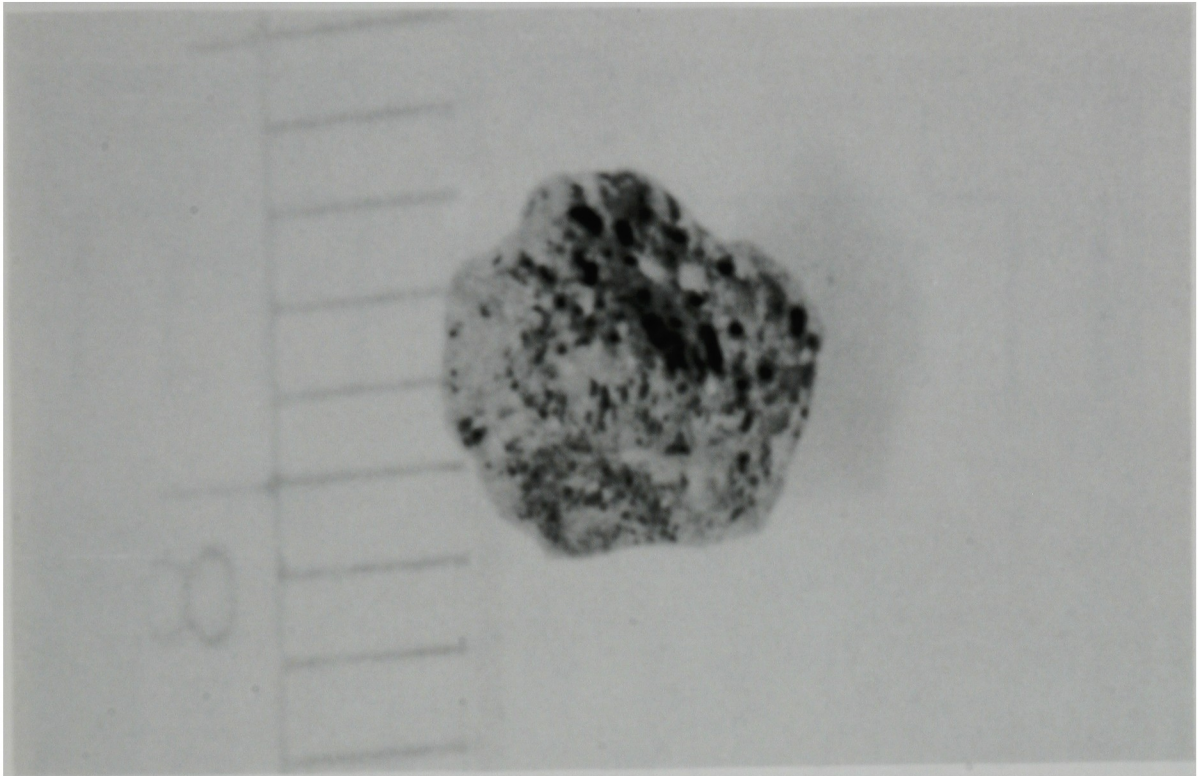


Figure A-8. Particle 1H from Sample 1 (surface of debris bed at H8 location), size range: 1680-4000 μm .

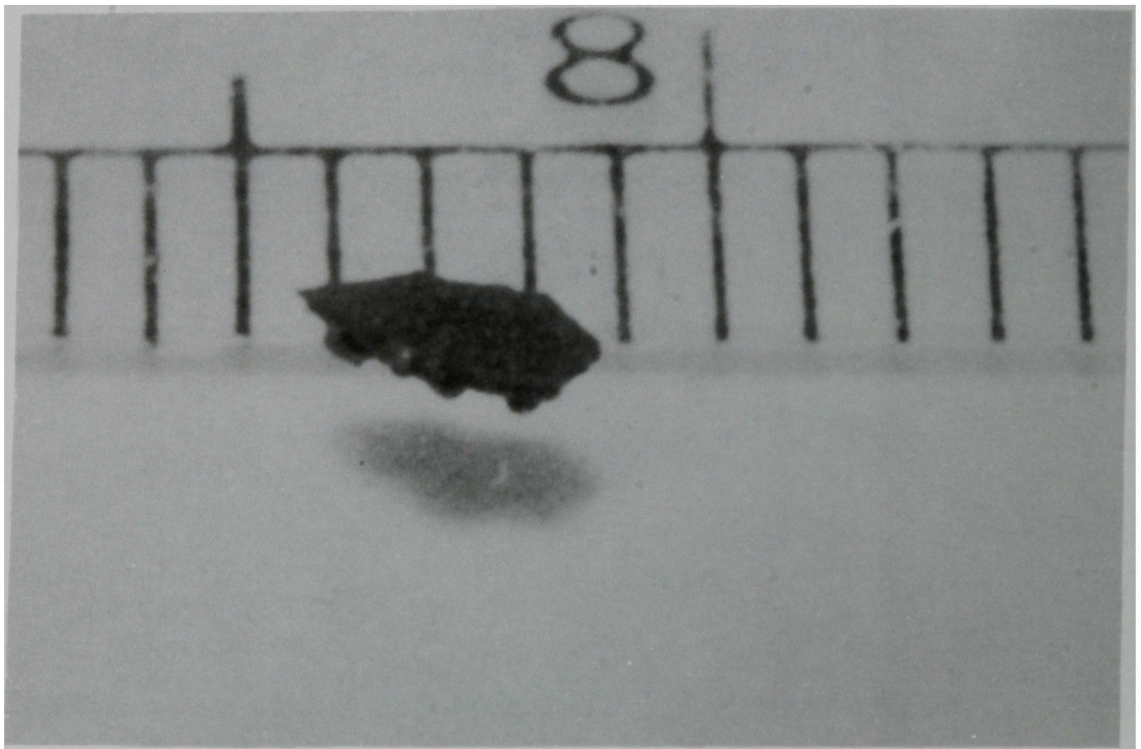
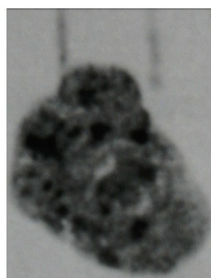
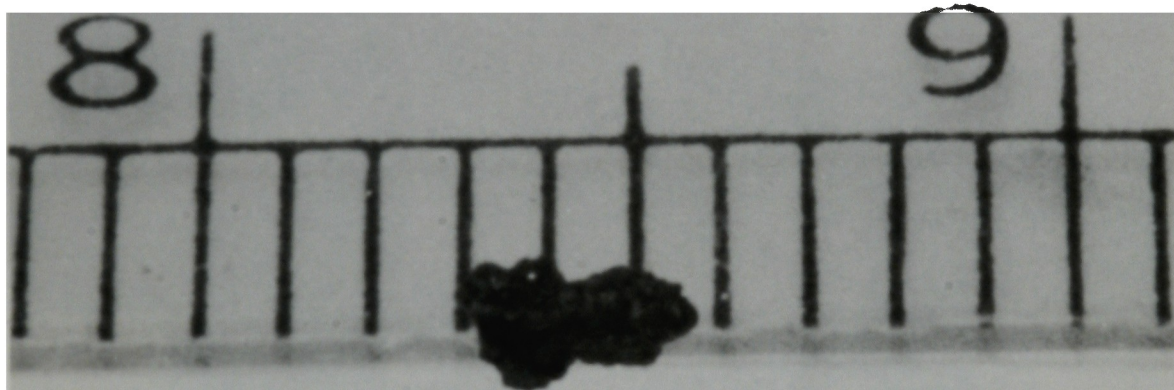


Figure A-9. Particle 1I from Sample 1 (surface of debris bed at H8 location), size range: 1000-1680 μm .



(a)



(b)

Figure A-10. Particles from Sample 1 (surface of debris bed at H8 location).

(a) Particle 1J, size range: 1000-1680 μm .

(b) Particle 1K, size range: 1000-1680 μm .

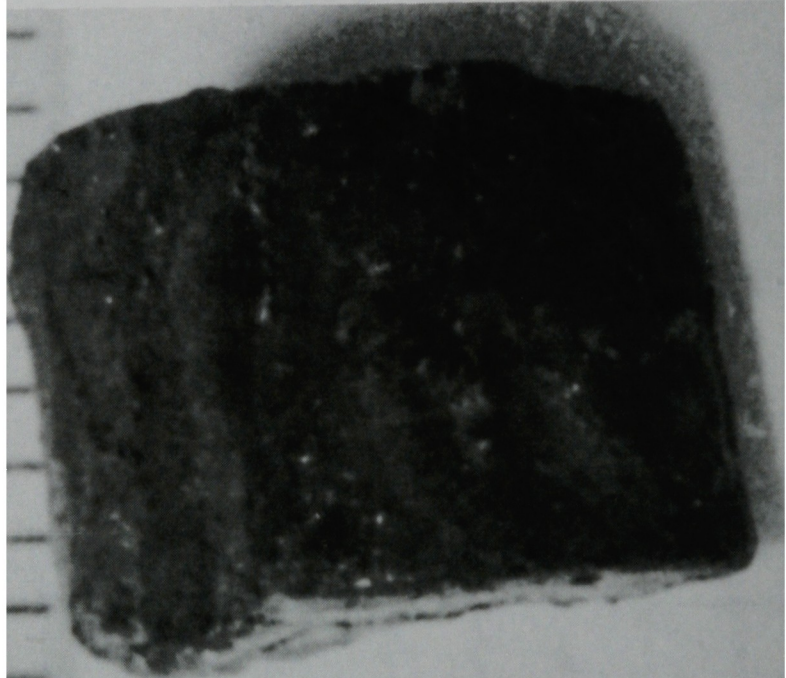
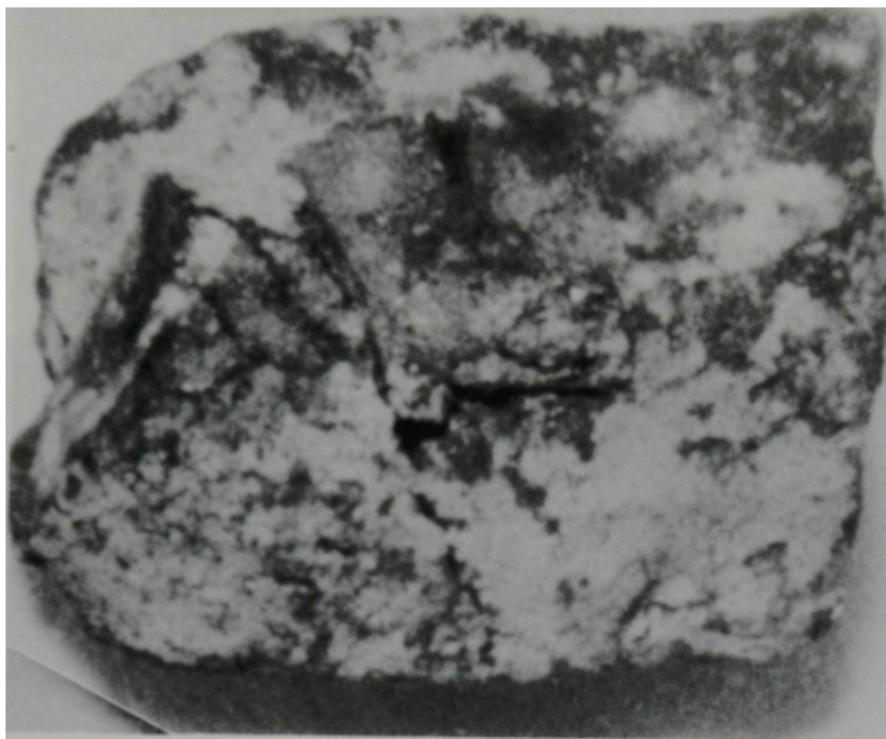
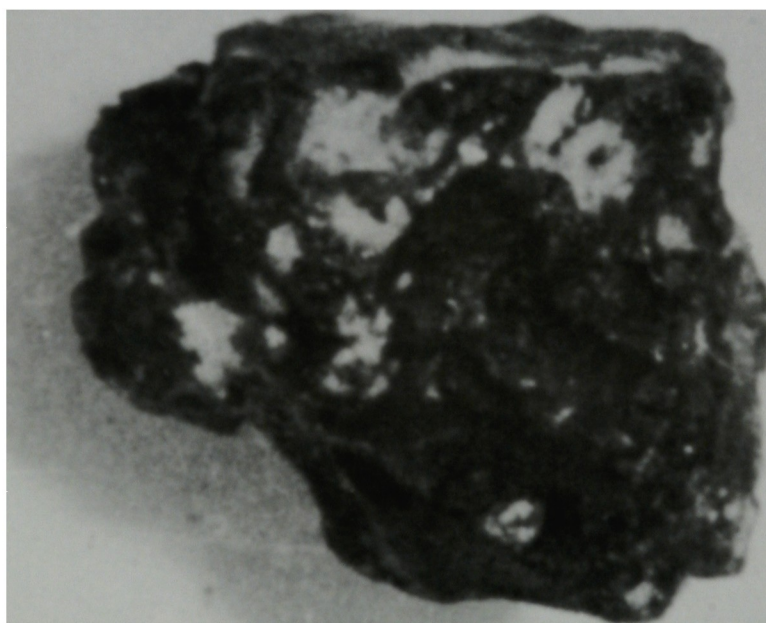


Figure A-11. Particle 4A from Sample 4 (surface of debris bed at E9 location), size range: $>4000\ \mu\text{m}$.



Front



Back

Figure A-12. Particle 4B from Sample 4 (surface of debris bed at E9 location), size range: $>4000\ \mu\text{m}$.

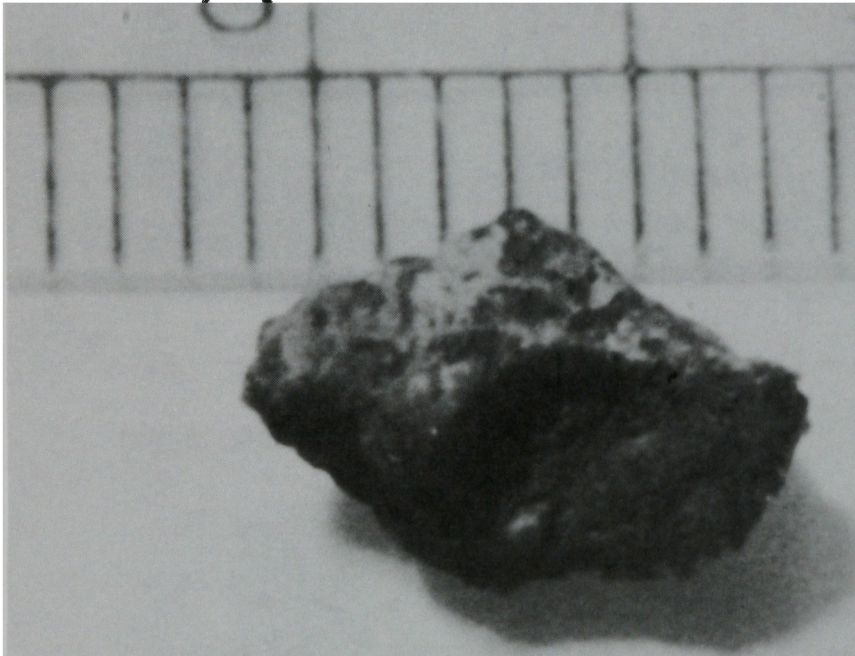


Figure A-13. Particle 4C from Sample 4 (surface of debris bed at E9 location), size range: $>4000\ \mu\text{m}$.

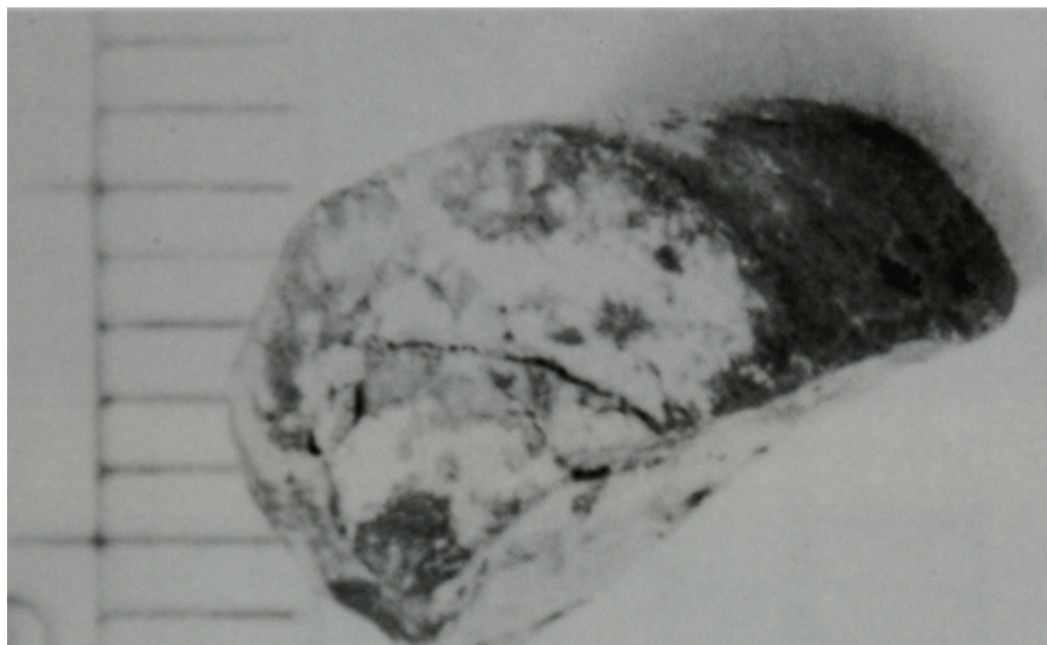
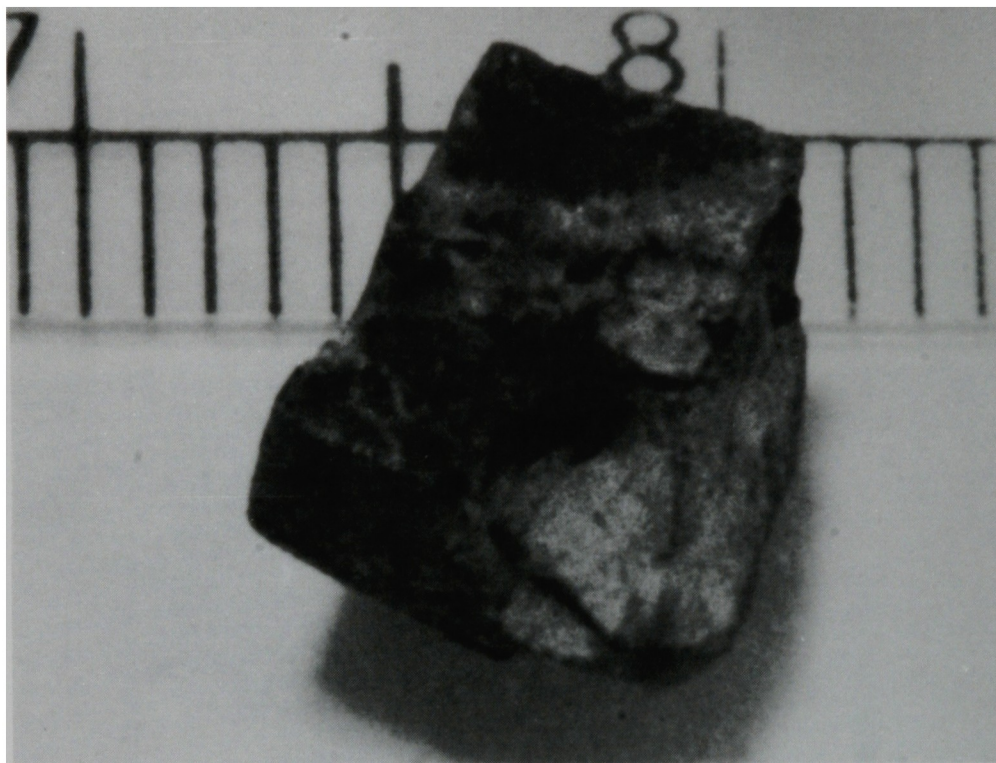
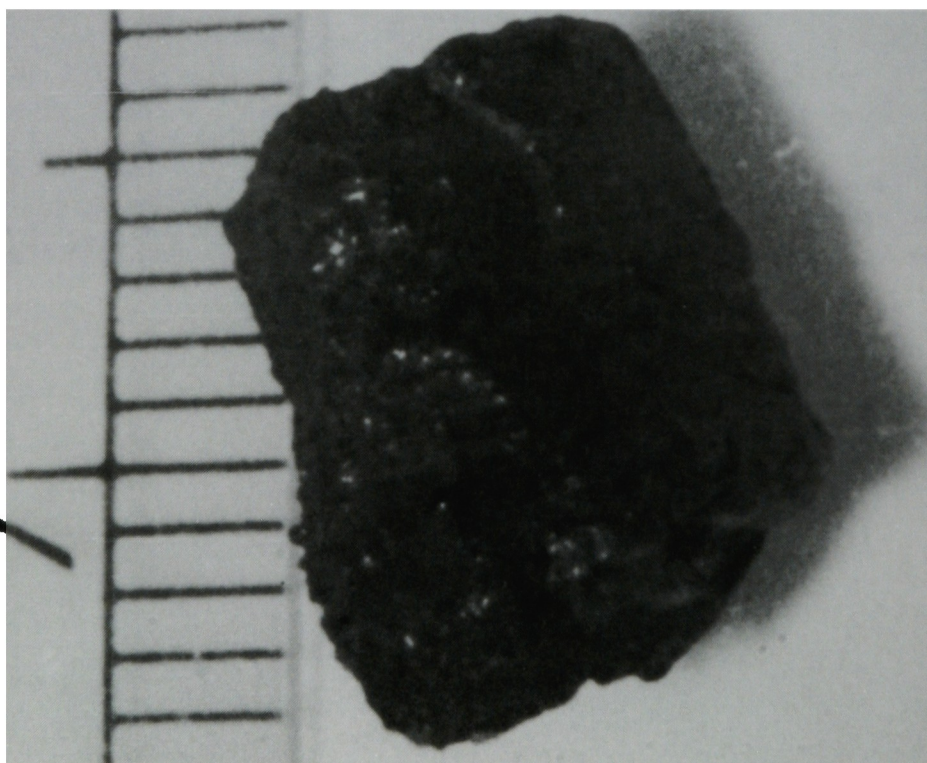


Figure A-14. Particle 4U from Sample 4 (surface of debris bed at E9 location), size range: $>4000\ \mu\text{m}$.

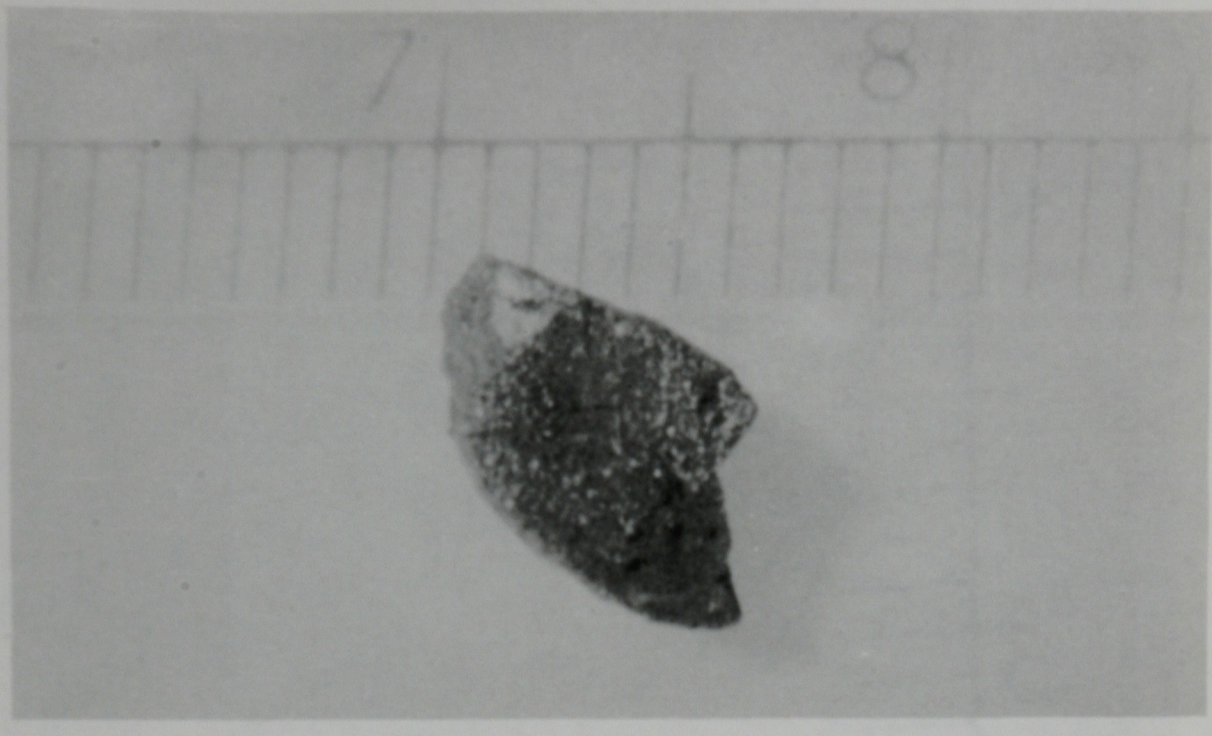


Front

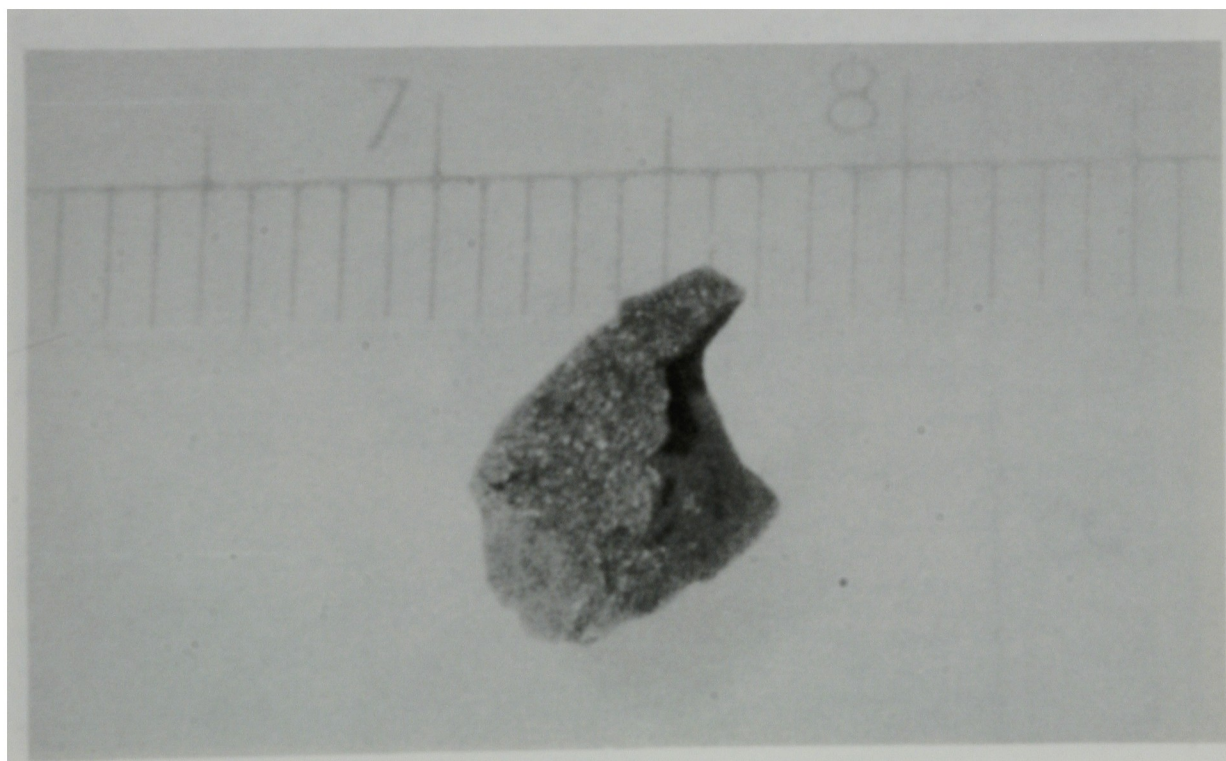


Back

Figure A-15. Particle 4E from Sample 4 (surface of debris bed at E9 location), size range: $>4000 \mu\text{m}$.

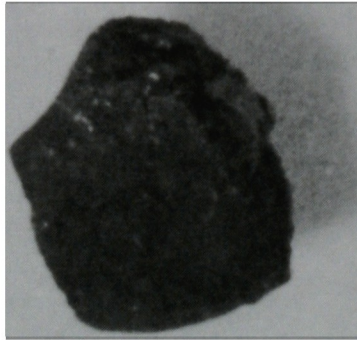
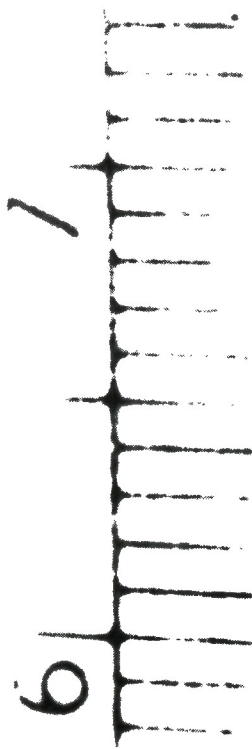


Front

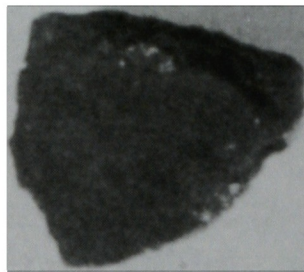
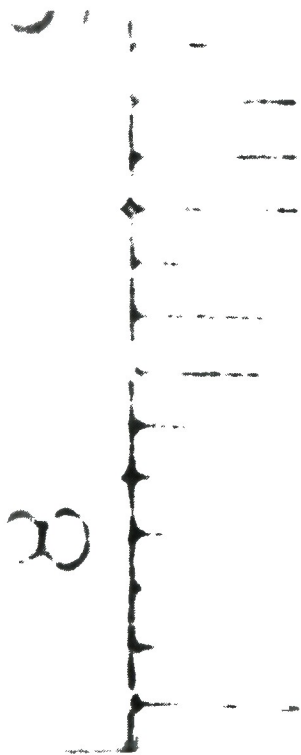


Back

Figure A-16. Particle 5A from Sample 5 (3 in. into debris bed at E9 location), size range: $>4000\text{ }\mu\text{m}$.



(a)

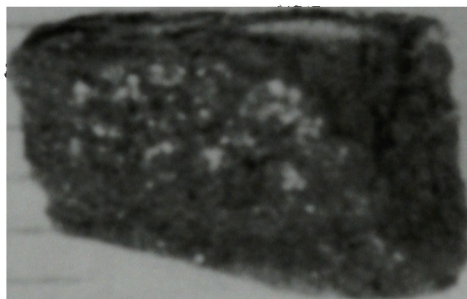


(b)

Figure A-17. Particles from Sample 5 (3 in. into debris bed at E9 location).
(a) Particle 5B, size range: $>4000\ \mu\text{m}$.
(b) Particle 5C, size range: $>4000\ \mu\text{m}$.

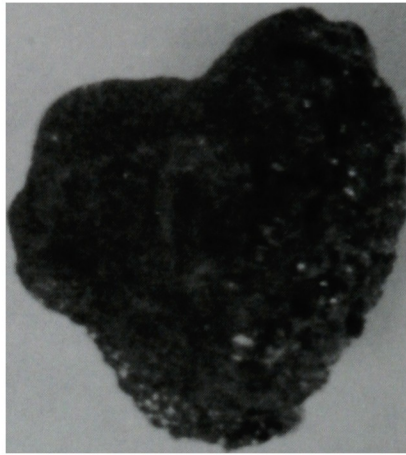


(a)

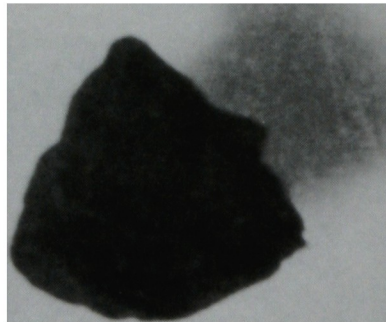


(b)

Figure A-18. Particles from Sample 5 (3 in. into debris bed at E9 location).
(a) Particle 5D, size range: $>4000\ \mu\text{m}$.
(b) Particle 5t, size range: $>4000\ \mu\text{m}$.



(a)

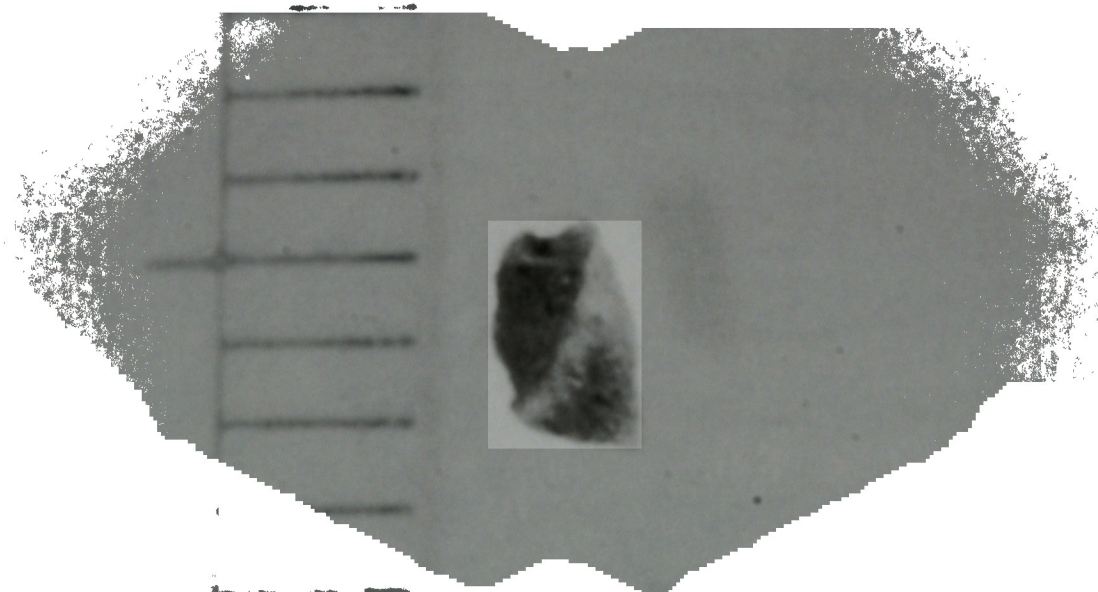


(b)

Figure A-19. Particles from Sample 5 (3 in. into debris bed at E9 location).
 (a) Particle 5F, size range: 1680-4000 μm .
 (b) Particle 5G, size range: 1680-4000 μm .



(a)



(b)

Figure A-20. Particles from Sample 5 (3 in. into debris bed at E9 location).

(a) Particle 50, size range: 1000-1680 μm .

(b) Particle 51, size range: 1000-1680 μm .

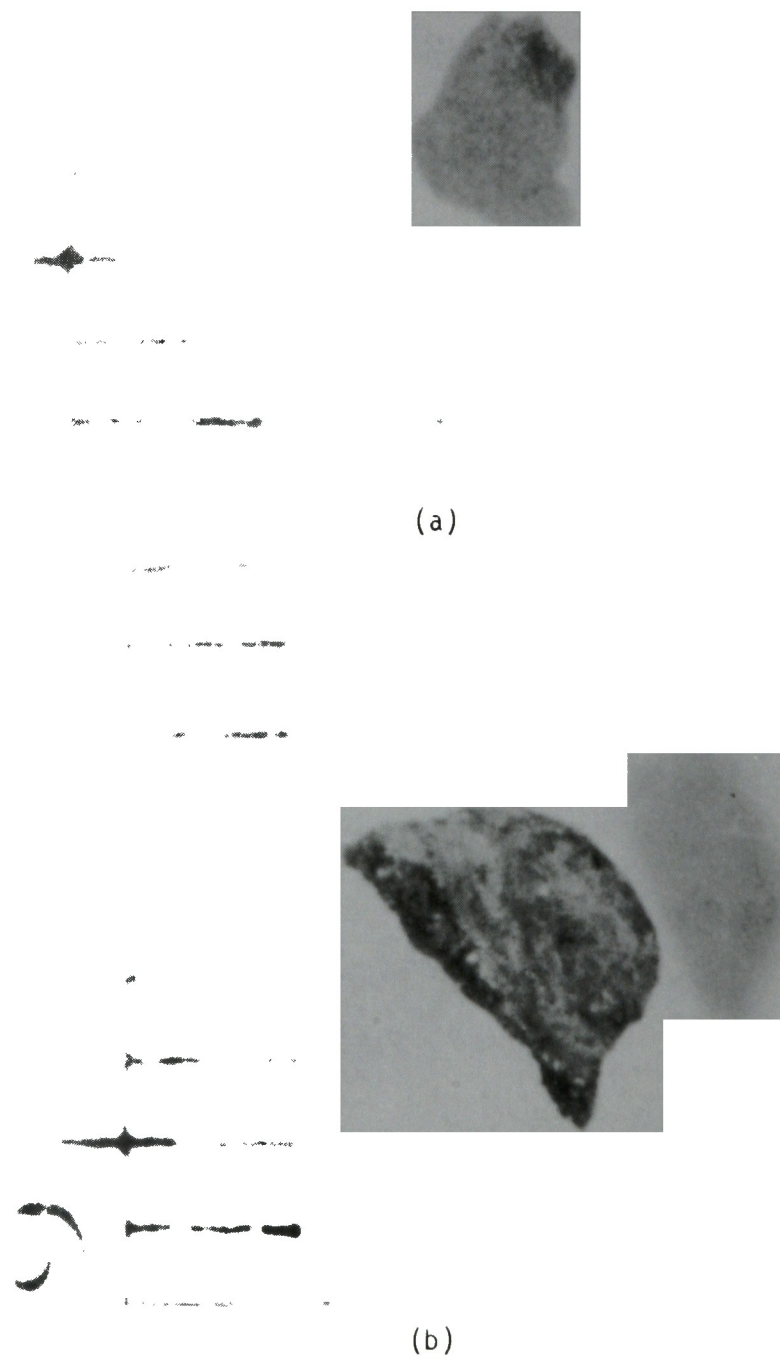
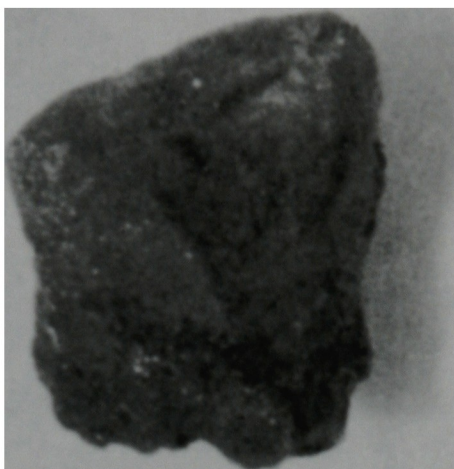


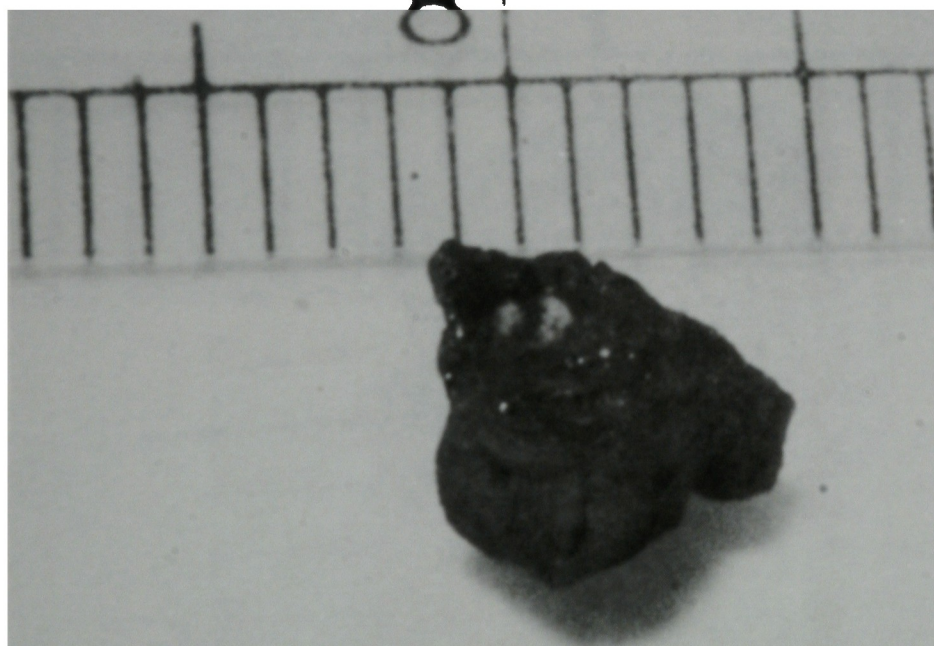
Figure A-21. Particles from Sample 5 (3 in. into debris bed at E9 location).

(a) Particle 5J, size range: 1000-1680 μm .

(b) Particle 5K, size range: 1000-1680 μm .

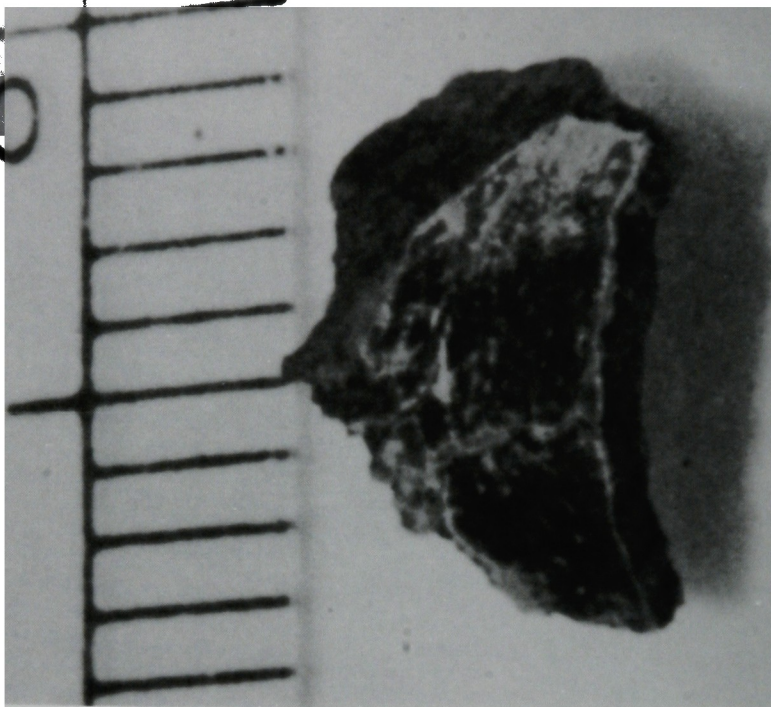


Front

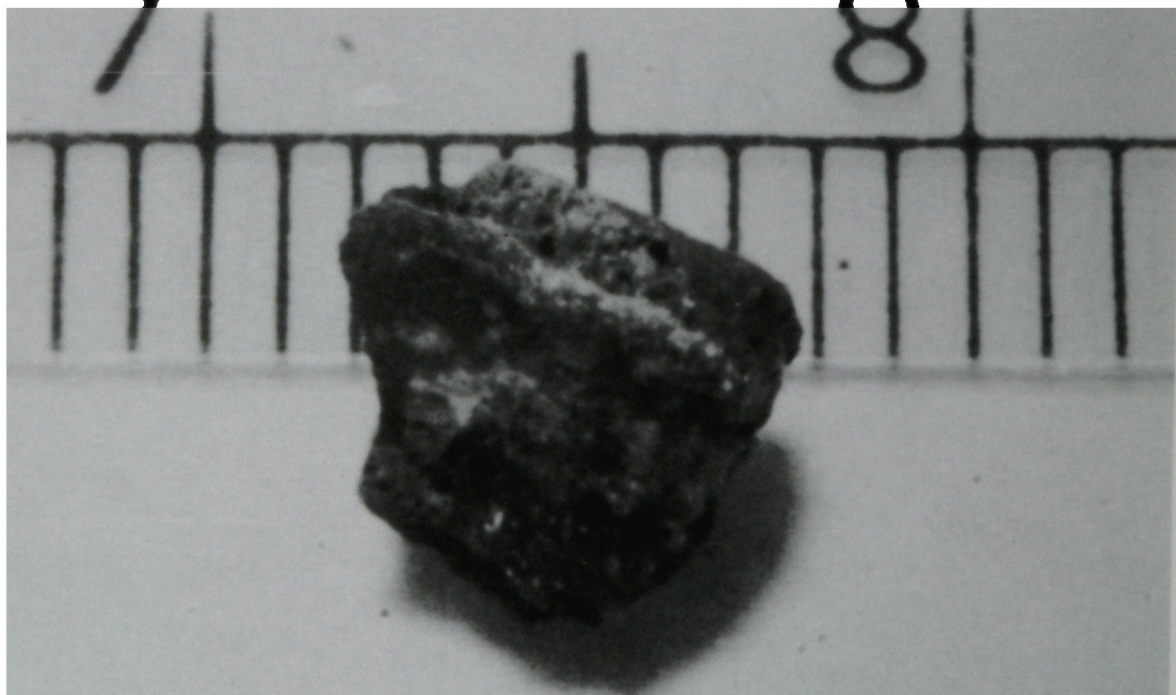


Back

Figure A-22. Particle 6A from Sample 6 (22 in. into debris bed at E9 location), size range: $>4000\ \mu\text{m}$.



(a)

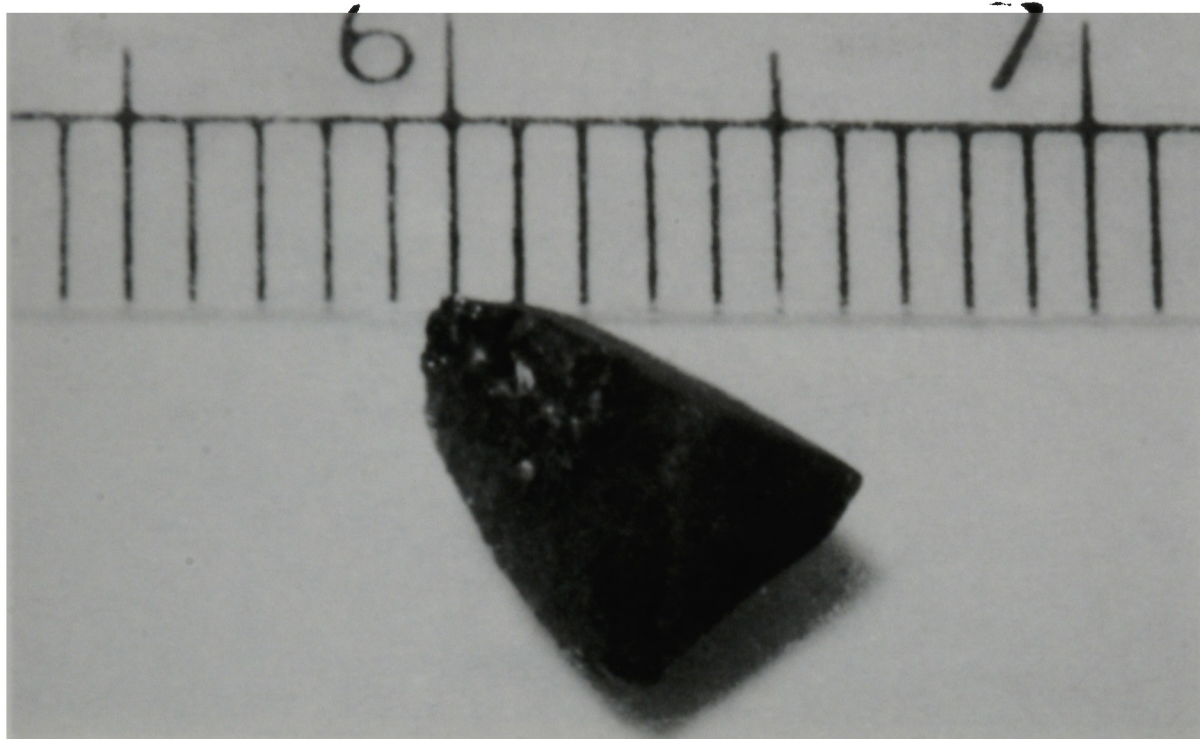


(b)

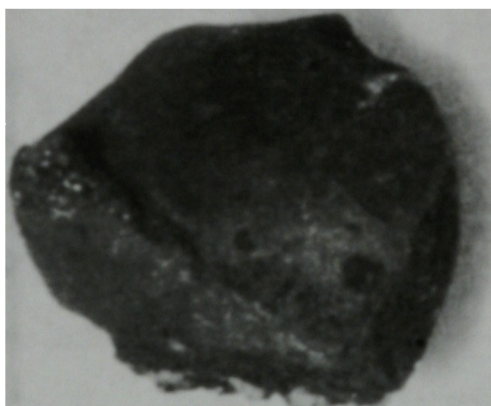
Figure A-23. Particles from Sample 6 (22 in. into debris bed at E9 location).

(a) Particle 6B, size range: $>4000\ \mu\text{m}$.

(b) Particle 6C, size range: $>4000\ \mu\text{m}$.

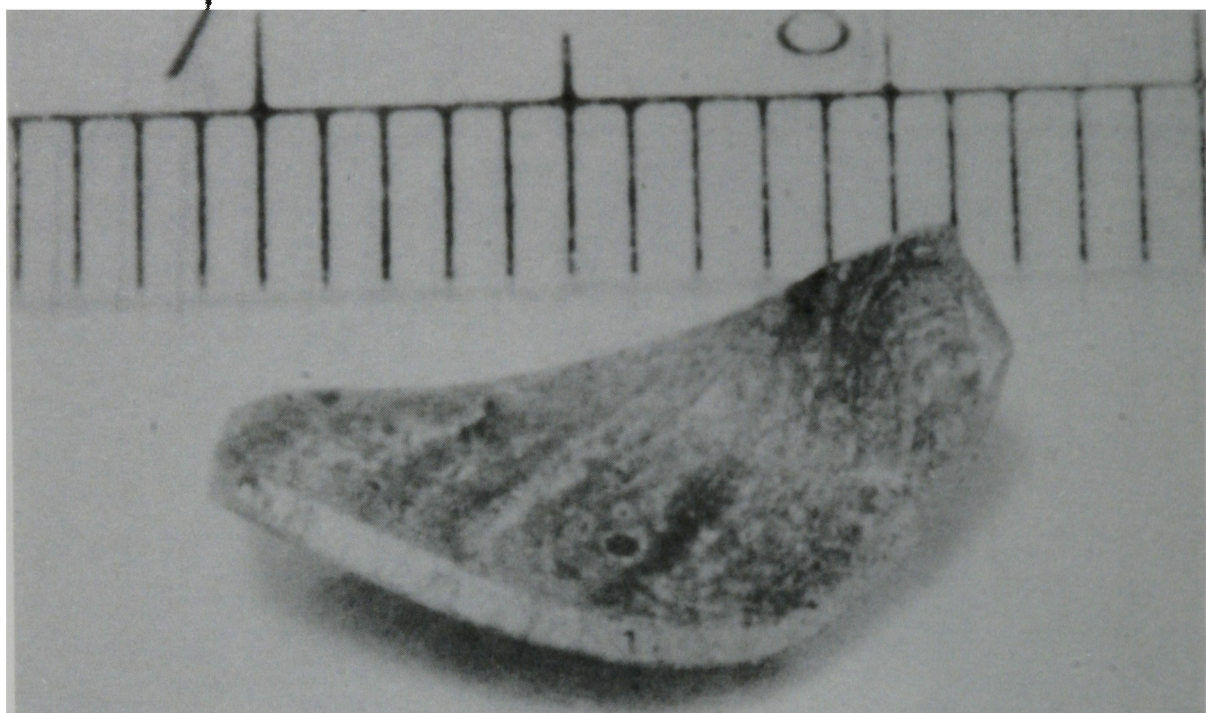


Front

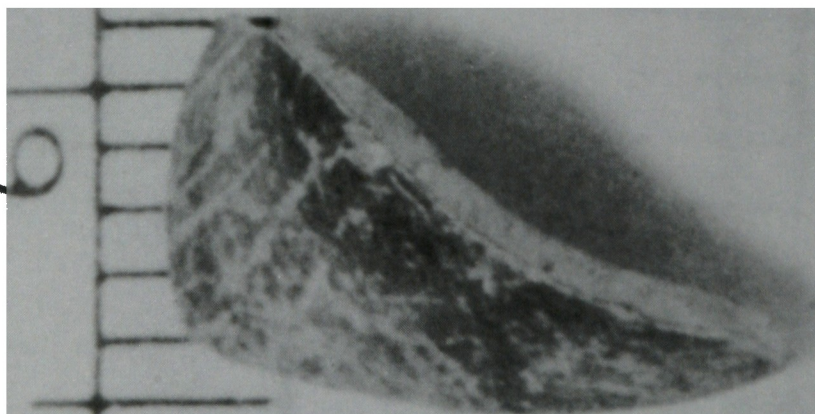


Back

Figure A-24. Particle 6D from Sample 6 (22 in. into debris bed at E9 location), size range: $>4000\ \mu\text{m}$.

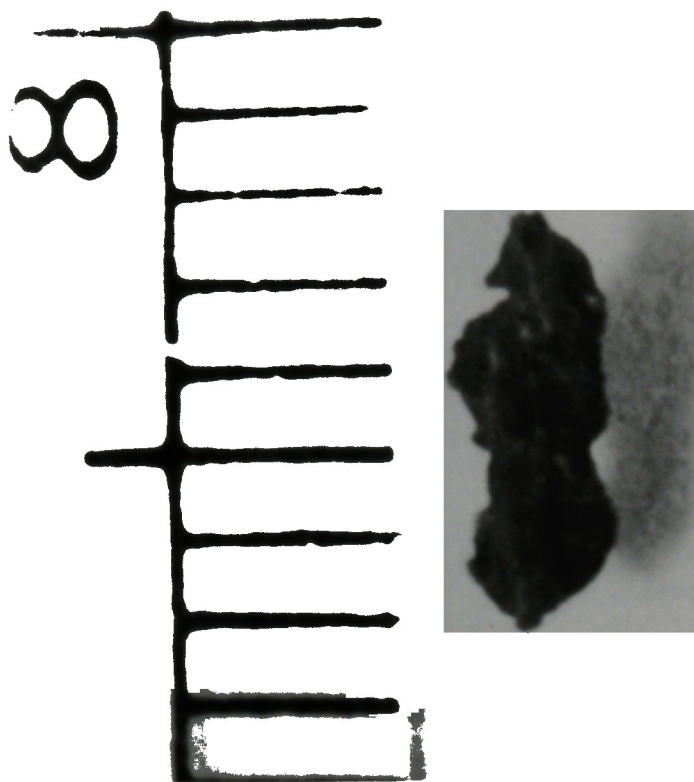


Front

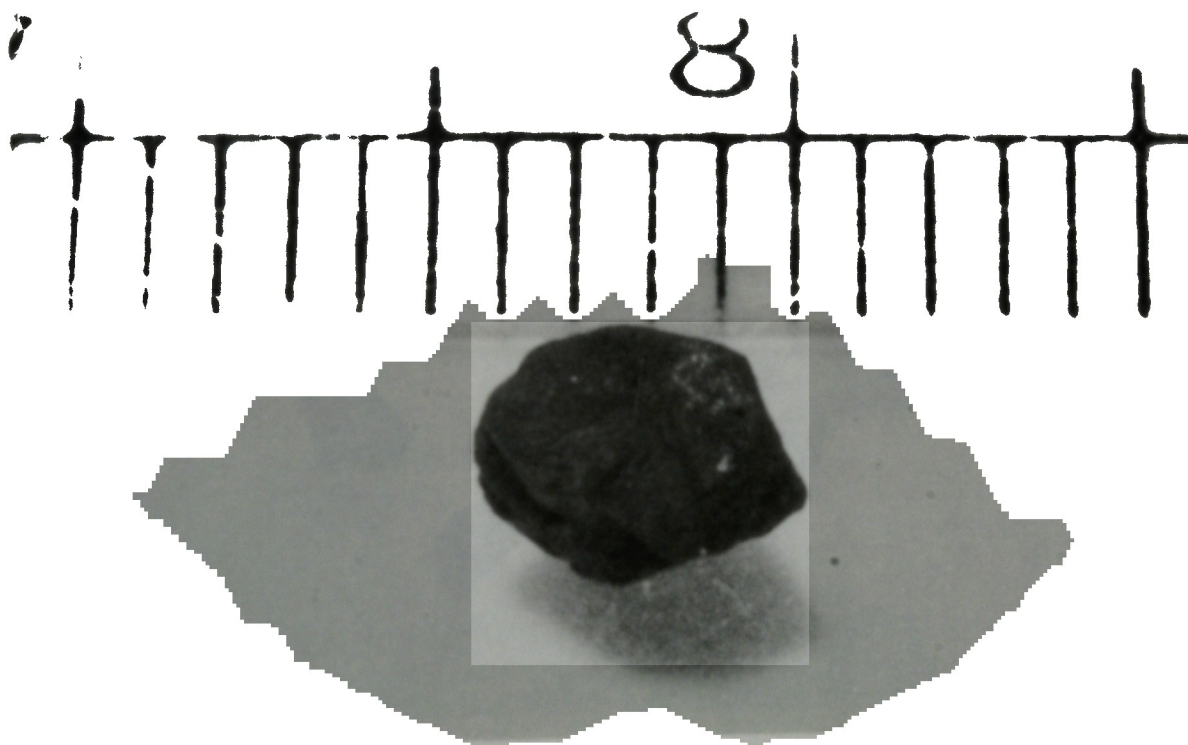


Back

Figure A-25. Particle 6E from Sample 6 (22 in. into debris bed at E9 location), size range: $>4000\ \mu\text{m}$.

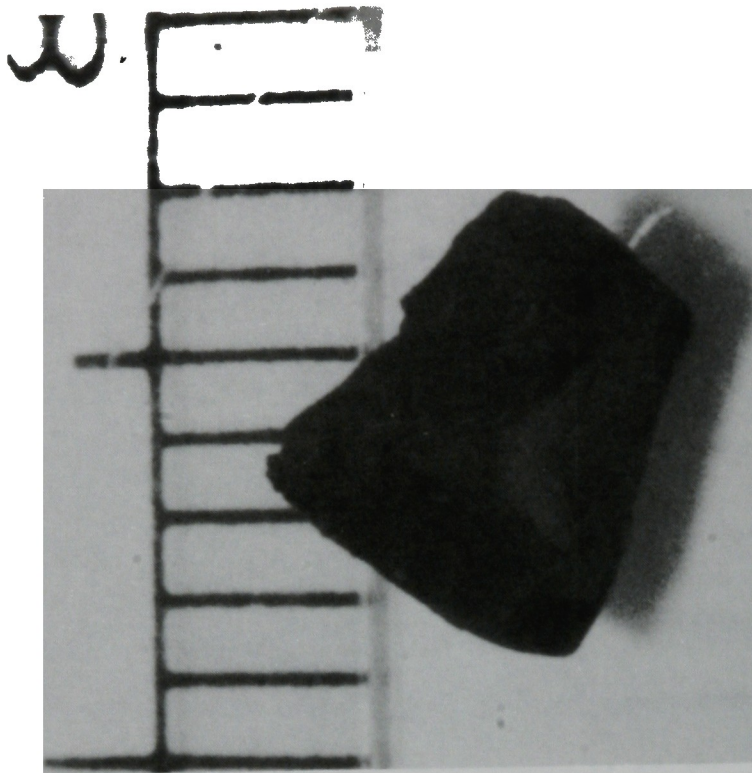


(a)

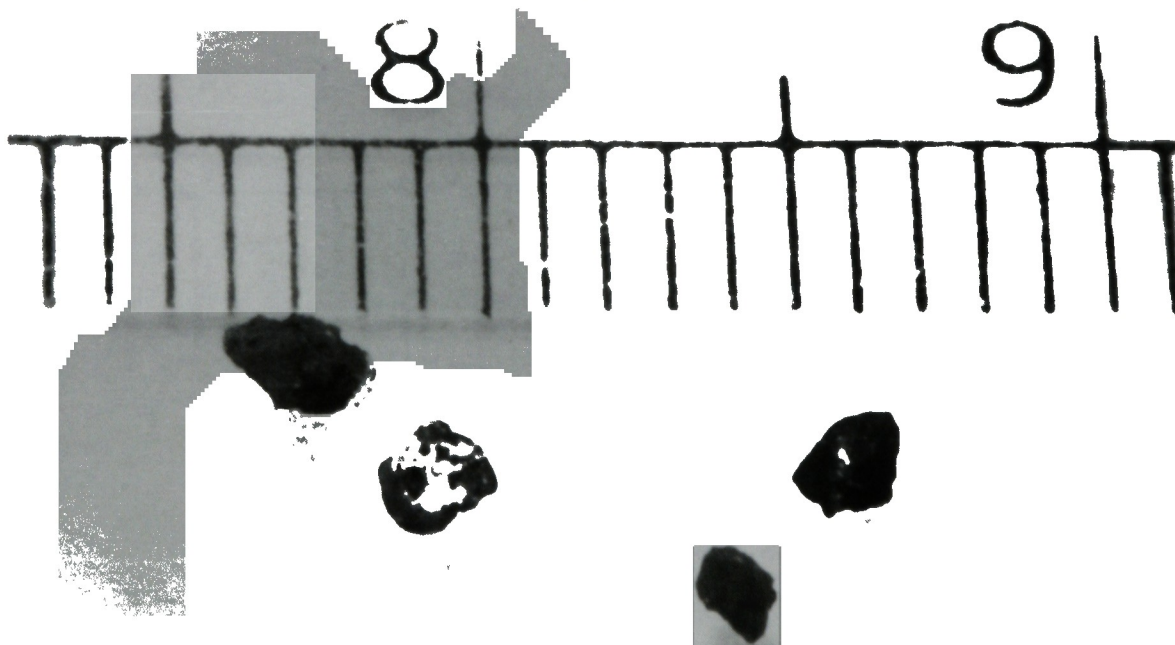


(b)

- Figure A-26. Particles from Sample 6 (22 in. into debris bed at E9 location).
- (a) Particle 6F, size range: 1680-4000 μm .
 - (b) Particle 6G, size range: 1680-4000 μm .



(a)



(b)

Figure A-27. Particles from Sample 6 (22 in. into debris bed at E9 location).

(a) Particle 6H, size range: 1680-4000 μm .

(b) Particle 6I, 6J, 6K size range: 1000-1680 μm .

APPENDIX B

CORE DEBRIS GAMMA SPECTROMETRY DATA

APPENDIX B

CORE DEBRIS GAMMA SPECTROMETRY DATA

Included in this appendix are the results of the gamma spectrometry results for the core debris samples. In the ^{241}Am is not reported as an effective efficiency curve has not yet been developed for this radionuclide. All other uncertainties are reported at the one sigma value with only counting statistics incorporated with the exception of ^{155}Eu . These based on extrapolated efficiencies and have a listed uncertainty of 20 percent. Corrections have been made to the data for the mass attenuation of the sample for the gamma rays used for analysis.

TABLE B-1. SAMPLE 1 HB SURFACE RADIONUCLIDE CONCENTRATION
($\mu\text{Ci/gm}$)

Radionuclide	$>4000_{\mu\text{m}}$ Particle 1 (1A)	$>4000_{\mu\text{m}}$ Particle 2 (1B)	$>4000_{\mu\text{m}}$ Particle 3 (1C)	$>4000_{\mu\text{m}}$ Particle 4 (1D)	$>4000_{\mu\text{m}}$ Particle 5 (1E)
^{60}Co	$2.55 \pm 0.14(+1)$	$1.81 \pm 0.19(+1)$	$8.7 \pm 1.1(0)$	$1.99 \pm 0.31(+1)$	$1.37 \pm 0.09(+1)$
^{106}Ru	$7.10 \pm 0.40(+1)$	$1.55 \pm 0.15(+3)$	$6.71 \pm 0.86(+1)$	$8.99 \pm 1.37(+2)$	$2.72 \pm 0.18(+2)$
$^{110\text{m}}\text{Ag}$	--	--	--	--	--
^{125}Sb	$1.20 \pm 0.07(+2)$	$7.82 \pm 0.82(+1)$	$1.23 \pm 0.23(+1)$	$1.36 \pm 0.22(+1)$	$9.24 \pm 0.61(+1)$
^{134}Cs	$5.36 \pm 0.31(0)$	$3.69 \pm 0.55(0)$	$7.57 \pm 0.86(+1)$	$1.08 \pm 0.17(+1)$	$3.54 \pm 0.23(+1)$
^{137}Cs	$2.98 \pm 0.16(+2)$	$6.68 \pm 0.67(+1)$	$1.31 \pm 0.15(+3)$	$2.02 \pm 0.31(+2)$	$8.38 \pm 0.54(+2)$
^{144}Ce	$1.74 \pm 0.14(+2)$	$3.84 \pm 0.41(+3)$	$2.81 \pm 0.34(+3)$	$3.14 \pm 0.49(+3)$	$7.32 \pm 0.59(+2)$
^{154}Eu	$7.98 \pm 0.96(-1)$	$5.86 \pm 0.61(+1)$	$4.78 \pm 0.57(+1)$	$4.63 \pm 0.71(+1)$	$1.05 \pm 0.08(+1)$
^{155}Eu	$9.5 \pm 1.9(0)$	$1.6 \pm 0.3(+2)$	$1.2 \pm 0.2(+1)$	$1.25 \pm 0.25(+2)$	$3.5 \pm 0.7(+1)$

TABLE B-1. (continued)

Radionuclide	1680-4000 μ m Particle 1 (1F)	1680-4000 μ m Particle 2 (1G)	1680-4000 μ m Particle 3 (1H)	1000-1680 μ m Particle 4 (1I)	1000-1680 μ m Particle 5 (1J)
⁶⁰ Co	8.1 \pm 0.8(0)	9.34 \pm 0.88(0)	7.85 \pm 0.49(+1)	1.67 \pm 0.20(+1)	1.95 \pm 0.11(0)
¹⁰⁶ Ru	4.39 \pm 0.49(+1)	7.33 \pm 0.74(+1)	1.07 \pm 0.07(+2)	7.00 \pm 0.85(+1)	8.9 \pm 0.6(0)
^{110m} Ag	--	--	--	7.43 \pm 0.92(0)	--
¹²⁵ Sb	2.06 \pm 0.23(+1)	1.84 \pm 0.24(+1)	1.48 \pm 0.13(+1)	2.17 \pm 0.25(+3)	1.1 \pm 0.1(0)
¹³⁴ Cs	1.12 \pm 0.09(+2)	9.98 \pm 0.86(+1)	6.29 \pm 0.44(0)	6.29 \pm 0.72(+1)	3.1 \pm 0.2(0)
¹³⁷ Cs	1.98 \pm 0.16(+3)	1.71 \pm 0.15(+3)	1.15 \pm 0.07(+2)	1.14 \pm 0.13(+3)	5.5 \pm 0.3(+1)
¹⁴⁴ Ce	3.06 \pm 0.27(+3)	2.31 \pm 0.22(+3)	2.18 \pm 0.15(+3)	ND	3.20 \pm 0.19(+2)
¹⁵⁴ Eu	5.73 \pm 0.50(+1)	3.54 \pm 0.33(+1)	3.02 \pm 0.20(+1)	9.8 \pm 2.5(-1)	5.4 \pm 0.3(0)
¹⁵⁵ Eu	1.24 \pm 0.25(+2)	9.5 \pm 1.9(+1)	8.3 \pm 1.8(+1)	ND	1.2 \pm 0.2(+1)

TABLE B-1. (continued)

Radionuclide	1000-1680 μ m Particle 3 (1K)	707-1000 μ m Aliquot	297-707 μ m Aliquot	149-279 μ m Aliquot	74-149 μ m Aliquot
⁶⁰ Co	8.2 \pm 0.7(0)	2.3 \pm 0.2(+2)	4.9 \pm 0.3(+1)	8.1 \pm 0.6(+1)	1.1 \pm 0.1(+2)
¹⁰⁶ Ru	4.6 \pm 0.4(+1)	5.6 \pm 0.4(+3)	1.5 \pm 0.1(+2)	1.5 \pm 0.1(+2)	2.7 \pm 0.3(+2)
^{110m} Ag	--	3.7 \pm 0.9(0)	1.1 \pm 0.2(0)	1.3 \pm 0.3(0)	1.6 \pm 0.4(0)
¹²⁵ Sb	4.9 \pm 0.8(0)	1.91 \pm 0.13(+3)	2.22 \pm 0.14(+2)	3.4 \pm 0.2(+2)	4.8 \pm 0.5(+2)
¹³⁴ Cs	5.1 \pm 0.4(0)	5.6 \pm 0.4(+1)	2.7 \pm 0.2(+1)	4.4 \pm 0.3(+1)	5.1 \pm 0.5(+1)
¹³⁷ Cs	8.7 \pm 0.7(+1)	1.06 \pm 0.4(+3)	6.5 \pm 0.4(+2)	9.1 \pm 0.6(+2)	1.0 \pm 0.1(+3)
¹⁴⁴ Ce	2.5 \pm 0.2(+3)	2.3 \pm 0.2(+3)	2.4 \pm 0.2(+3)	1.55 \pm 0.12(+3)	1.7 \pm 0.2(+3)
¹⁵⁴ Eu	4.8 \pm 0.4(+1)	4.5 \pm 0.4(+1)	4.3 \pm 0.3(+1)	2.4 \pm 0.2(+1)	3.4 \pm 0.4(+1)
¹⁵⁵ Eu	1.0 \pm 0.2(+2)	1.1 \pm 0.2(+2)	9.7 \pm 1.9(+1)	6.7 \pm 1.3(+1)	6.9 \pm 1.4(+1)

TABLE B-1. (continued)

<u>Radionuclide</u>	<u>30-74μm Aliquot</u>
^{60}Co	$6.56 \pm 0.47(+1)$
^{106}Ru	$1.09 \pm 0.08(+2)$
$^{110\text{m}}\text{Ag}$	$1.01 \pm 0.18(0)$
^{125}Sb	$2.03 \pm 0.14(+2)$
^{134}Cs	$3.24 \pm 0.23(+1)$
^{137}Cs	$6.14 \pm 0.43(+2)$
^{144}Ce	$7.12 \pm 0.65(+2)$
^{154}Eu	$1.13 \pm 0.10(+1)$
^{155}Eu	$2.56 \pm 0.50(+1)$

TABLE B-2. SAMPLE 3 H8 22-INCHES RADIONUCLIDE CONCENTRATIONS
($\mu\text{Ci/gm}$)

Radionuclide	$>4000_{\mu\text{m}}$ Particle 1 (3A)	$>4000_{\mu\text{m}}$ Particle 2 (3B)	$>4000_{\mu\text{m}}$ Particle 3 (3C)	$>4000_{\mu\text{m}}$ Particle 4 (3D)	$>4000_{\mu\text{m}}$ Particle 5 (3E)
^{60}Co	$4.67 \pm 0.27(+1)$	$5.94 \pm 0.41(+1)$	$1.30 \pm 0.08(+1)$	$2.03 \pm 0.29(0)$	$1.33 \pm 0.24(0)$
^{106}Ru	$6.25 \pm 0.36(+2)$	$3.76 \pm 0.35(0)$	$4.03 \pm 0.24(+2)$	$1.46 \pm 0.08(+3)$	$1.43 \pm 0.08(+3)$
$^{110\text{m}}\text{Ag}$	--	--	--	--	--
^{125}Sb	$4.63 \pm 0.29(+1)$	$6.95 \pm 0.50(0)$	$1.86 \pm 0.13(+1)$	$1.34 \pm 0.08(+2)$	$1.25 \pm 0.08(+2)$
^{134}Cs	$3.25 \pm 0.26(0)$	$5.00 \pm 0.42(-1)$	$2.23 \pm 0.18(0)$	$5.66 \pm 0.32(+1)$	$5.19 \pm 0.30(+1)$
^{137}Cs	$5.87 \pm 0.34(+1)$	$1.17 \pm 0.08(+1)$	$4.65 \pm 0.28(+1)$	$9.49 \pm 0.52(+2)$	$8.36 \pm 0.47(+2)$
^{144}Ce	$1.77 \pm 0.12(+3)$	$5.79 \pm 0.52(+1)$	$1.75 \pm 0.11(+3)$	$3.73 \pm 0.24(+3)$	$3.92 \pm 0.25(+3)$
^{154}Eu	$3.00 \pm 0.19(+1)$	$7.15 \pm 0.75(-1)$	$2.24 \pm 0.14(+1)$	$6.67 \pm 0.41(+1)$	$6.83 \pm 0.42(+1)$
^{155}Eu	$7.4 \pm 1.5(+1)$	$2.92 \pm 0.59(0)$	$6.99 \pm 0.43(+1)$	$1.59 \pm 0.32(+2)$	$1.36 \pm 0.27(+2)$

TABLE B-2. (continued)

Radionuclide	1680-4000 μ m Particle 1 (3F)	1680-4000 μ m Particle 2 (3G)	1680-4000 μ m Particle 3 (3H)	1000-1680 μ m Particle 4 (3I)	1000-1680 μ m Particle 5 (3J)
^{60}Co	$3.3 \pm 0.5(0)$	$6.41 \pm 0.75(0)$	$8.6 \pm 1.0(0)$	$7.13 \pm 0.49(+1)$	$1.62 \pm 0.19(+1)$
^{106}Ru	$2.6 \pm 0.3(+3)$	$1.81 \pm 0.21(+2)$	$5.06 \pm 0.66(+1)$	$2.39 \pm 0.17(+2)$	$1.45 \pm 0.17(+2)$
$^{110\text{m}}\text{Ag}$	--	--	--	--	--
^{125}Sb	$9.6 \pm 1.1(+1)$	$1.88 \pm 0.22(+1)$	$6.1 \pm 1.8(0)$	$4.45 \pm 0.38(+1)$	$1.69 \pm 0.21(+1)$
^{134}Cs	$4.4 \pm 0.5(+1)$	$1.06 \pm 0.12(+1)$	$9.2 \pm 1.0(+1)$	$4.80 \pm 0.33(+1)$	$4.59 \pm 0.55(0)$
^{137}Cs	$7.5 \pm 0.9(+2)$	$3.95 \pm 0.45(+2)$	$1.58 \pm 0.18(+3)$	$9.32 \pm 0.63(+2)$	$7.28 \pm 0.83(+1)$
^{144}Ce	$7.0 \pm 0.8(+3)$	$5.70 \pm 0.69(+2)$	$2.17 \pm 0.26(+3)$	$2.55 \pm 0.19(+3)$	$9.3 \pm 1.3(+2)$
^{154}Eu	$1.18 \pm 0.14(+2)$	$4.34 \pm 0.55(0)$	$3.55 \pm 0.42(+1)$	$4.29 \pm 0.31(+1)$	$1.65 \pm 0.20(+1)$
^{155}Eu	$3.1 \pm 0.6(+2)$	$2.82 \pm 0.33(+1)$	$7.8 \pm 1.6(+1)$	$1.13 \pm 0.23(+2)$	$4.05 \pm 0.47(+1)$

TABLE B-2. (continued)

Radionuclide	1000-1680 μ m Particle 3 (3K)	707-1000 μ m Aliquot	297-707 μ m Aliquot	149-279 μ m Aliquot	74-149 μ m Aliquot
⁶⁰ Co	6.41 \pm 0.41(0)	9.21 \pm 0.54(+1)	2.21 \pm 0.18(+1)	6.61 \pm 0.37(+1)	8.59 \pm 0.61(+1)
¹⁰⁶ Ru	4.17 \pm 0.28(+1)	2.07 \pm 0.14(+2)	1.19 \pm 0.09(+2)	3.09 \pm 0.17(+2)	2.33 \pm 0.17(+2)
^{110m} Ag	--	--	--	--	1.22 \pm 0.33(0)
¹²⁵ Sb	9.00 \pm 0.81(0)	3.37 \pm 0.25(+1)	1.93 \pm 0.19(+1)	1.09 \pm 0.06(+2)	1.93 \pm 0.14(+2)
¹³⁴ Cs	1.16 \pm 0.07(+1)	3.10 \pm 0.20(+1)	3.50 \pm 0.27(+1)	4.31 \pm 0.24(+1)	5.15 \pm 0.37(+1)
¹³⁷ Cs	2.05 \pm 0.12(+2)	5.40 \pm 0.34(+2)	8.35 \pm 0.65(+2)	9.00 \pm 0.49(+2)	9.05 \pm 0.64(+2)
¹⁴⁴ Ce	2.53 \pm 0.16(+3)	2.38 \pm 0.16(+3)	1.80 \pm 0.15(+3)	1.64 \pm 0.10(+3)	1.48 \pm 0.12(+3)
¹⁵⁴ Eu	4.69 \pm 0.28(+1)	4.46 \pm 0.30(+1)	3.16 \pm 0.26(+1)	2.59 \pm 0.16(+1)	2.30 \pm 0.19(+1)
¹⁵⁵ Eu	1.10 \pm 0.22(+2)	1.00 \pm 0.20(+2)	3.83 \pm 0.31(+1)	8.2 \pm 1.6(+3)	6.3 \pm 1.3(+1)

TABLE B-2. (continued)

Radionuclide	30-74 μ m Aliquot	20-30 μ m Aliquot
^{60}Co	$1.40 \pm 0.09(+2)$	$1.02 \pm 0.26(+2)$
^{106}Ru	$6.50 \pm 0.44(+2)$	$2.46 \pm 0.63(+2)$
$^{110\text{m}}\text{Ag}$	--	--
^{125}Sb	$2.21 \pm 0.15(+2)$	$1.78 \pm 0.46(+2)$
^{134}Cs	$5.16 \pm 0.35(+1)$	$2.87 \pm 0.74(+1)$
^{137}Cs	$8.90 \pm 0.60(+2)$	$6.6 \pm 1.7(+2)$
^{144}Ce	$1.19 \pm 0.09(+3)$	$7.5 \pm 2.0(+2)$
^{154}Eu	$1.73 \pm 0.14(+1)$	$1.05 \pm 0.28(+1)$
^{155}Eu	$4.9 \pm 1.0(+1)$	$3.07 \pm 0.79 (+1)$

TABLE B-3. SAMPLE 4 - LOCATION E9 SURFACE RADIONUCLIDE CONCENTRATIONS

Radionuclide	Particle 1 (4A)	Particle 2 (4B)	Particle 3 (4C)	Particle 4 (4D)	Particle 5 (4E)
^{60}Co	$1.42 \pm 0.16(+2)$	$1.13 \pm 0.07(+1)$	$2.51 \pm 0.17(+2)$	$2.75 \pm 0.51(0)$	$2.71 \pm 0.27(+1)$
^{106}Ru	$3.35 \pm 0.38(+3)$	$2.38 \pm 0.15(+2)$	$6.00 \pm 0.41(+2)$	$1.47 \pm 0.18(+3)$	$1.87 \pm 0.20(+3)$
$^{110\text{m}}\text{Ag}$	--	--	--	--	--
^{125}Sb	$2.00 \pm 0.24(+2)$	$6.81 \pm 0.53(0)$	$4.94 \pm 0.38(+1)$	$1.51 \pm 0.19(+2)$	$8.77 \pm 0.98(+1)$
^{134}Cs	$1.02 \pm 0.12(+2)$	$1.73 \pm 0.13(0)$	$1.34 \pm 0.10(+1)$	$1.75 \pm 0.22(+2)$	$3.33 \pm 0.36(+1)$
^{137}Cs	$1.71 \pm 0.19(+3)$	$3.57 \pm 0.22(+1)$	$3.65 \pm 0.24(+2)$	$3.92 \pm 0.48(+3)$	$5.46 \pm 0.58(+2)$
^{144}Ce	$8.6 \pm 1.0(+3)$	$7.74 \pm 0.53(+2)$	$2.51 \pm 0.19(+3)$	$4.60 \pm 0.59(+3)$	$5.18 \pm 0.56(+3)$
^{154}Eu	$1.50 \pm 0.17(+2)$	$9.32 \pm 0.6(0)$	$2.03 \pm 0.16(+1)$	$6.05 \pm 0.78(+1)$	$8.64 \pm 0.93(+1)$
^{155}Eu	$3.15 \pm 0.63(+2)$	$2.96 \pm 0.59(+1)$	$1.07 \pm 0.21(+2)$	$6.2 \pm 1.2(+1)$	$1.76 \pm 0.19(+2)$

TABLE B-4. SAMPLE 5 - LOCATION E9 - 3 INCHES RADIONUCLIDE CONCENTRATIONS

Radionuclide	$>4000\mu\text{m}$ Particle 1 (5A)	$>4000\mu\text{m}$ Particle 2 (5B)	$>4000\mu\text{m}$ Particle 3 (5C)	$>4000\mu\text{m}$ Particle 4 (5D)	$>4000\mu\text{m}$ Particle 5 (5E)
^{60}Co	$3.77 \pm 0.67(+1)$	$4.51 \pm 0.31(+1)$	$3.94 \pm 0.28(+1)$	$2.81 \pm 0.25(0)$	$1.20 \pm 0.09(+2)$
^{106}Ru	$2.21 \pm 0.39(+3)$	$1.25 \pm 0.08(+3)$	$1.04 \pm 0.07(+3)$	$5.40 \pm 0.36(+2)$	$1.19 \pm 0.08(+3)$
$^{110\text{m}}\text{Ag}$	--	--	--	--	--
^{125}Sb	$1.67 \pm 0.30(+2)$	$1.47 \pm 0.10(+2)$	$2.47 \pm 0.24(+1)$	$3.86 \pm 0.28(+1)$	$3.00 \pm 0.22(+2)$
^{134}Cs	$2.33 \pm 0.42(+1)$	$1.53 \pm 0.11(+1)$	$9.55 \pm 0.75(0)$	$2.25 \pm 0.15(+1)$	$6.78 \pm 0.55(0)$
^{137}Cs	$3.92 \pm 0.69(+2)$	$2.95 \pm 0.20(+2)$	$1.64 \pm 0.11(+2)$	$6.89 \pm 0.45(+2)$	$1.48 \pm 0.11(+2)$
^{144}Ce	$6.6 \pm 1.2(+3)$	$3.84 \pm 0.27(+3)$	$3.15 \pm 0.24(+3)$	$1.81 \pm 0.13(+3)$	$2.13 \pm 0.17(+3)$
^{154}Eu	$1.20 \pm 0.21(+2)$	$5.93 \pm 0.42(+1)$	$4.27 \pm 0.32(+1)$	$1.58 \pm 0.12(+1)$	$3.82 \pm 0.29(+1)$
^{155}Eu	$2.72 \pm 0.54(+2)$	$1.33 \pm 0.27(+2)$	$1.35 \pm 0.27(+2)$	$8.1 \pm 1.6(+1)$	$9.9 \pm 2.0(+1)$

TABLE B-4. (continued)

Radionuclide	1680-4000 μ m Particle 1 (5F)	1680-4000 μ m Particle 2 (5G)	1680-4000 μ m Particle 3 (5H)	1000-1680 μ m Particle 4 (5I)	1000-1680 μ m Particle 5 (5J)
^{60}Co	$2.07 \pm 0.19(0)$	$3.10 \pm 0.18(+1)$	$1.0 \pm 0.2 (+2)$	$6.57 \pm 0.40(-1)$	$1.09 \pm 0.18(0)$
^{106}Ru	$5.58 \pm 0.34(+2)$	$6.93 \pm 0.38(+2)$	$2.8 \pm 0.5(+3)$	$1.44 \pm 0.09(+3)$	$1.29 \pm 0.09(+3)$
$^{110\text{m}}\text{Ag}$	--	--	--	--	--
^{125}Sb	$6.35 \pm 0.40(+1)$	$1.32 \pm 0.11(+1)$	$6.1 \pm 0.1(+2)$	$1.02 \pm 0.07(+2)$	$1.16 \pm 0.08(+2)$
^{134}Cs	$2.92 \pm 0.18(+1)$	$2.86 \pm 0.26(0)$	$3.6 \pm 0.6(+2)$	$3.17 \pm 0.20(+1)$	$3.29 \pm 0.23(+1)$
^{137}Cs	$7.90 \pm 0.47(+2)$	$3.78 \pm 0.21(+1)$	$6.5 \pm 1.1(+3)$	$5.08 \pm 0.31(+2)$	$5.36 \pm 0.37(+2)$
^{144}Ce	$1.86 \pm 0.12(+3)$	$2.36 \pm 0.14(+3)$	$1.1 \pm 0.2(+4)$	$3.56 \pm 0.25(+3)$	$3.40 \pm 0.26(+3)$
^{154}Eu	$1.73 \pm 0.12(+1)$	$2.94 \pm 0.18(+1)$	$2.2 \pm 0.4(+2)$	$6.26 \pm 0.42(+1)$	$6.23 \pm 0.45(+1)$
^{155}Eu	$7.4 \pm 1.5(+1)$	$1.02 \pm 0.20(+2)$	$5.1 \pm 1.0(+2)$	$1.62 \pm 0.32(+2)$	$1.39 \pm 0.28(+2)$

TABLE B-4. (continued)

<u>Radionuclide</u>	<u><16 mesh Aliquot</u>
^{60}Co	$5.53 \pm 0.34(+1)$
^{106}Ru	$6.53 \pm 0.40(+2)$
$^{110\text{m}}\text{Ag}$	--
^{125}Sb	$8.01 \pm 0.55(+1)$
^{134}Cs	$9.85 \pm 0.59(+1)$
^{137}Cs	$1.71 \pm 0.10(+3)$
^{144}Ce	$2.24 \pm 0.17(+3)$
^{154}Eu	$3.54 \pm 0.25(+1)$
^{155}Eu	$1.06 \pm 0.20(+2)$

TABLE B-5. SAMPLE 6 - LOCATION E9 - 22 INCHES RADIONUCLIDE CONCENTRATIONS

Radionuclide	^{>4000μm} Particle 1 (6A)	^{>4000μm} Particle 2 (6B)	^{>4000μm} Particle 3 (6C)	^{>4000μm} Particle 4 (6D)	^{>4000μm} Particle 5 (6E)
⁶⁰ Co	6.07 ± 0.67(0)	1.66 ± 0.09(0)	3.34 ± 0.23(0)	ND	1.24 ± 0.09(0)
¹⁰⁶ Ru	1.07 ± 0.11(+3)	2.39 ± 0.23(0)	1.16 ± 0.07(+2)	9.15 ± 0.62(+2)	1.32 ± 0.14(0)
^{110m} Ag	--	--	--	--	--
¹²⁵ Sb	9.74 ± 0.99(+1)	3.05 ± 0.17(+2)	4.22 ± 0.26(+1)	6.95 ± 0.53(+1)	2.40 ± 0.16(+1)
¹³⁴ Cs	3.90 ± 0.39(+1)	7.11 ± 0.40(0)	9.73 ± 0.59(0)	5.47 ± 0.38(+1)	2.22 ± 0.15(0)
¹³⁷ Cs	1.19 ± 0.12(+3)	1.24 ± 0.07(+3)	1.82 ± 0.11(+2)	1.30 ± 0.09(+3)	4.41 ± 0.29(+1)
¹⁴⁴ Ce	3.65 ± 0.38(+3)	2.84 ± 0.98(+3)	1.96 ± 0.17(+2)	2.66 ± 0.21(+3)	1.91 ± 0.38(0)
¹⁵⁴ Eu	2.88 ± 0.30(+1)	ND	2.93 ± 0.25(0)	3.25 ± 0.25(+1)	ND
¹⁵⁵ Eu	1.51 ± 0.30(+2)	2.21 ± 0.88(+1)	1.03 ± 0.07(+1)	1.16 ± 0.23(+2)	ND

TABLE B-5. (continued)

Radionuclide	1680-4000 μ m Particle 1 (6F)	1680-4000 μ m Particle 2 (6G)	1680-4000 μ m Particle 3 (6H)	1000-1680 μ m Particle 4 (6I)	1000-1680 μ m Particle 5 (6J)
^{60}Co	$4.89 \pm 0.35(0)$	$9.3 \pm 2.1(-1)$	ND	$2.74 \pm 0.16(+2)$	$7.33 \pm 0.43(0)$
^{106}Ru	$7.0 \pm 1.0(0)$	$1.03 \pm 0.06(+3)$	$8.05 \pm 0.45(+2)$	$2.64 \pm 0.16(+3)$	$2.92 \pm 0.16(+2)$
$^{110\text{m}}\text{Ag}$	--	--	--	--	--
^{125}Sb	$1.46 \pm 0.11(+1)$	$9.97 \pm 0.66(+1)$	$8.16 \pm 0.50(+1)$	$8.28 \pm 0.49(+2)$	$1.78 \pm 0.11(+1)$
^{134}Cs	$3.25 \pm 0.20(+1)$	$1.69 \pm 0.09(+2)$	$4.67 \pm 0.26(+1)$	$2.08 \pm 0.34(0)$	$4.97 \pm 0.57(-1)$
^{137}Cs	$6.22 \pm 0.38(+2)$	$3.79 \pm 0.21(+3)$	$1.07 \pm 0.06(+3)$	$2.98 \pm 0.18(+1)$	$1.10 \pm 0.06(+1)$
^{144}Ce	$1.84 \pm 0.35(+1)$	$3.06 \pm 0.20(+3)$	$2.50 \pm 0.16(+3)$	$3.20 \pm 0.34(+2)$	$6.90 \pm 0.44(+2)$
^{154}Eu	ND	$4.34 \pm 0.28(+1)$	$2.46 \pm 0.16(+1)$	$5.04 \pm 0.64(0)$	$1.34 \pm 0.08(+1)$
^{155}Eu	ND	$1.37 \pm 0.27(+2)$	ND	$2.7(0)$	$4.2(0)$

TABLE B-5. (continued)

Radionuclide	1000-1680 μ m Particle 1 (6K)	707-1000 μ m Aliquot	297-707 μ m Aliquot	149-279 μ m Aliquot	74-149 μ m Aliquot
⁶⁰ Co	6.87 \pm 0.55(0)	1.43 \pm 0.08(+2)	5.15 \pm 0.29(+1)	9.21 \pm 0.59(+1)	1.11 \pm 0.06(+2)
¹⁰⁶ Ru	5.81 \pm 0.35(+2)	4.20 \pm 0.23(+2)	2.19 \pm 0.13(+2)	2.94 \pm 0.17(+2)	3.74 \pm 0.21(+2)
^{110m} Ag	--	--	--	--	--
¹²⁵ Sb	8.15 \pm 0.59(+1)	8.77 \pm 0.52(+1)	9.77 \pm 0.57(+1)	1.46 \pm 0.08(+2)	1.89 \pm 0.11(+2)
¹³⁴ Cs	1.76 \pm 0.10(+2)	5.66 \pm 0.31(+1)	5.82 \pm 0.32(+1)	5.36 \pm 0.30(+1)	4.81 \pm 0.27(+1)
¹³⁷ Cs	4.06 \pm 0.24(+3)	1.23 \pm 0.07 (+3)	1.13 \pm 0.06(+3)	1.07 \pm 0.06(+3)	9.58 \pm 0.53(+2)
¹⁴⁴ Ce	3.48 \pm 0.24(+3)	2.29 \pm 0.15(+3)	2.11 \pm 0.149(+3)	1.40 \pm 0.09(+3)	1.27 \pm 0.09(+3)
¹⁵⁴ Eu	5.07 \pm 0.349(+1)	3.63 \pm 0.22(+1)	3.55 \pm 0.22(+1)	2.16 \pm 0.14(+1)	2.14 \pm 0.14(+1)
¹⁵⁵ Eu	3.53 \pm 0.24(+1)	1.07 \pm 0.21(+2)	9.19 \pm 1.80(+1)	6.7 \pm 1.3(+1)	7.8 \pm 1.6(+1)

TABLE B-5. (continued)

<u>Radionuclide</u>	<u>30-74μm Aliquot</u>
^{60}Co	$1.25 \pm 0.09(+2)$
^{106}Ru	$5.23 \pm 0.37(+2)$
$^{110\text{m}}\text{Ag}$	--
^{125}Sb	$1.67 \pm 0.12(+2)$
^{134}Cs	$5.00 \pm 0.35(+1)$
^{137}Cs	$9.54 \pm 0.67(+2)$
^{144}Ce	$1.11 \pm 0.09(+3)$
^{154}Eu	$1.83 \pm 0.14(+1)$
^{155}Eu	$4.5 \pm 0.9(+1)$

APPENDIX C

FISSILE/FERTILE MATERIAL ANALYSIS

APPENDIX C

FISSILE/FERTILE MATERIAL ANALYSIS

All sample aliquots removed from the core debris samples were analyzed both by gamma ray spectrometry and by delayed neutron analysis. This table presents the preliminary results of the delayed neutron analysis. These results may change slightly due to change in the calibration curves for these data. The analysis was performed by first measuring the total fissile/fertile material contents using a fast neutron flux at the Coupled Fast Reactivity Measurement Facility (CFRMF) and subsequently measuring the fissile material content (i.e., ^{235}U plus ^{239}Pu) in a thermal neutron flux field at the CFRMF. It has been determined that the ^{239}Pu component is negligible (<0.2 wt%) and therefore the component principally measured is ^{235}U . The effect of the ^{239}Pu is to increase the measured fissile material content 5-8%.

TABLE C-1. FISSILE/FERTILE MATERIAL CONCENTRATIONS SAMPLE 1 HB Surface

Identification	^{238}U (mg)	Fissile (mg)	Fissile (wt percent)	Sample Weight (mg)
>4000 μm Particle 1 (1A)	$7.9 \pm 0.6(0)$	$2.4 \pm 0.2(-1)$	3.0 ± 0.3	84
>4000 μm Particle 2 (1B)	$1.10 \pm 0.07(+1)$	$2.3 \pm 0.2(-1)$	2.0 ± 0.2	12
>4000 μm Particle 3 (1C)	$5.70 \pm 0.6(0)$	$1.4 \pm 0.2(-1)$	$2.4 \pm 0.4(0)$	10
>4000 μm Particle 4 (1D)	$5.9 \pm 0.8(0)$	$1.4 \pm 0.2(-1)$	$2.4 \pm 0.4(0)$	7
>4000 μm Particle 5 (1E)	$5.5 \pm 0.6(0)$	$1.4 \pm 0.2(-1)$	$2.5 \pm 0.4(0)$	29
1680-4000 μm Particle 1 (1F)	$1.09 \pm 0.07(+1)$	$2.6 \pm 0.2(-1)$	$2.4 \pm 0.2(0)$	16
1680-4000 μm Particle 2 (1G)	$8.2 \pm 0.7(0)$	$1.7 \pm 0.2(-1)$	$2.0 \pm 0.3(0)$	15
1680-4000 μm Particle 3 (1H)	$1.5 \pm 0.1(+1)$	$4.2 \pm 0.2(-1)$	$2.7 \pm 0.2(0)$	33
1000-1680 μm Particle 1 (1I)	--	--	--	10
1000-1680 μm Particle 2 (1J)	$1.46 \pm 0.08(+1)$	$3.3 \pm 0.2(-1)$	$2.2 \pm 0.2(0)$	210
1000-1680 μm Particle 3 (1K)	$1.00 \pm 0.07(+1)$	$2.5 \pm 0.2(-1)$	$2.5 \pm 0.2(0)$	19
707-1000 μm Aliquot	$1.65 \pm 0.09(+1)$	$3.8 \pm 0.2(-1)$	$2.2 \pm 0.2(0)$	26
297-707 μm Aliquot	$1.62 \pm 0.09(+1)$	$4.1 \pm 0.2(-1)$	$2.4 \pm 0.2(0)$	29
149-297 μm Aliquot	$9.0 \pm 0.6(0)$	$2.1 \pm 0.2(-1)$	$2.3 \pm 0.2(0)$	23
74-149 μm Aliquot	$5.4 \pm 0.6(0)$	$1.2 \pm 0.2(-1)$	$2.1 \pm 0.4(0)$	12
30-74 μm Aliquot	$3.9 \pm 0.5(0)$	$8.2 \pm 1.7(-1)$	$2.1 \pm 0.5(0)$	22

NA - Data not available for this report

TABLE C-1. (continued)

Identification	^{238}U (mg)	Fissile (mg)	Fissile (wt percent)	Sample Weight (mg)
>4000 μm Particle 1 (3A)	$2.1 \pm 0.1(+1)$	$6.2 \pm 0.4(-1)$	$2.8 \pm 0.2(0)$	56
>4000 μm Particle 2 (3B)	<0.7(0)	<1.6(-2)	--	23
>4000 μm Particle 3 (3C)	NA	NA	NA	39
>4000 μm Particle 4 (3D)	$7.9 \pm 0.3(+1)$	$1.9 \pm 0.06(0)$	$2.3 \pm 0.1(0)$	97
>4000 μm Particle 5 (3E)	$5.6 \pm 0.2(+1)$	$1.3 \pm 0.04(0)$	$2.3 \pm 0.1(0)$	69
1680-4000 μm Particle 1 (3F)	NA	NA	NA	10
1680-4000 μm Particle 2 (3G)	NA	NA	NA	10
1680-4000 μm Particle 3 (3H)	$5.4 \pm 0.7(0)$	$1.0 \pm 0.2(-1)$	$1.9 \pm 0.4(0)$	10
1000-1680 μm Particle 1 (3I)	NA	NA	NA	25
1000-1680 μm Particle 2 (3J)	$4.6 \pm 0.6(0)$	$1.2 \pm 0.2(-1)$	$2.4 \pm 0.4(0)$	24
1000-1680 μm Particle 3 (3K)	$1.8 \pm 0.1(+1)$	$6.4 \pm 0.2(-1)$	$2.3 \pm 0.1(0)$	45
707-1000 μm Aliquot	NA	NA	NA	30
297-707 μm Aliquot	NA	NA	NA	18
149-297 μm Aliquot	NA	NA	NA	114
74-149 μm Aliquot	NA	NA	NA	22
30-74 μm Aliquot	$6.9 \pm 0.7(0)$	$1.8 \pm 0.2(-1)$	$2.6 \pm 0.4(0)$	25
20-30 μm Aliquot	$1.3 \pm 0.6(0)$	$2.2 \pm 1.6(-1)$	$1.7 \pm 1.5(0)$	4

TABLE C-1. (continued)

Identification	^{238}U (mg)	Fissile (mg)	Fissile (wt percent)	Sample Weight (mg)
>4000 μm Particle 1 (4A)	NA	NA	NA	10
>4000 μm Particle 2 (4B)	$6.1 \pm 0.6(0)$	$2.1 \pm 0.2(-1)$	$3.4 \pm 0.5(0)$	33
>4000 μm Particle 3 (4C)	NA	NA	NA	28
>4000 μm Particle 4 (4D)	NA	NA	NA	9
>4000 μm Particle 5 (4E)	NA	NA	NA	11

TABLE C-1. (continued)

Identification	²³⁸ U (mg)	Fissile (mg)	Fissile (wt percent)	Sample Weight (mg)
<4000 μm Particle 1 (6A)	NA	NA	NA	12
<4000 μm Particle 2 (6B)	>0.016	>0.73	--	65
<4000 μm Particle 3 (6C)	1.4 ± 0.5(0)	6.4 ± 0.2(-1)	4.4 ± 1.9(0)	40
<4000 μm Particle 4 (6D)	1.9 ± 0.1(+1)	5.6 ± 0.2(-1)	2.9 ± 0.2(0)	25
<4000 μm Particle 5 (6E)	>0.5	>0.02	--	26
1680-4000 μm Particle 1 (6F)	>0.5	>0.02	--	33
1680-4000 μm Particle 2 (6G)	7.3 ± 0.3(+1)	2.14 ± 0.06(0)	2.8 ± 0.1(0)	94
1680-4000 μm Particle 3 (6H)	8.6 ± 0.3(+1)	2.4 ± 0.07(0)	2.7 ± 0.1(0)	1010
1000-1680 μm Particle 1 (6I)	4.0 ± 0.6(0)	1.2 ± 0.2(-1)	3.0 ± 0.6(0)	41
1000-1680 μm Particle 2 (6J)	8.9 ± 0.7(0)	2.8 ± 0.2(-1)	3.1 ± 0.3(0)	71
1000-1680 μm Particle 3 (6K)	3.1 ± 0.1(0)	9.2 ± 0.3(-1)	2.8 ± 0.2(0)	43
707-1000 μm Aliquot	7.7 ± 0.3(+1)	2.07 ± 0.06(0)	2.6 ± 0.1(0)	1390
297-707 μm Aliquot	6.9 ± 0.3(+1)	1.71 ± 0.05(0)	2.4 ± 0.1(0)	1300
149-297 μm Aliquot	4.9 ± 0.2(+1)	1.75 ± 0.06(0)	2.7 ± 0.2(0)	1350
74-149 μm Aliquot	3.2 ± 0.1(+1)	8.00 ± 0.03(0)	2.4 ± 0.1(0)	87
30-74 μm Aliquot	5.6 ± 0.6(0)	1.6 ± 0.2 (-1)	2.8 ± 0.4(0)	22

TABLE C-1. (continued)

Identification	²³⁸ U (mg)	Fissile (mg)	Fissile (wt percent)	Sample Weight (mg)
>4000 μ m Particle 1 (5A)	NA	NA	NA	6
>4000 μ m Particle 2 (5B)	2.3 \pm 0.1(+1)	5.5 \pm 0.2(-1)	2.4 \pm 0.2(0)	26
>4000 μ m Particle 3 (5C)	NA	NA	NA	24
>4000 μ m Particle 4 (5D)	NA	NA	NA	27
>4000 μ m Particle 5 (5E)	7.7 \pm 0.6(0)	2.4 \pm 0.2(-1)	3.0 \pm 0.3(0)	21
1680-4000 μ m Particle 1 (5F)	2.2 \pm 0.1(+1)	6.5 \pm 0.3(-1)	2.9 \pm 0.2(0)	39
1680-4000 μ m Particle 2 (5G)	NA	NA	NA	89
1000-1680 μ m Particle 1 (5H)	NA	NA	NA	6
1000-1680 μ m Particle 2 (5I)	2.7 \pm 0.1(+1)	8.1 \pm 0.3(-1)	2.9 \pm 0.2(0)	37
1000-1680 μ m Particle 3 (5J)	1.7 \pm 0.9(+1)	4.5 \pm 0.2(-1)	2.7 \pm 0.2(0)	24
<1000 μ m Aliquot	1.9 \pm 0.1(+1)	6.0 \pm 0.3(-1)	3.0 \pm 0.2(0)	428

